LA-UR-15-23681
Approved for public release; distribution is unlimited.

Title:	Multi-functional carbon nanomaterials: Tailoring morphology for multidisciplinary applications
Author(s):	Dervishi, Enkeleda
Intended for:	This is a presentation for James L Smith Materials Research Seminar
Issued:	2015-05-14

Multi-functional carbon nanomaterials: Tailoring morphology for multidisciplinary applications

Enkeleda Dervishi, Ph.D.

Marie Curie Distinguished Postdoctoral Fellow

MPA-CINT

Los Alamos NATIONAL LABORATORY

U.S. DEPARTMENT OF ENERGY | Office of Science

UALR Center for Integrative Nanotechnology Sciences

Sandia National Laboratories

Outline

- Introduction to carbon nanomaterials
- Reaction conditions affecting the growth of carbon nanotubes and graphene
  - *Catalyst Composition*
  - *Reaction Temperature*
  - *Hydrocarbon Source*
- Graphene-Nanotube Hybrids
- Applications of nanomaterials
- Conclusions
- Acknowledgements

Carbon-based Nanomaterials

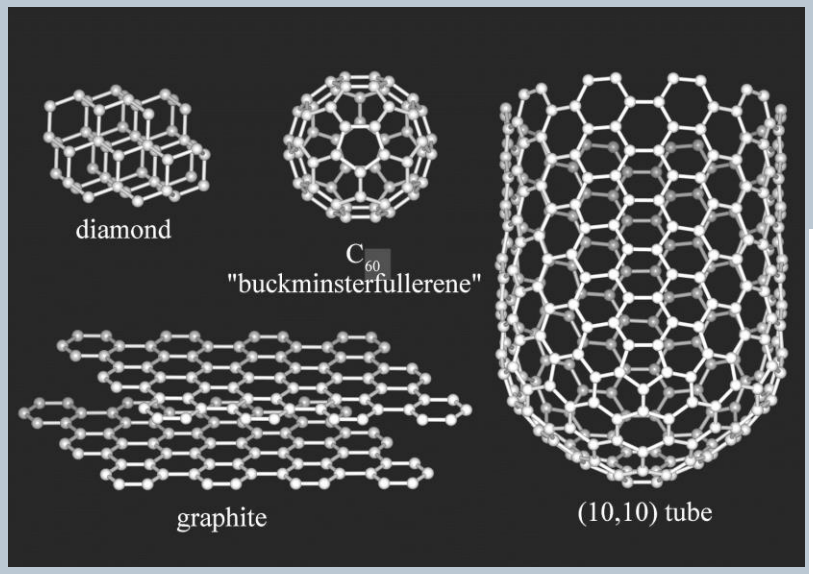

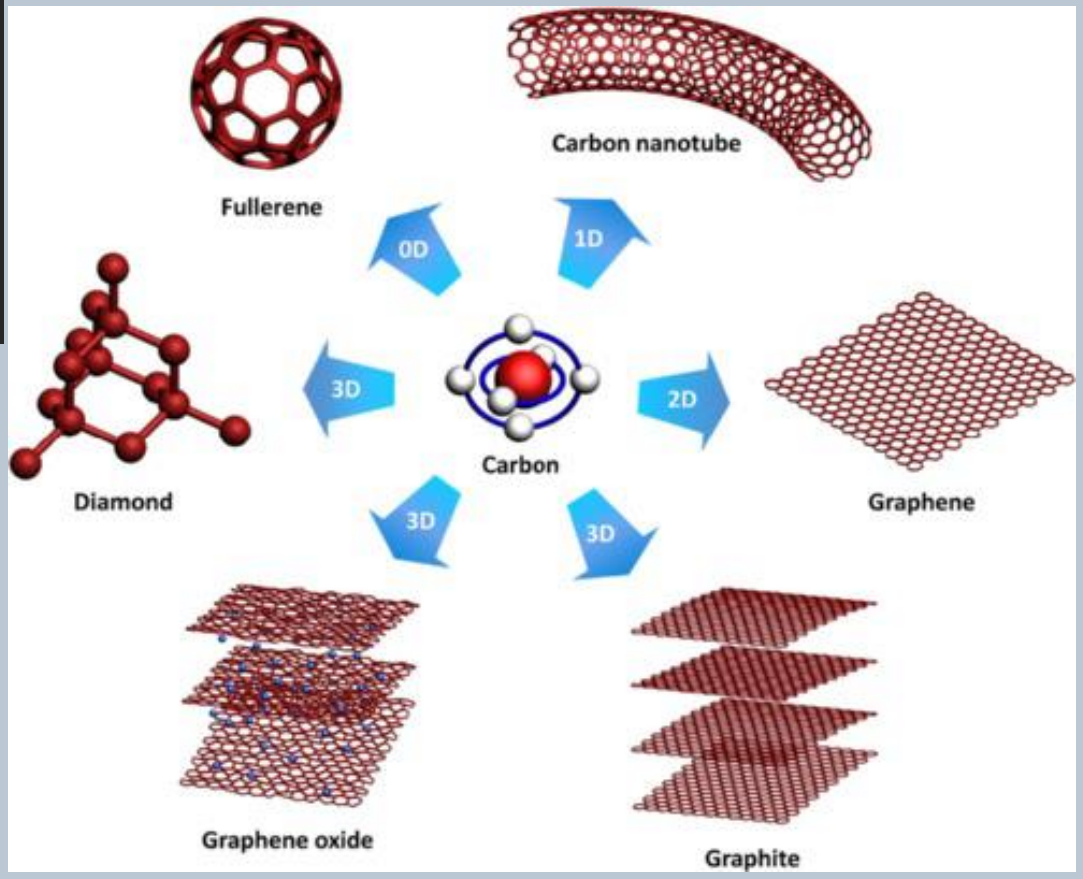

http://cohesion.rice.edu/naturalsciences/smalley/emplibrary/allotropes.jpg

http://www.nanoconvergencejournal.com/content/pdf/s40580-014-0015-5.pdf

Los Alamos NATIONAL LABORATORY

U.S. DEPARTMENT OF ENERGY | Office of Science

UALR Center for Integrative Nanotechnology Sciences

Sandia National Laboratories

Graphene

- Mono-layer 2D atomic thick structure formed from hexagons of carbon atoms bound together by sp^2 hybrid bonds
- This semi-metal structure is an exciting new material for a wide range of applications

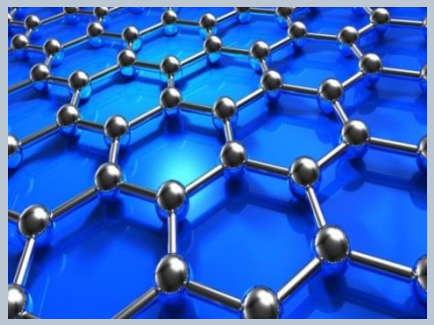

http://www.gizmag.com/polymer-graphene-substitute-kist/32824/pictures

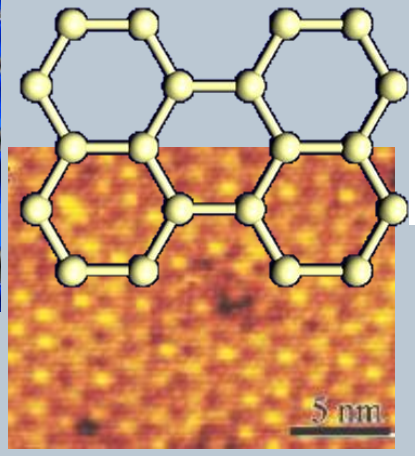

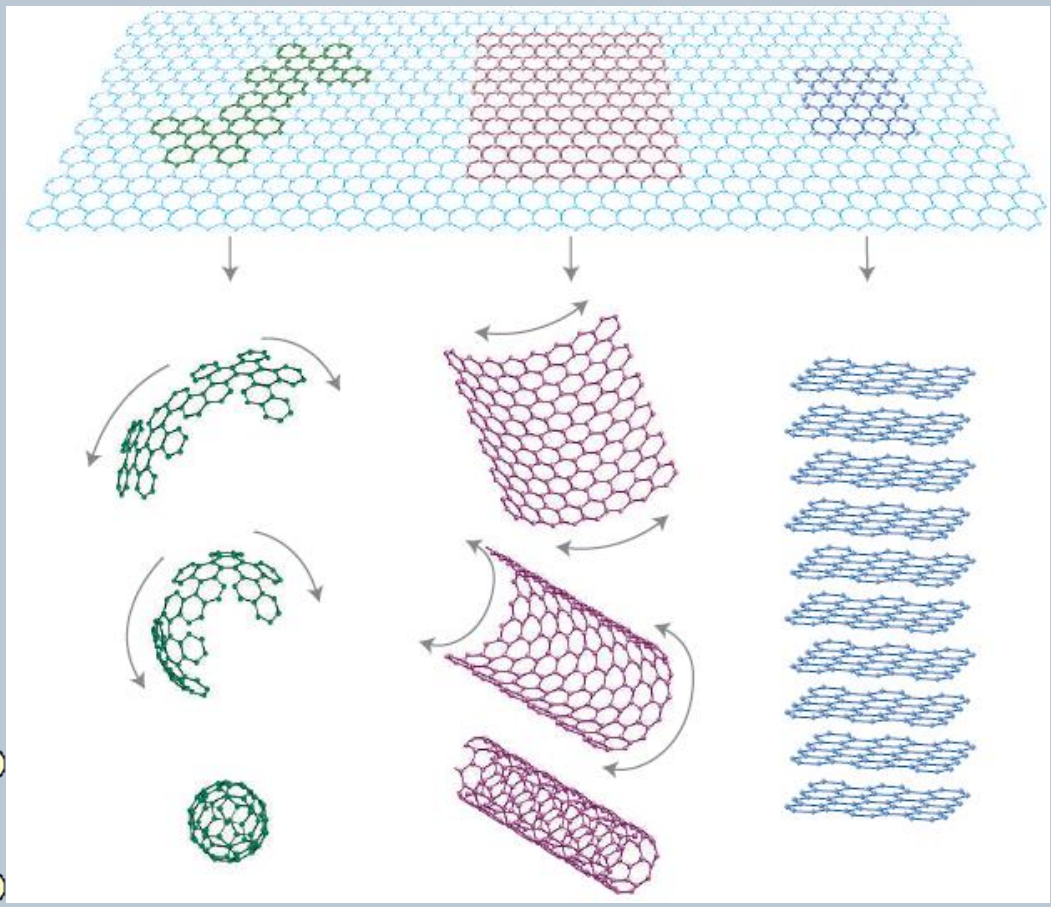

Mother of all graphitic forms

A. K. Geim[1] & K. S. Novoselov,[1] *Nature Materials,* 6, 183 -191, 2007.

Los Alamos NATIONAL LABORATORY

U.S. DEPARTMENT OF ENERGY | Office of Science

UALR Center for Integrative Nanotechnology Sciences

Sandia National Laboratories

Properties of Graphene

- High carrier mobility at room temperature (exceeding 15,000 $cm^2 \cdot V^{-1} \cdot s^{-1}$).
- Resistivity of the graphene sheet is ~10^{-6} Ω·cm, less than the resistivity of silver (Ag).
- Bandgap engineering through doping and constraining dimensions of large-area graphene (e. g. nanoribbons and nano-graphene structures).
- High thermal conductivity (4800-5300 W/m·K).
- High Young's modulus (~1,100 Gpa) and high fracture strength (125 Gpa) (200 times stronger than structural steel).
- Monolayer graphene absorbs ≈ 2.3% of white light (97.7 % transmittance).

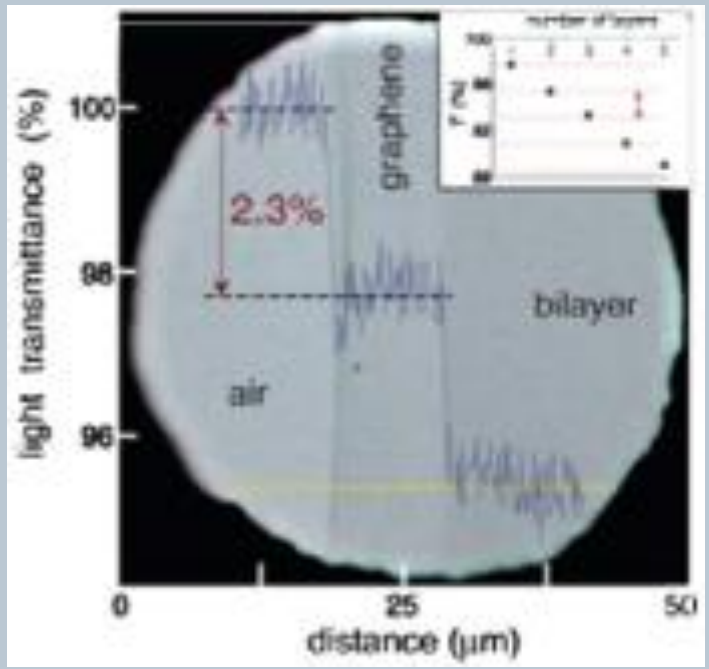

S. Chae and Y. Lee, *Nano Convergence,* 1, 15, 2014.

Carbon nanotubes (CNTs)

- Can be viewed as a sheet of graphene rolled up to a cylindrical and hollow structure.
- Usually 1-2 nm in diameter and several microns in length.
- Unique 1D material with exceptional properties enabling new technologies.

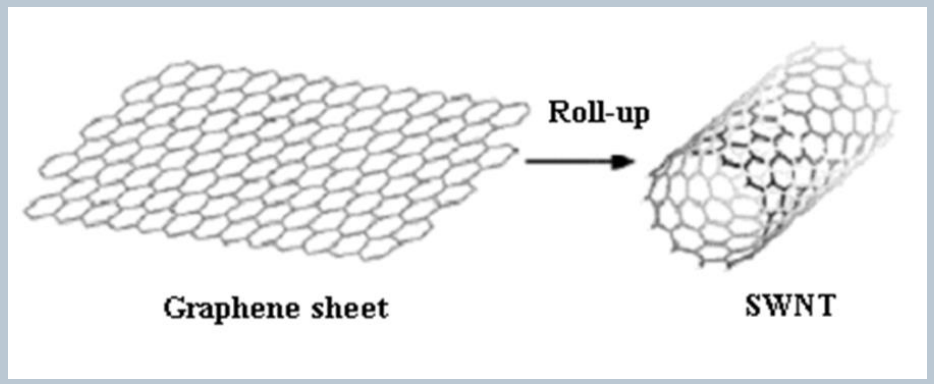

CNTs

- **SWCNTs** — **Metallic or Semiconductor**
- **MWCNTs** — **Metallic**
  $d_{intertubes}$ = 0.34nm

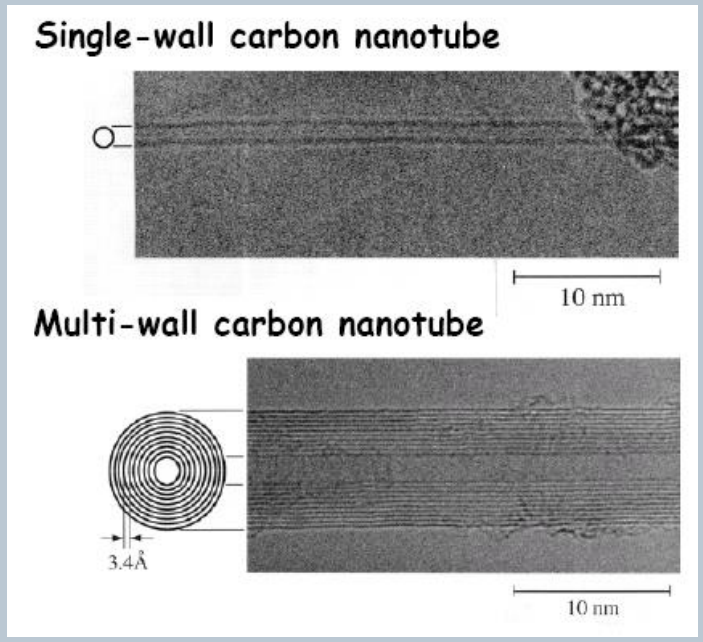

http://www.mb.tn.tudelft.nl/user/dekker/files/carbonnanotubes.pdf

Properties of Carbon Nanotubes

Mechanical properties		Thermal properties at room temperature	
Young's modulus of multiwall nanotubes	~1–1.2 TPa [25, 26]	Thermal conductivity of single wall nanotube	1750–5800 W mK [28]
Young's modulus of single wall nanotube ropes	~1 TPa [27]	Thermal conductivity of multiwall nanotube	>3000 W mK [29]
Tensile strength of single wall nanotube ropes	~60 GPa [25]		
Electrical properties		**Electronic properties**	
Typical resistivity of single and multiwall nanotube	10^{-6} Ω m [22, 30]	Single wall nanotube bandgap—	
		whose n–m is divisible by 3	0 eV [22] (metallic)
Typical maximum current density	10^{7}–10^{9} A cm^{2} [31, 32]	whose n–m is nondivisible by 3	0.4–0.7 eV [20, 21] (semiconducting)
Quantized conductance, theoretical/measured	$(6.5\ \text{k}\Omega)^{-1}/(12.9\ \text{k}\Omega)^{-1}$ [22, 33]	Multiwall nanotube bandgap	~0 eV [22] (nonsemiconducting)

K. Teo and Ch. Singh "Catalytic Synthesis of Carbon Nanotubes and Nanofibers", *Encyclopedia of Nanoscience and Nanotechnology*, Volume 1, pp. 665-686, 2004.

Applications of carbon nanotubes and graphene

- **Nanoelectronics** (Electronic devices nanoelectronic circuits for high speed computers)
- **Nanocomposite Materials** (plastics, metals, glass, ceramics et.)
- **Hydrogen storage and Li^+ battery**
- **Scanning probe tips**
- **Biomedical and bio-nano-sensors (Tissue and Bone Regeneratio, Cancer Treatment, Drug Delivery**

- **Filters**
- **Special Coatings for Defense Applications** (Static Discharge Dissipation, Armor Improvement, Smart" Bullet-proof vests with sensors incorporated)
- **Field Emission (Flat Panel Displays)**
- **Electromagnetic Shielding**
- **Advanced Aerospace Composites**
- **Energy storage mediums**
- **Fuel Cell Electrodes**

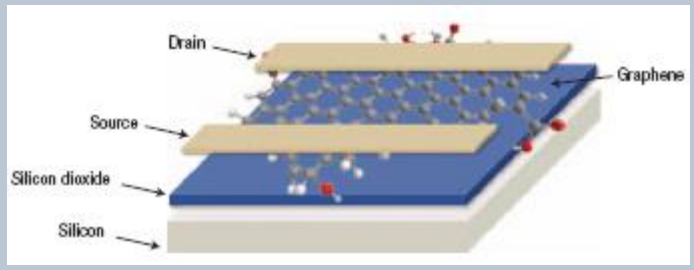

Graphene Transistor

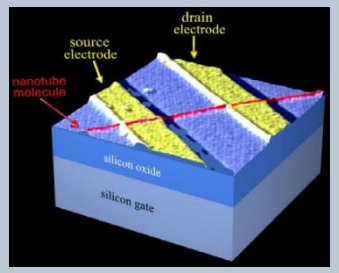

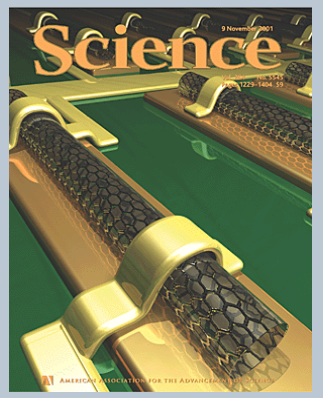

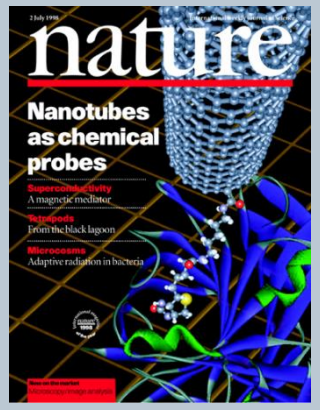

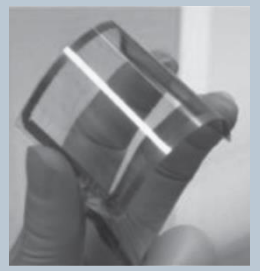

b) An assembled graphene/PET touc showing outstanding fl exibility.(c) A graphene-based touch-screen panel connected to a computer with control software. Reproduced with permission. [122] *Jinhong Du , Songfeng Pei , Laipeng Ma , and Hui-Ming Cheng Adv. Mater.* **2014**, *26*, 1958–1991

Reaction conditions affecting the growth of carbon nanotubes and graphene

Los Alamos NATIONAL LABORATORY
U.S. DEPARTMENT OF ENERGY
Office of Science
UALR Center for Integrative Nanotechnology Sciences
Sandia National Laboratories

Chemical vapor deposition

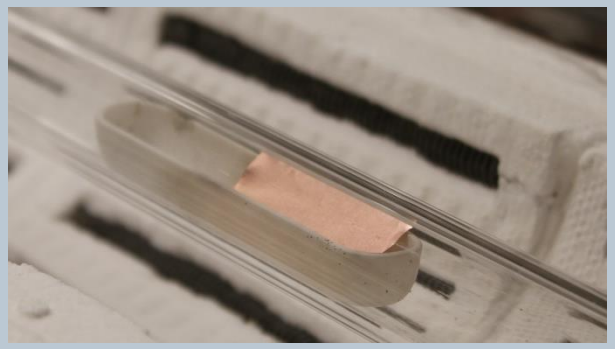

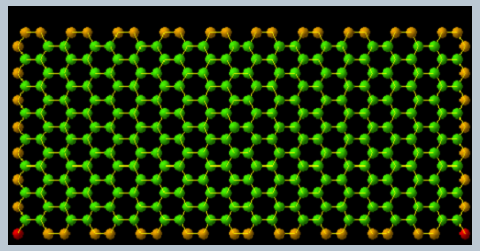

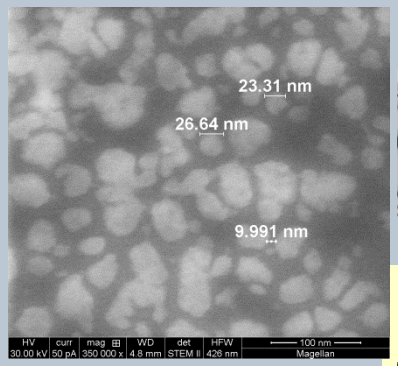

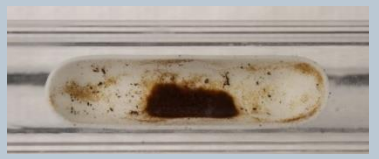

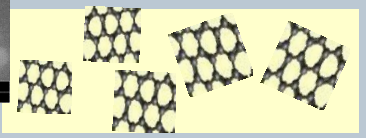

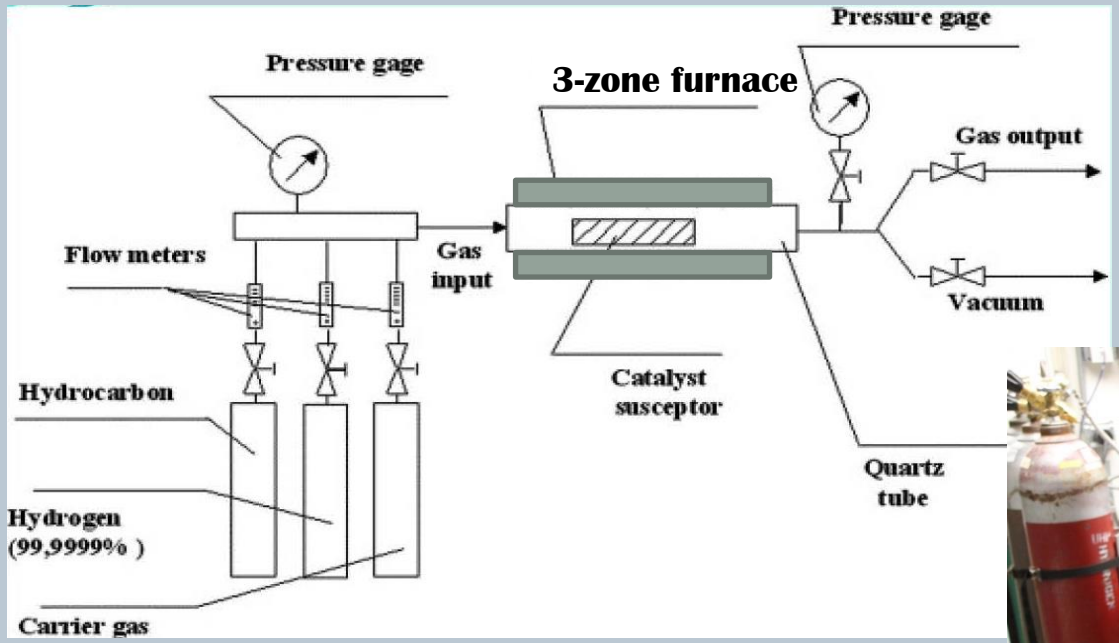

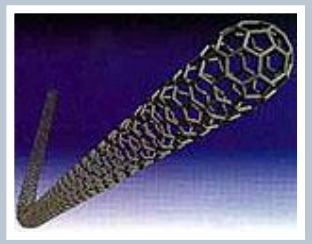

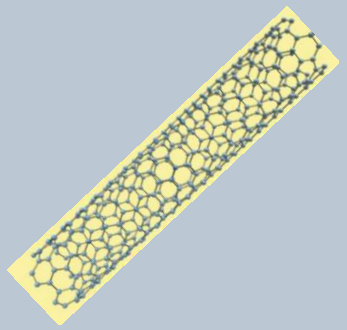

Synthesis of carbon nanotubes

- The growth of catalyst-grown CNTs occurs through the precipitation of dissolved carbon from a catalytic particle surface.
- Growth terminates when the catalyst particle gets poisoned by impurities or after the formation of a stable metal carbide.

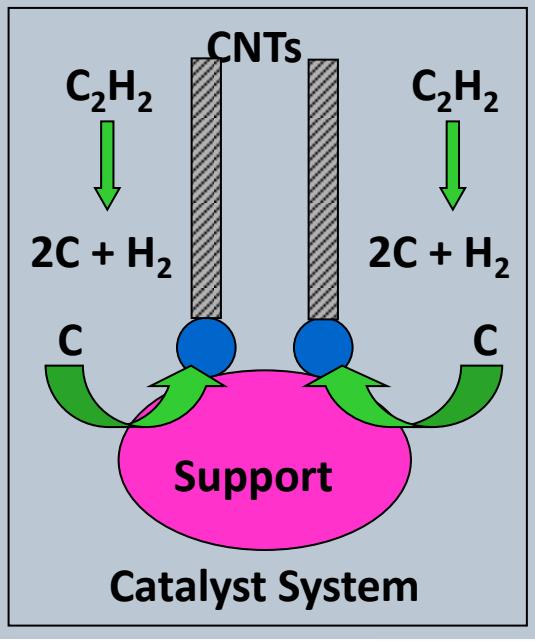

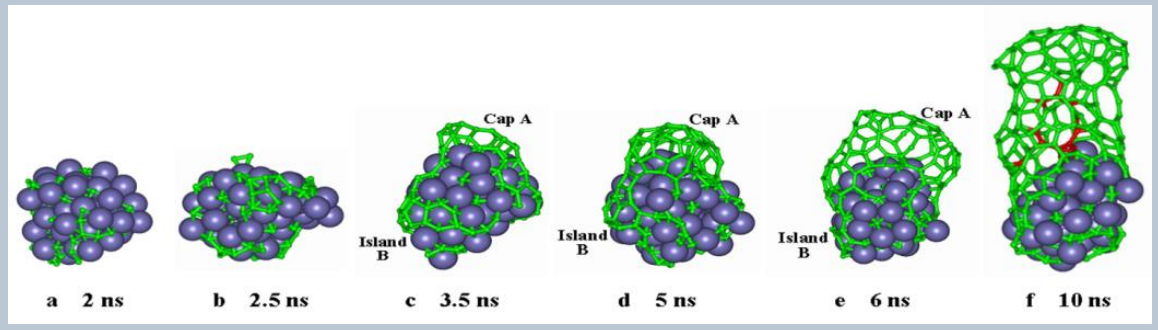

Molecular Simulation

http://www.mb.tn.tudelft.nl/user/dekker/files/carbonnanotubes.pdf

Reaction Parameters

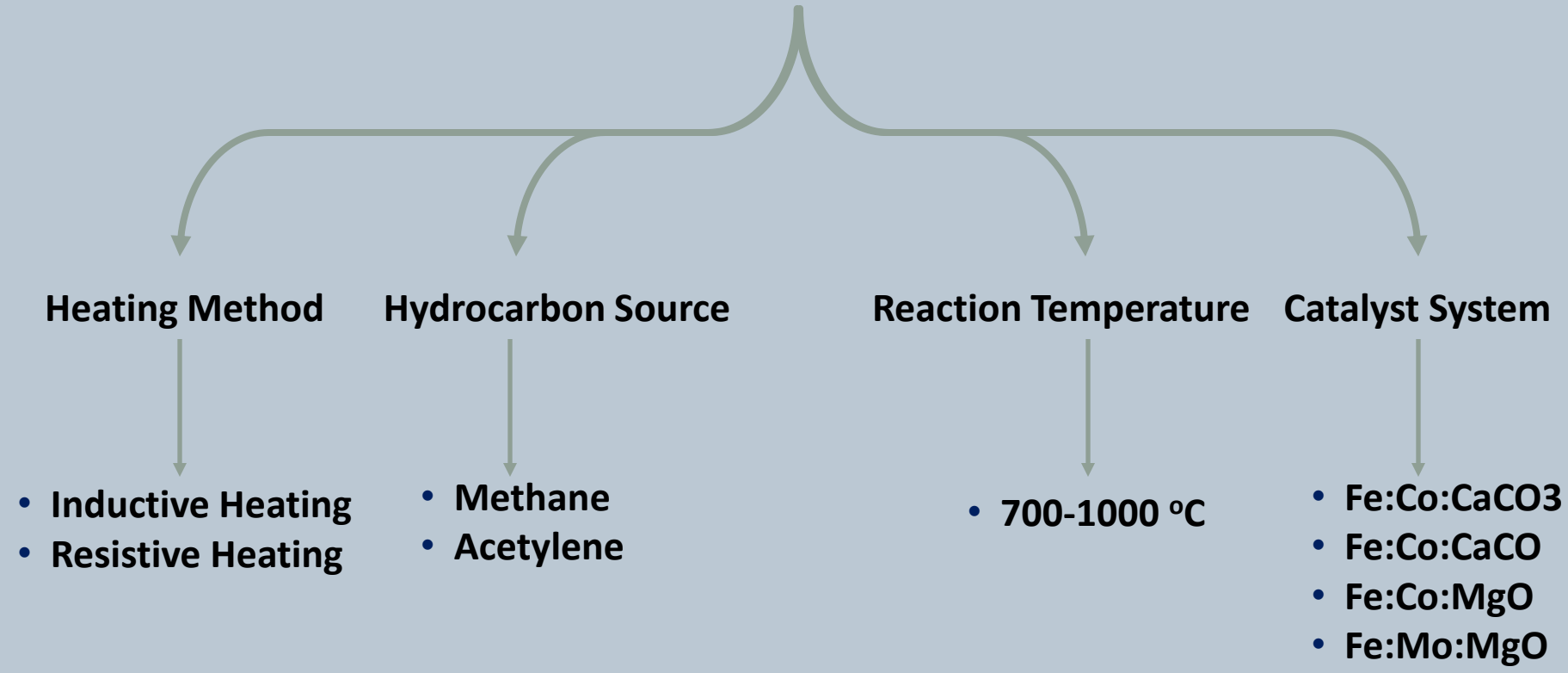

Synthesis of nanotubes with controlled properties

- Diameter distribution
- Yield
- Crystallinity
- Wall number

Growth of Carbon Nanotubes on FeCo/MgO

- Catalyst Composition (Metal to Support ratio)
- Reaction/Synthesis Temperature
- Hydrocarbon Source (CH_4 and C_2H_2)

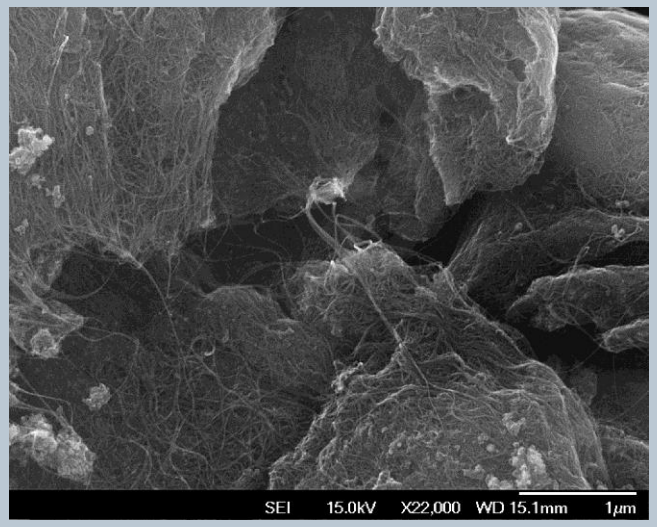

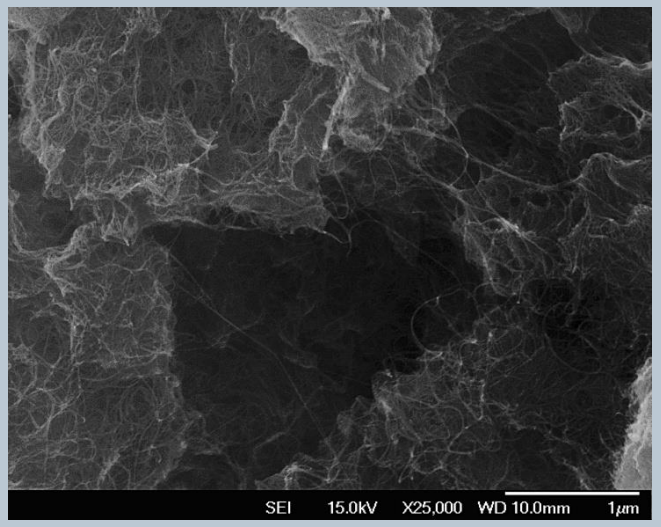

Experimental Details

- **The relative catalyst ratio of Fe to Co (total 5 wt. %) was varied on a MgO support**
- **At 850 °C, CH_4 or C_2H_2 was used for the CNT growth at 40 ml/min and 4.5 ml/min, respectively for 30 minutes.**

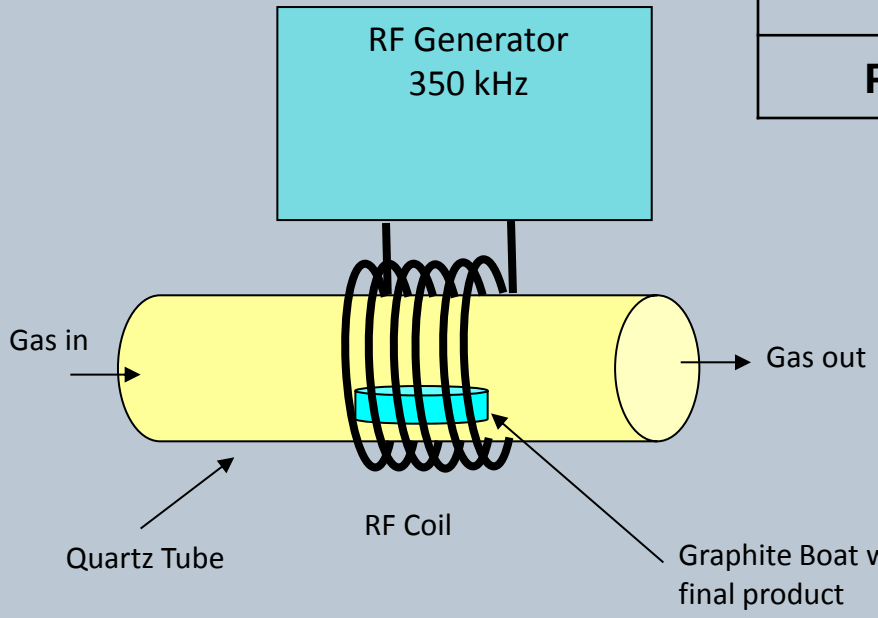

Sample	SA_{BET} (m^2/ g)
Fe:Co (0:5 wt.%)/MgO	16.22
Fe:Co (1.65:3.35 wt.%)/MgO	18.03
Fe:Co (2.5:2.5 wt.%)/MgO	35.45
Fe:Co (3.35:1.65 wt.%)/MgO	18.81
Fe:Co (5:0 wt.%)/MgO	25.52

$$\eta(\%) = \left[\frac{m_{ar} - m_b}{m_{br}} \right] * 100$$

m_{ar} - mass of the sample after the synthesis, m_{br} - mass of the catalyst before the reaction, and m_b - mass of the catalyst after the blank experiment.

E. Dervishi et al., *Particulate Science and Technology: An International Journal, 27(3), 222 -237, 2009.*

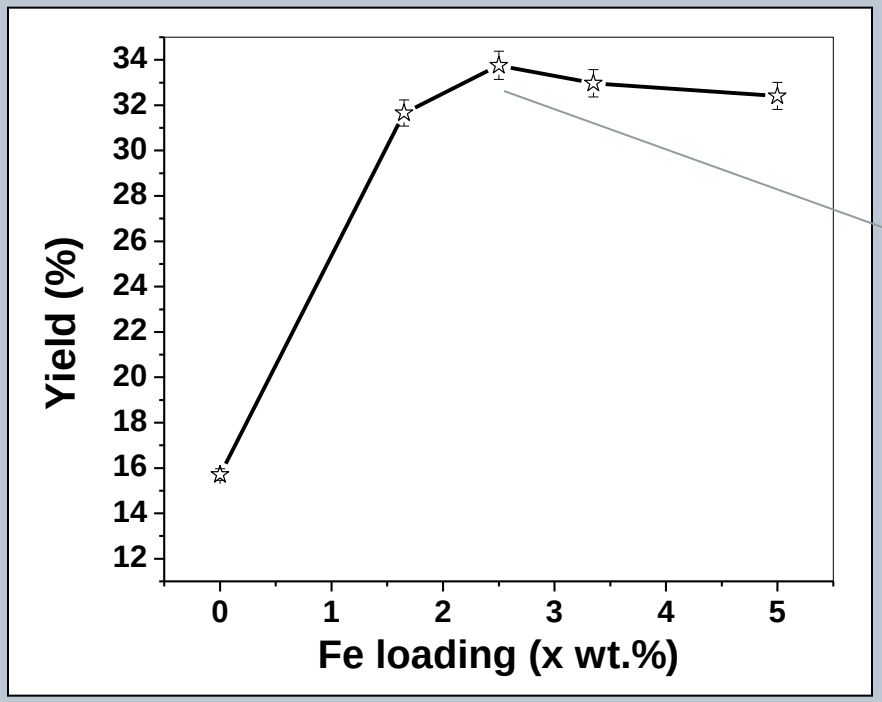

Acetylene

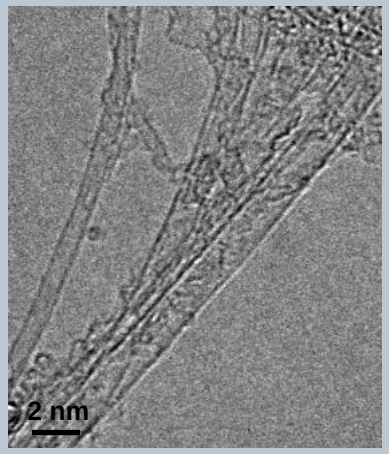

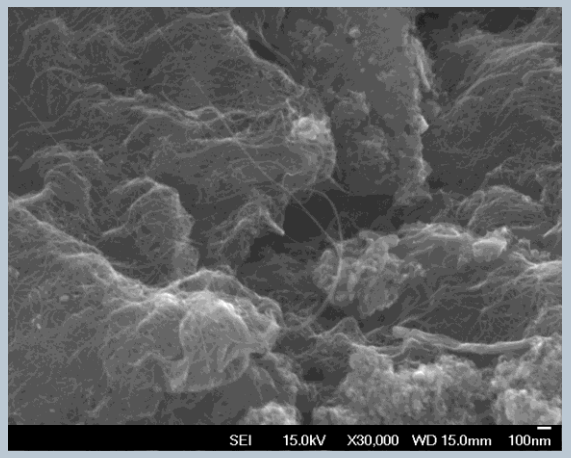

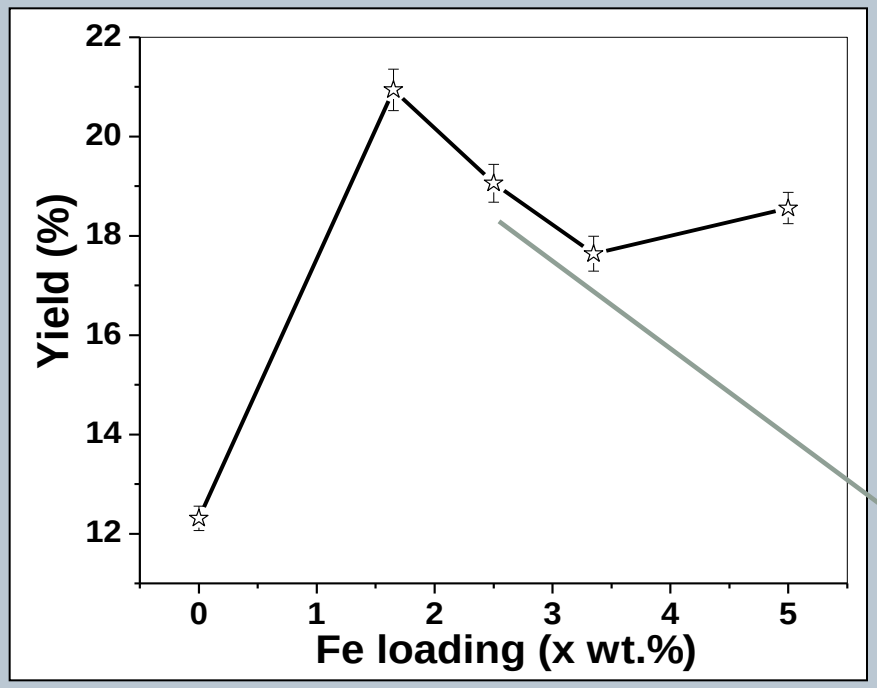

Methane

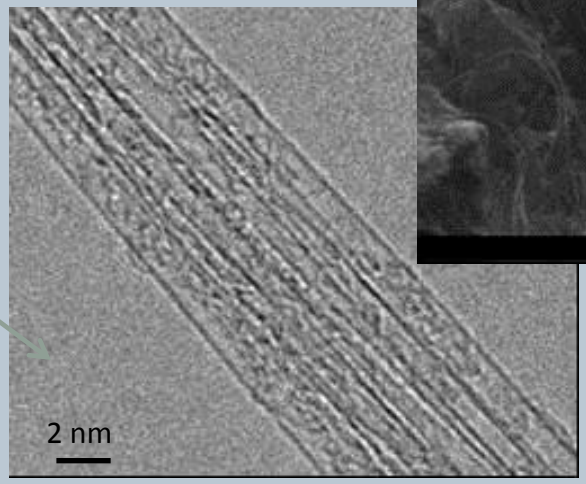

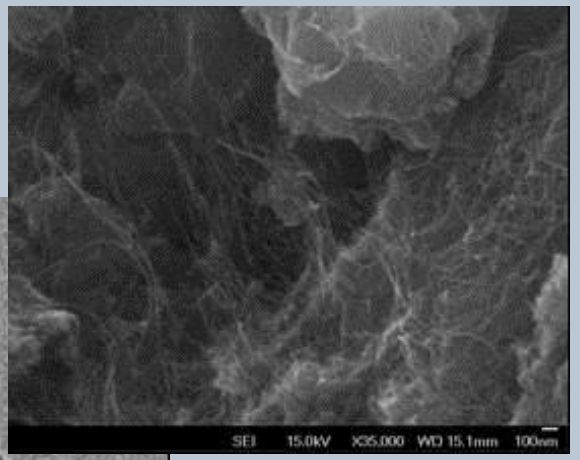

E.Dervishi et al., *Particulate Science and Technology: An International Journal, 27(3), 222 -237, 2009.*

SWCNTs synthesized with CH_4

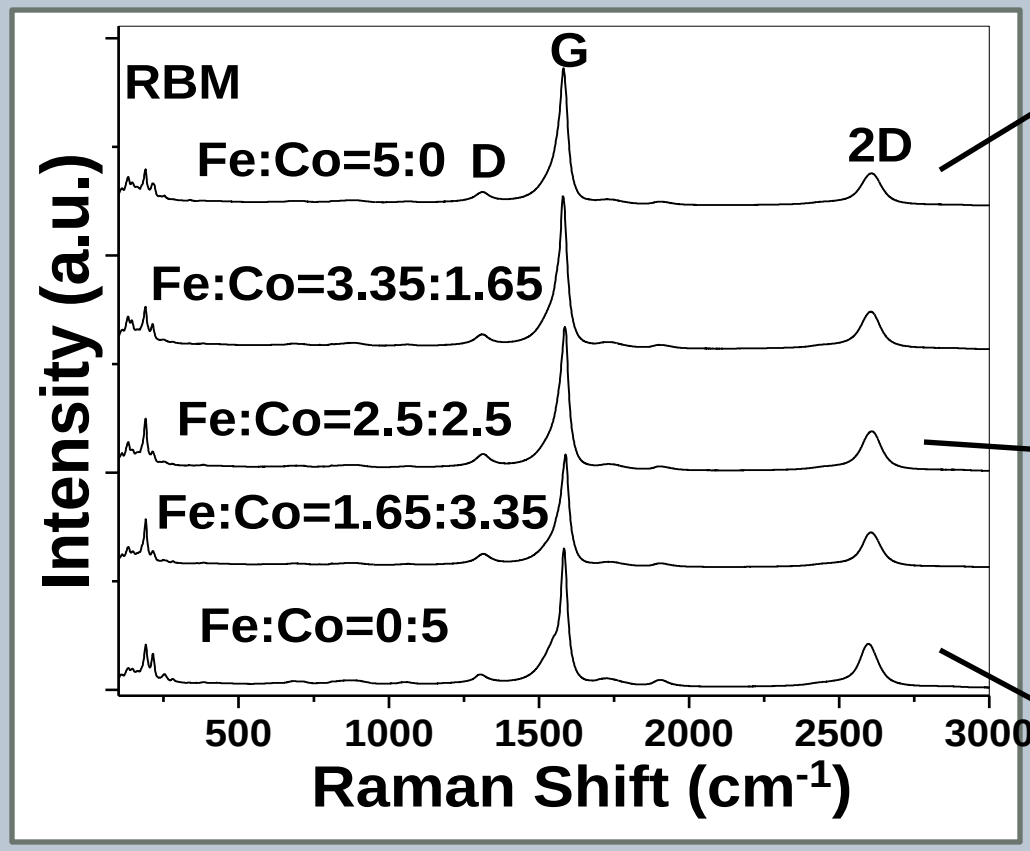

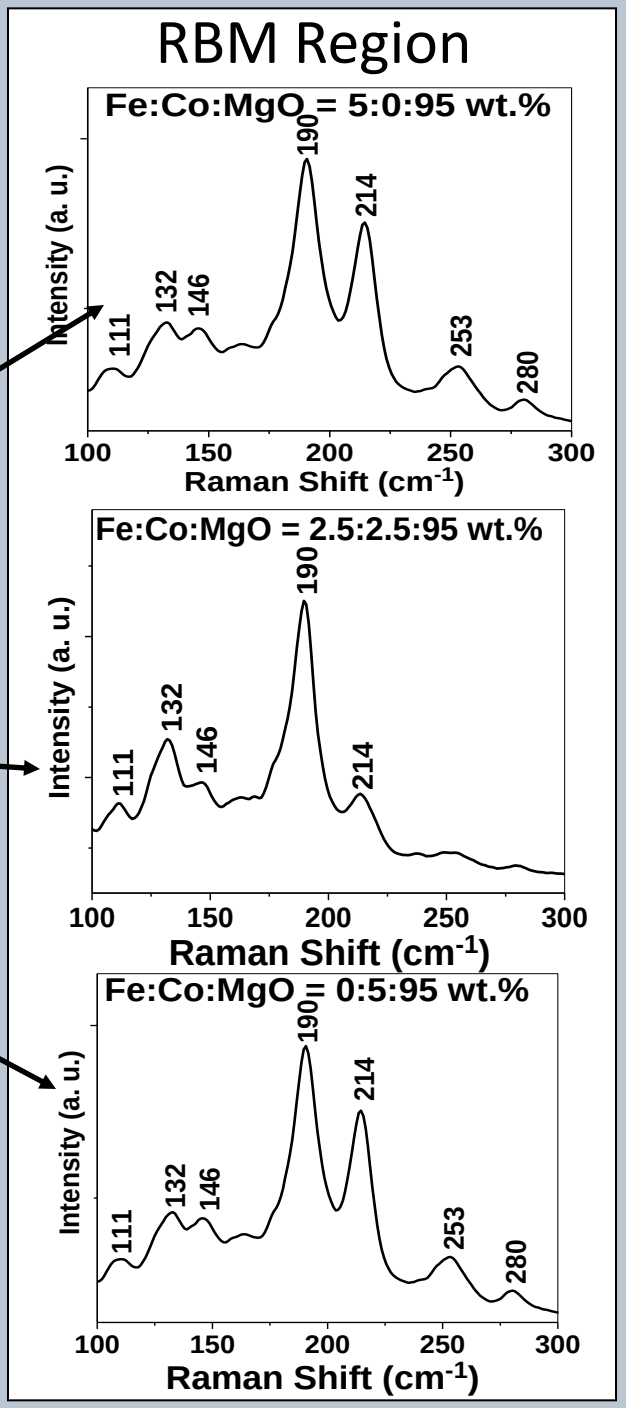

Influence of the reaction temperature using optimized catalyst system

Reaction Parameters

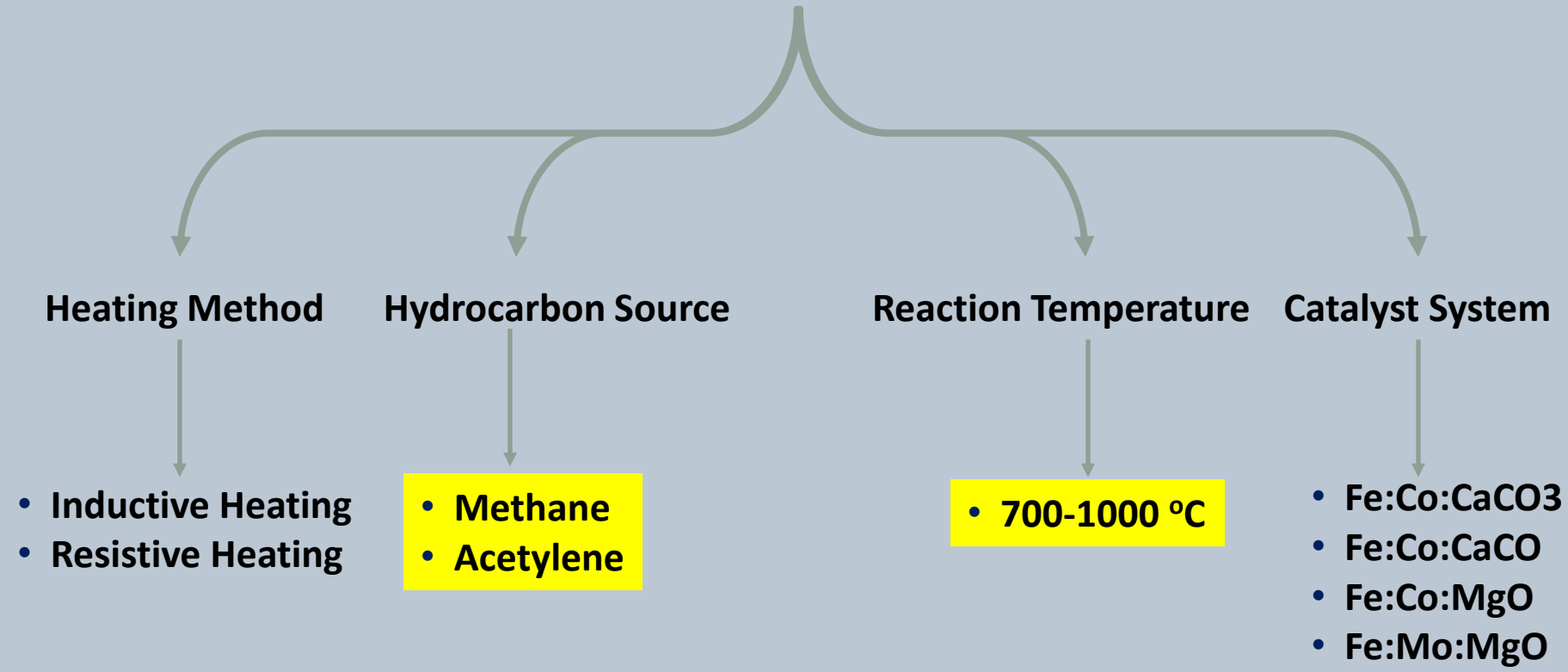

CNTs synthesized with methane at various temperatures

- CNTs were synthesized on the Fe:Co:MgO (2.5:2.5:95 wt.%) catalyst system
- CH_4 was introduced at 40 ml/min for 30 min and the reaction temperature was varied from 700-1000 ^oC, in 50 degree increments.

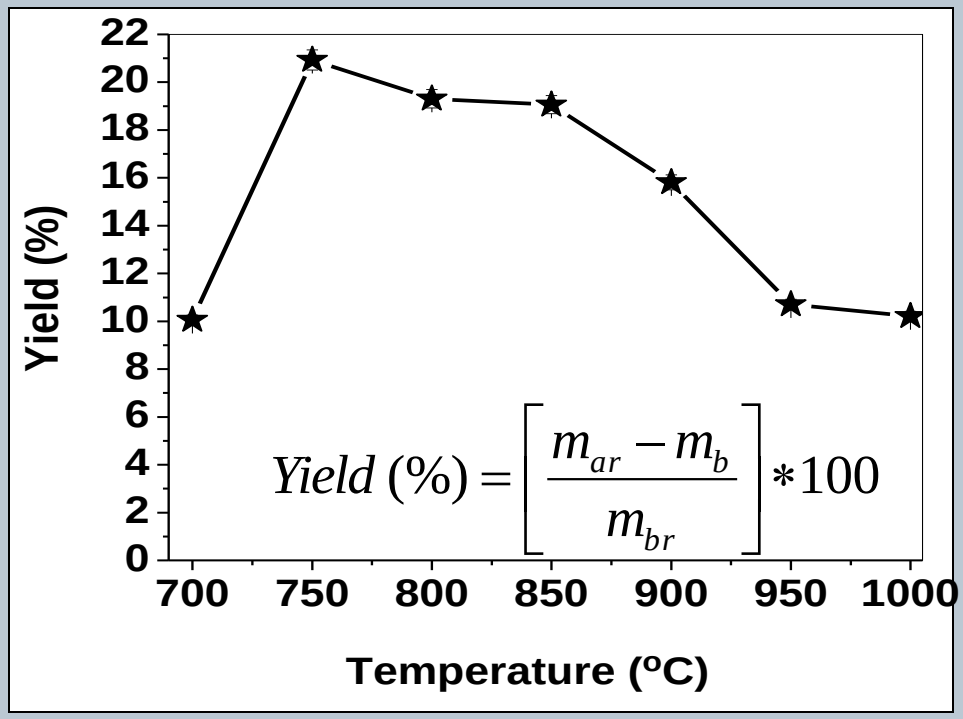

The catalyst system was heat treated for 30 minutes at 800 ^oC and 1000 ^oC for surface area analysis.

Sample	$SA_{BET}(m^2/g)$	Pore Size(nm)
Cat_800	25.45	16.45
Cat_1000	16.21	21.50

E. Dervishi et al., *Journal of Materials Chemistry, 19(19), 3004-3012, 2009. Identified as a 'hot article' and highlighted on the hot papers section.*

STEM analysis of the Catalyst system

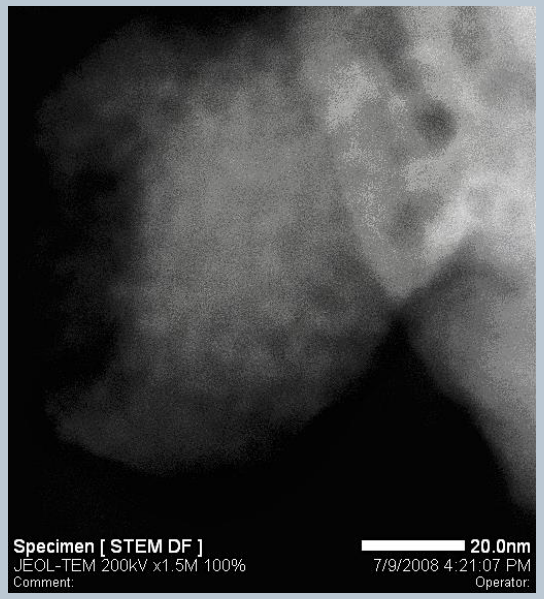

Heat treated at 800 °C

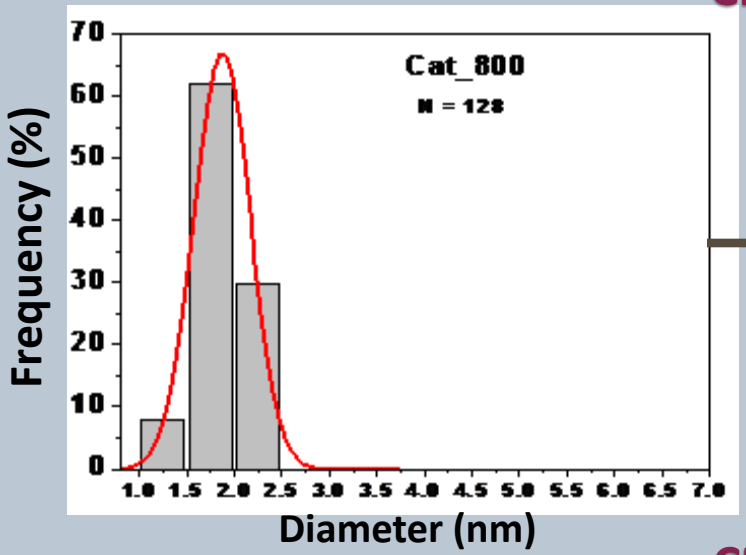

CNTs synthesized at 800 °C

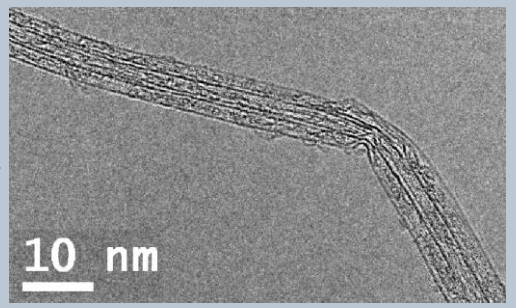

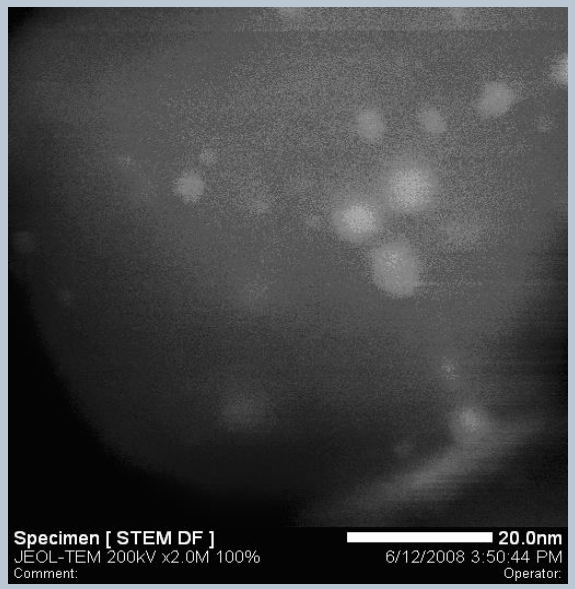

Heat treated at 1000 °C

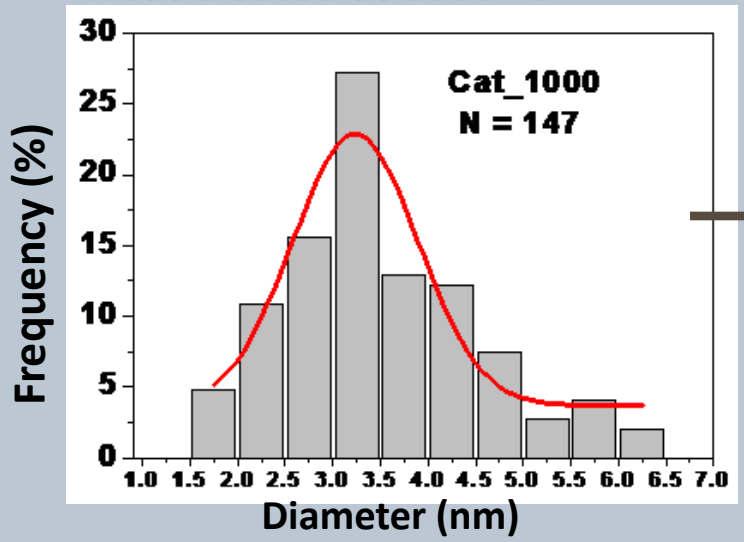

CNTs synthesized at 1000 °C

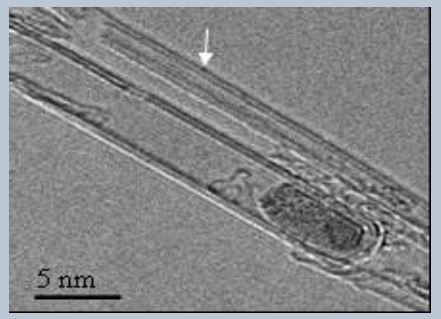

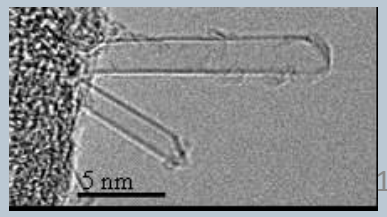

SWCNTs synthesized at 800 °C and 1000 °C

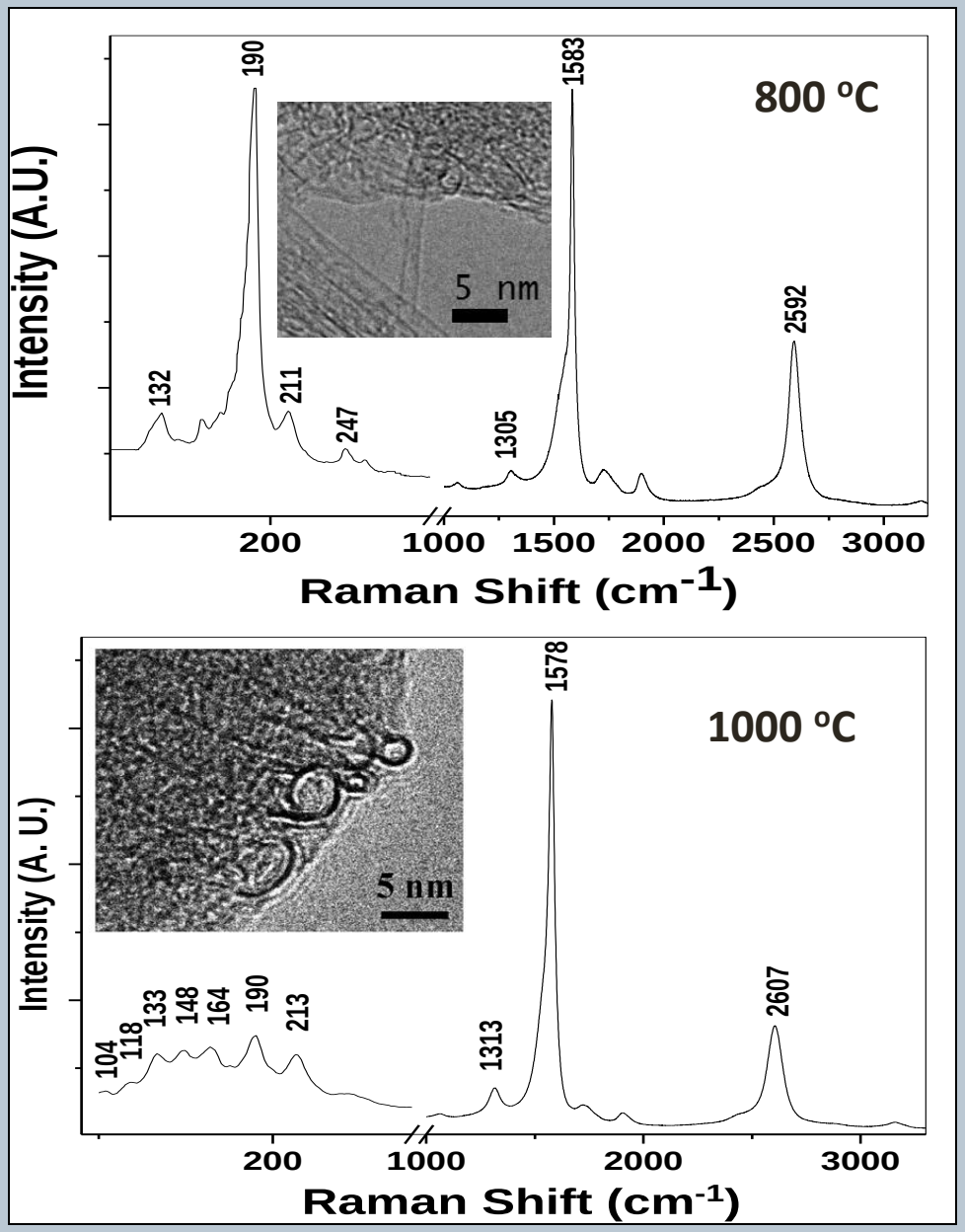

RBM region

Sample	$\lambda_{exc.}$ = 633 nm	$\lambda_{exc.}$ = 514 nm
	d (nm)	
CNT_800	1.91; 1.3; 1.16; 0.98	1.36; 1.23
CNT_1000	2.49; 2.16; 1.9;1.69; 1.51; 1.3; 1.15	1.34; 1.21; 1.004; 0.93; 0.8;

$$\omega_{RBM}\,(cm^{-1}) = \frac{\alpha}{d(nm)} + a$$

CNTs synthesized with acetylene at various temperatures

Fe:Co:MgO (2.5:2.5:95 wt.%) catalytic system

- **Argon was used as a carrier gas at 150 ml/min.**
- **C_2H_2 was utilized for the CNT growth at 4.5 ml/min for 30 minutes.**
- **The reaction temperature was varied from 700-1000 ^oC, in 50 degree increments.**

E. Dervishi et al., *Chemistry of Materials, 21(22), 5491-5498, 2009.*

A versatitle catalyst system (FeCo/MgO) for synthesis of nanotubes and graphene

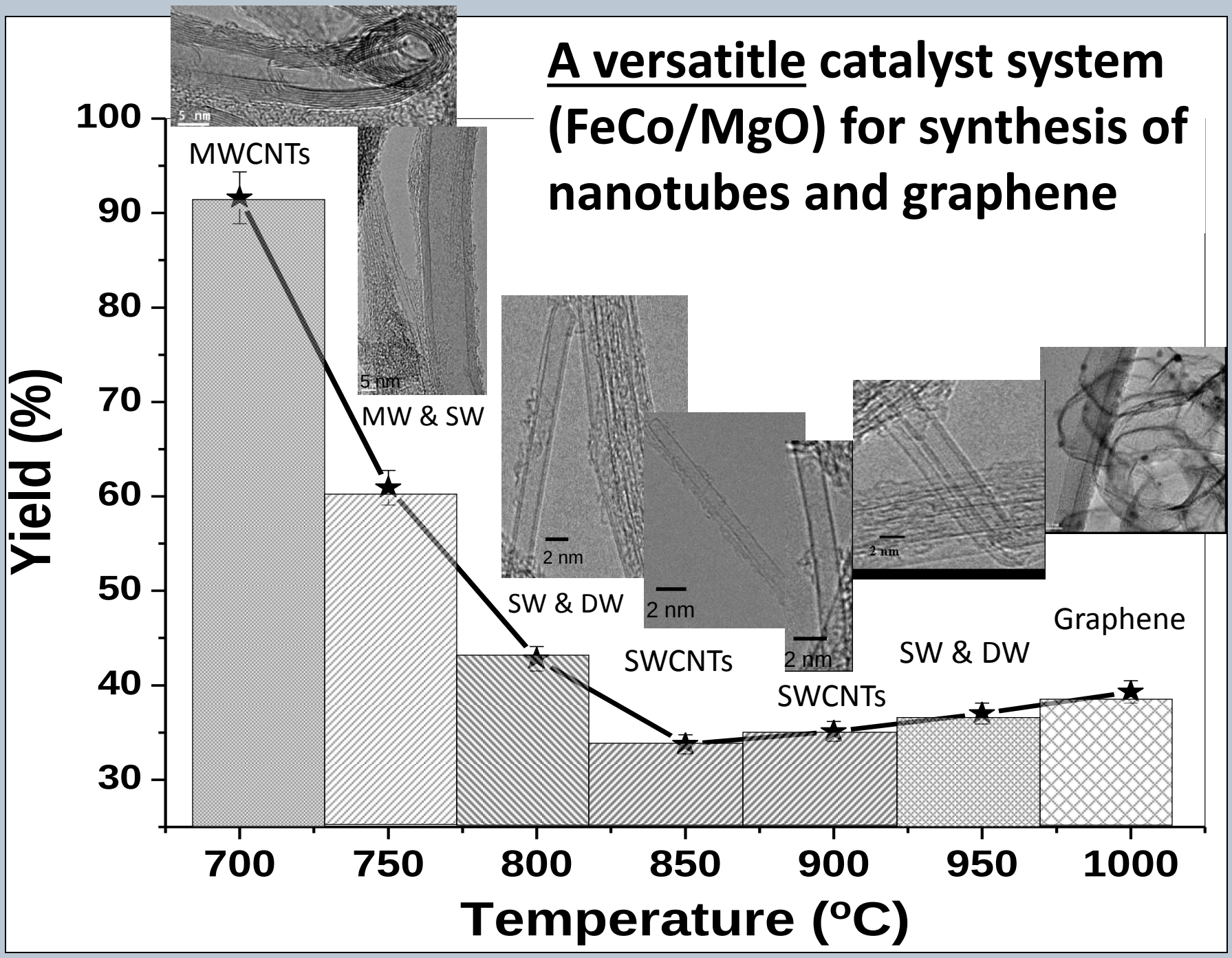

Synthesis of nano-graphene

Reaction Parameters

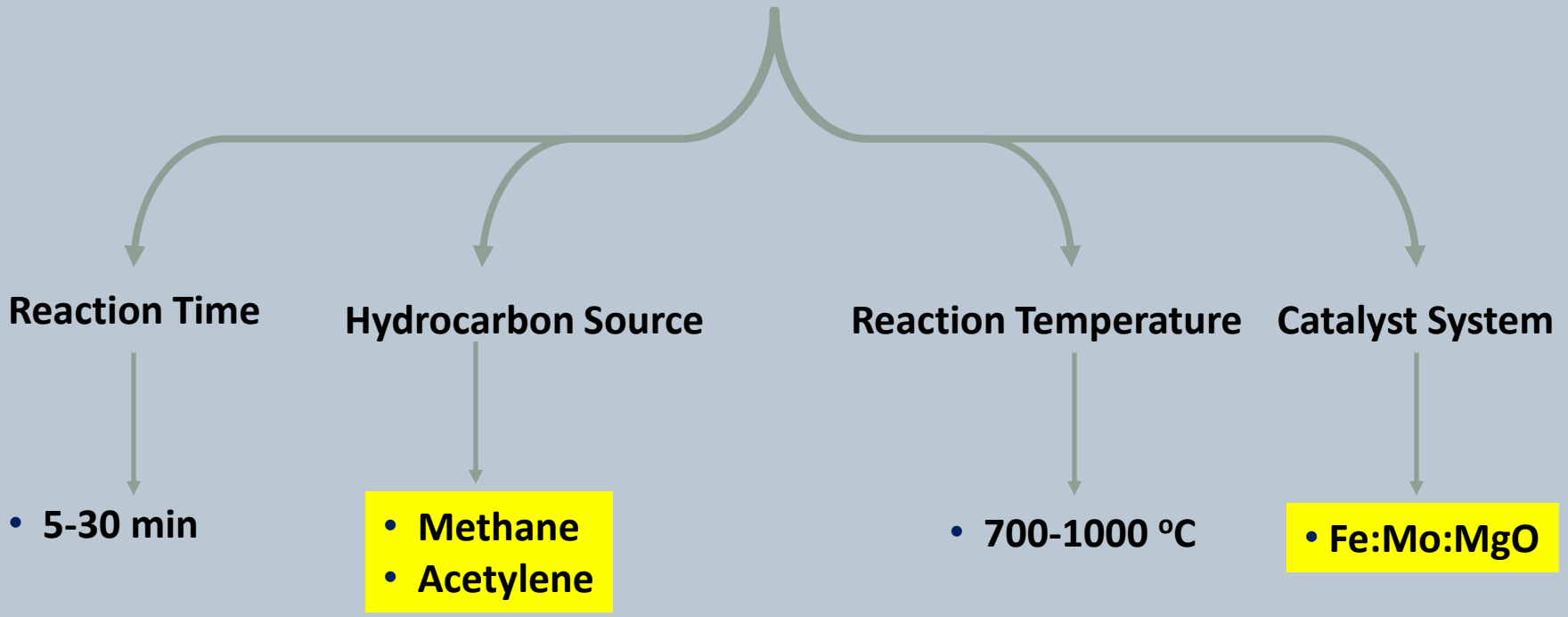

Large Scale Graphene Synthesis

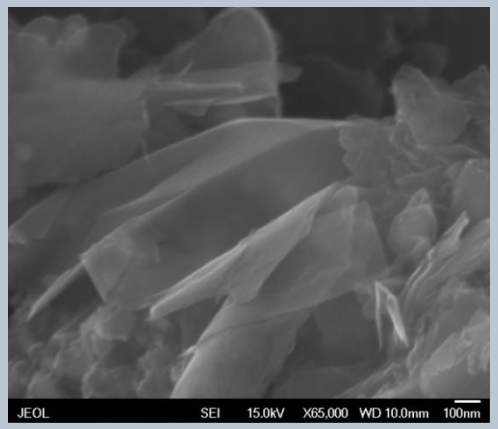

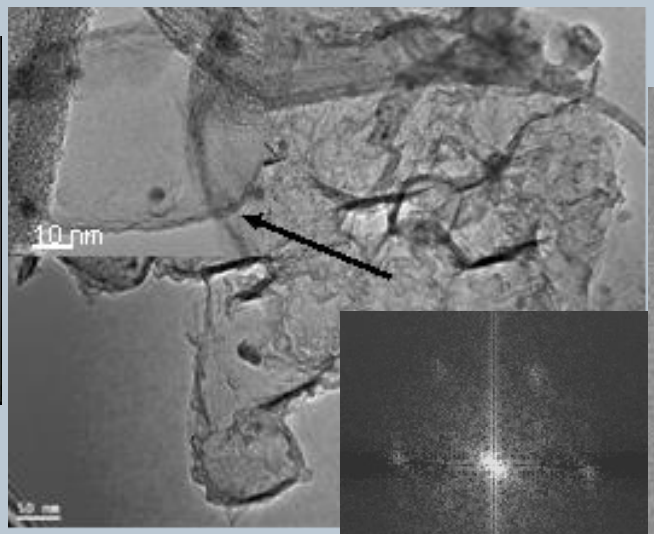

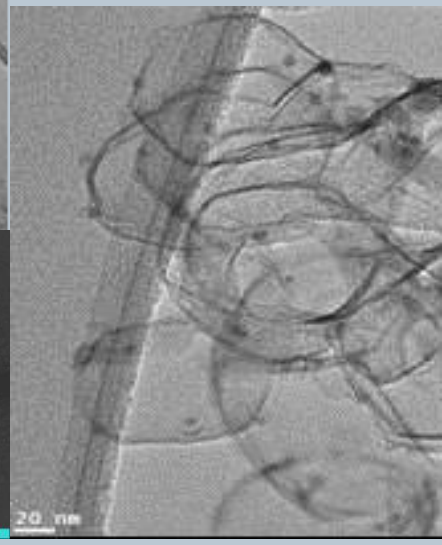

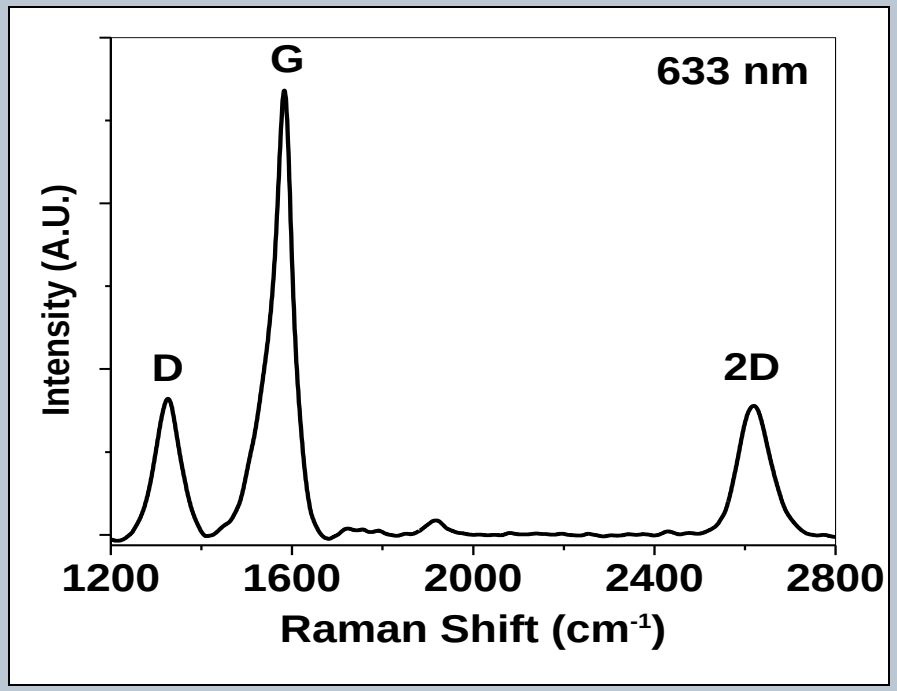

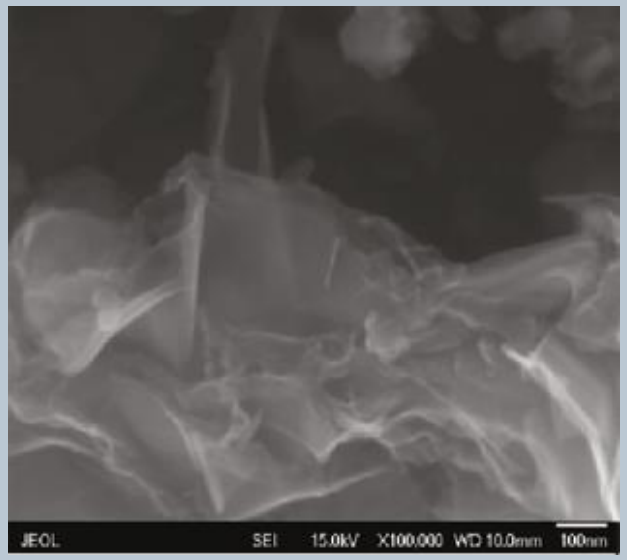

E. Dervishi et al., *Chemical Communications, 27, 4061-4063, 2009.*

Few-layer nano-graphene structures synthesized on a multifunctional Fe:Mo:MgO catalyst system

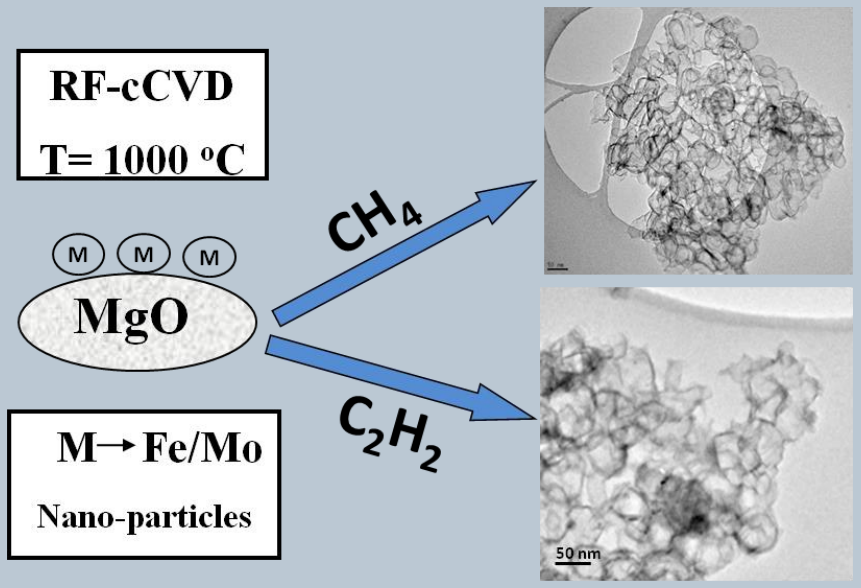

Fe:Mo:MgO (1:0.1:110 molar ratio) catalyst system

Sample Name	$SA_{BET}(m^2/g)$
G_M	**176.75**
G_A	**295.7**

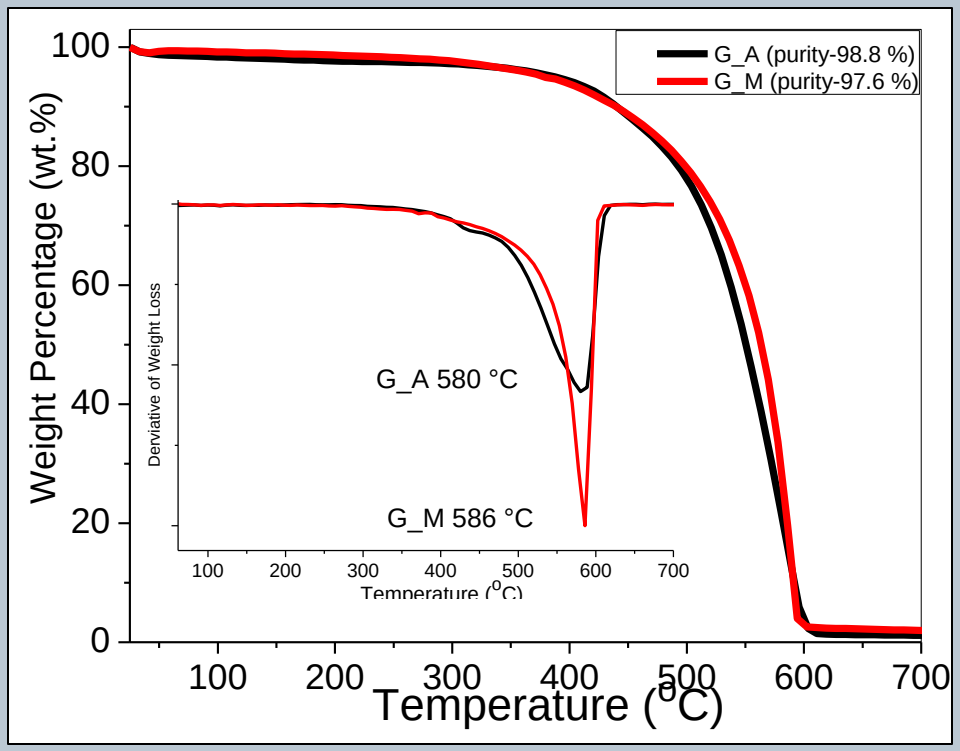

Thermogravimetrical analysis of the graphene sheets synthesized with methane ("G_M") and acetylene ("G_A").

E. Dervishi et al., *Journal of Materials Science, 47 (4), 1910-1919, 2012.*

The role of Hydrocarbon Source

Methane

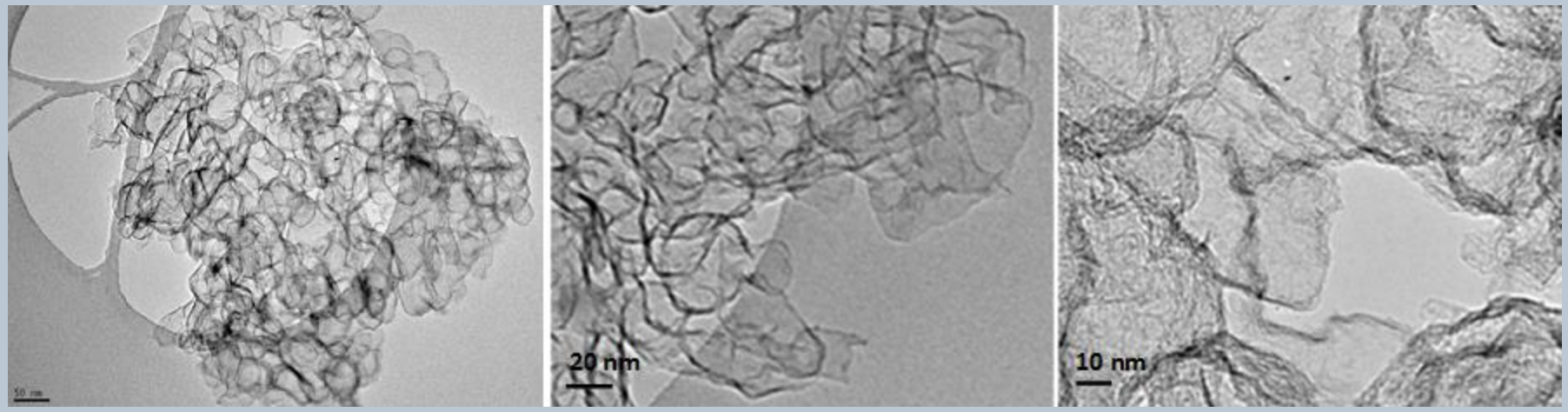

Acetylene

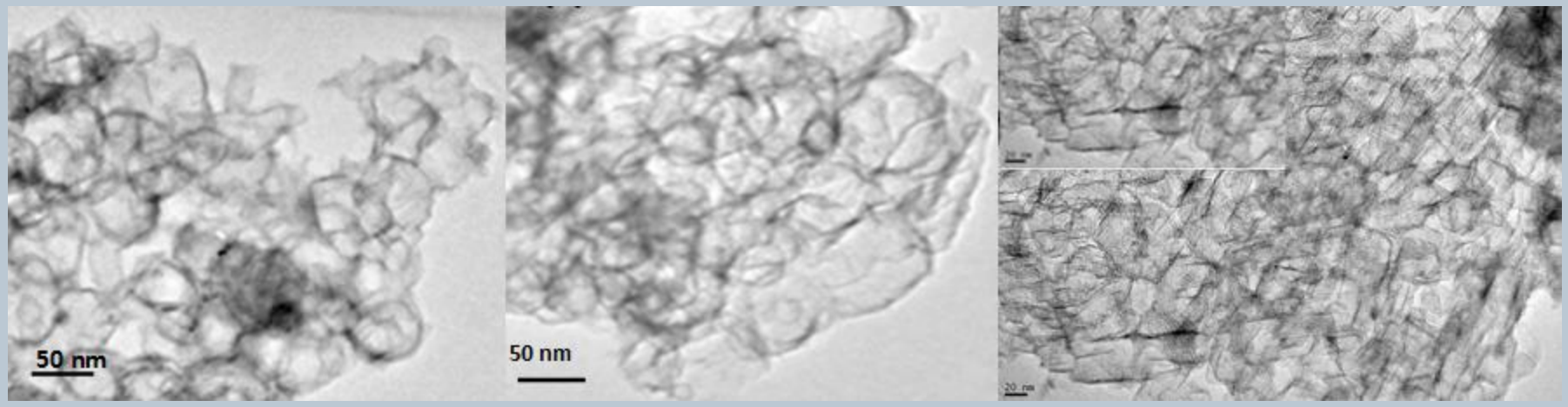

Reaction time (acetylene as the hydrocarbon source)

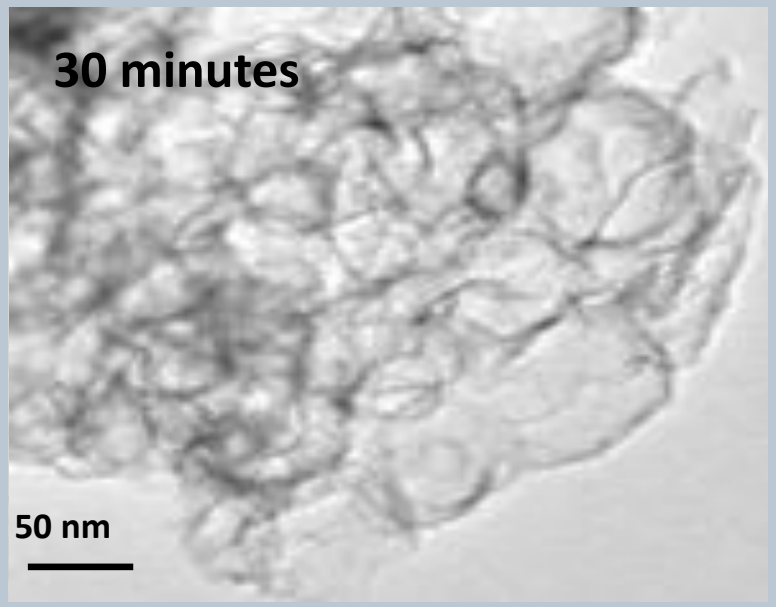

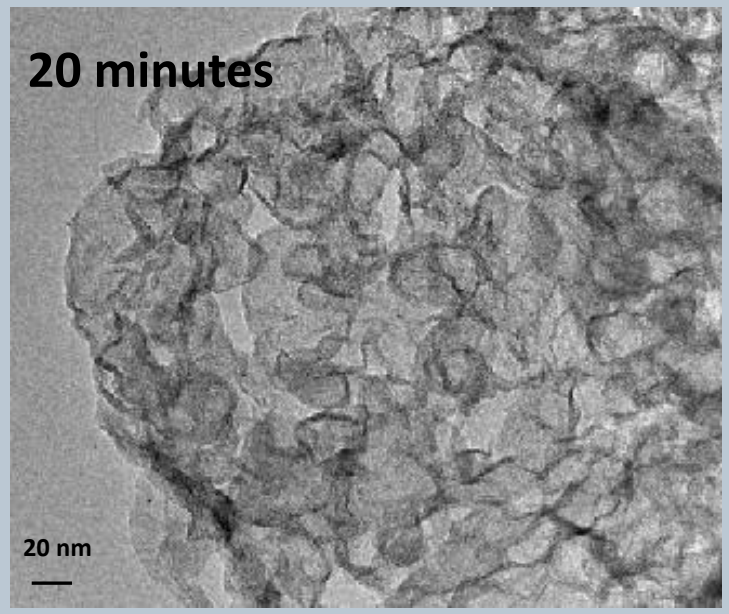

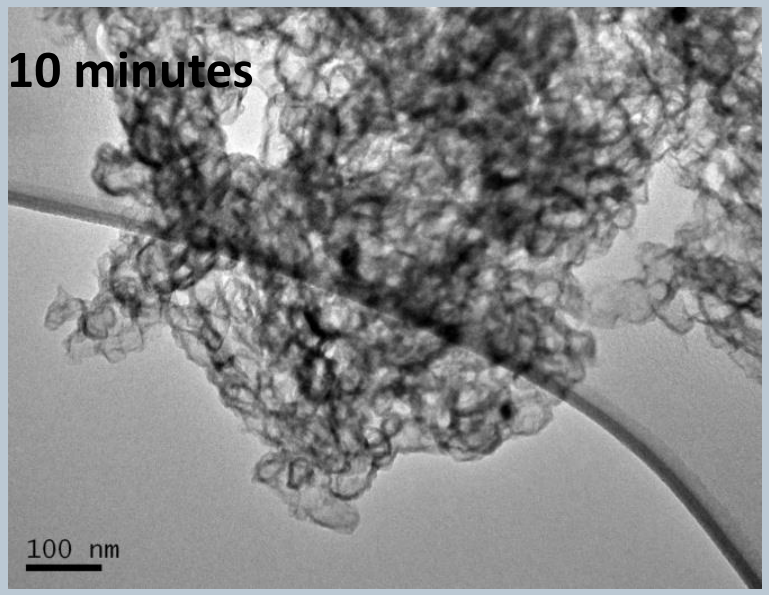

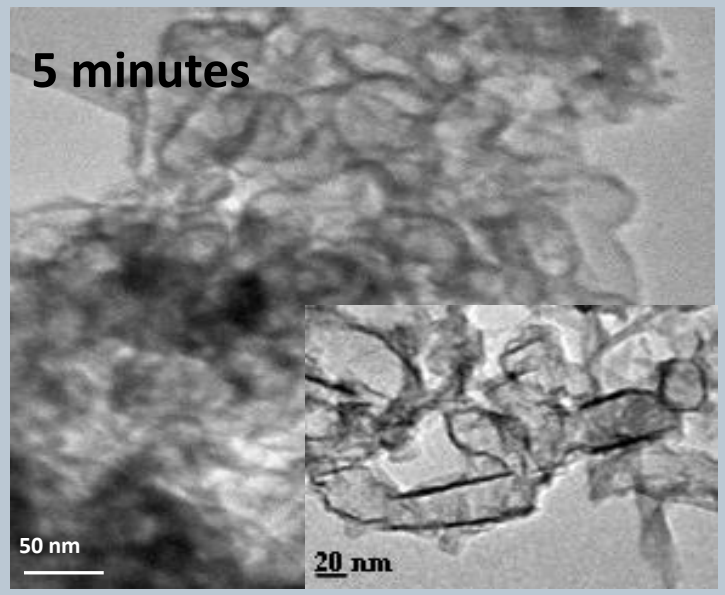

E. Dervishi et al., *Journal of Materials Science, 47 (4), 1910-1919, 2012.*

Reaction Parameters

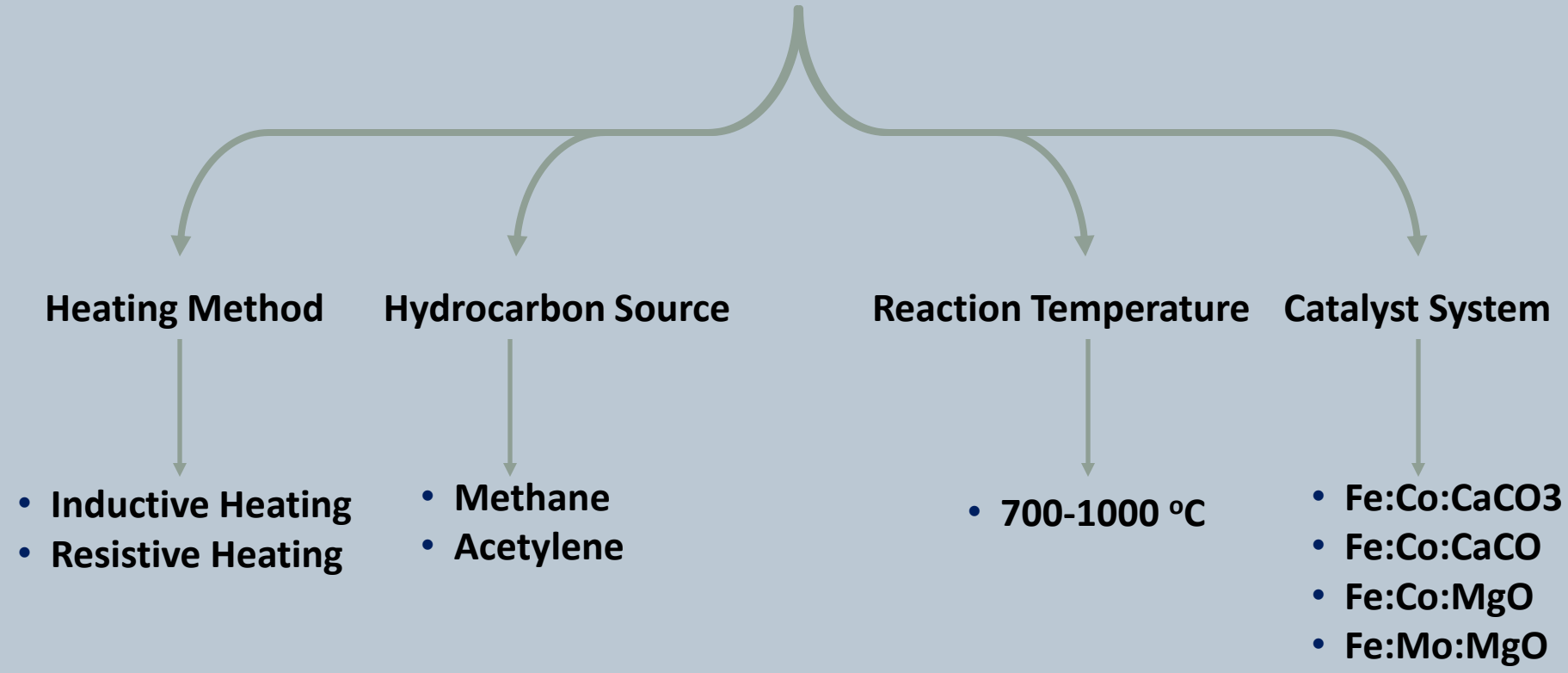

Synthesis of nanotubes with controlled properties

- Diameter distribution
- Yield
- Crystallinity
- Wall number

Large area graphene

- Large-area graphene sheets were grown on Cu foil (Alfa Aesar Po #: 46365) via chemical vapor deposition.
- The foil was first heated up to 950 °C under an Argon/Hydrogen mixture at 200 sccm for 90 minutes. Next, the furnace temperature was raised to 1020 °C and methane was introduced at 15 sccm for 20 min, at a total pressure of 10 Torr. Finally, the sample was rapidly cooled down under an Argon/Hydrogen mixture.

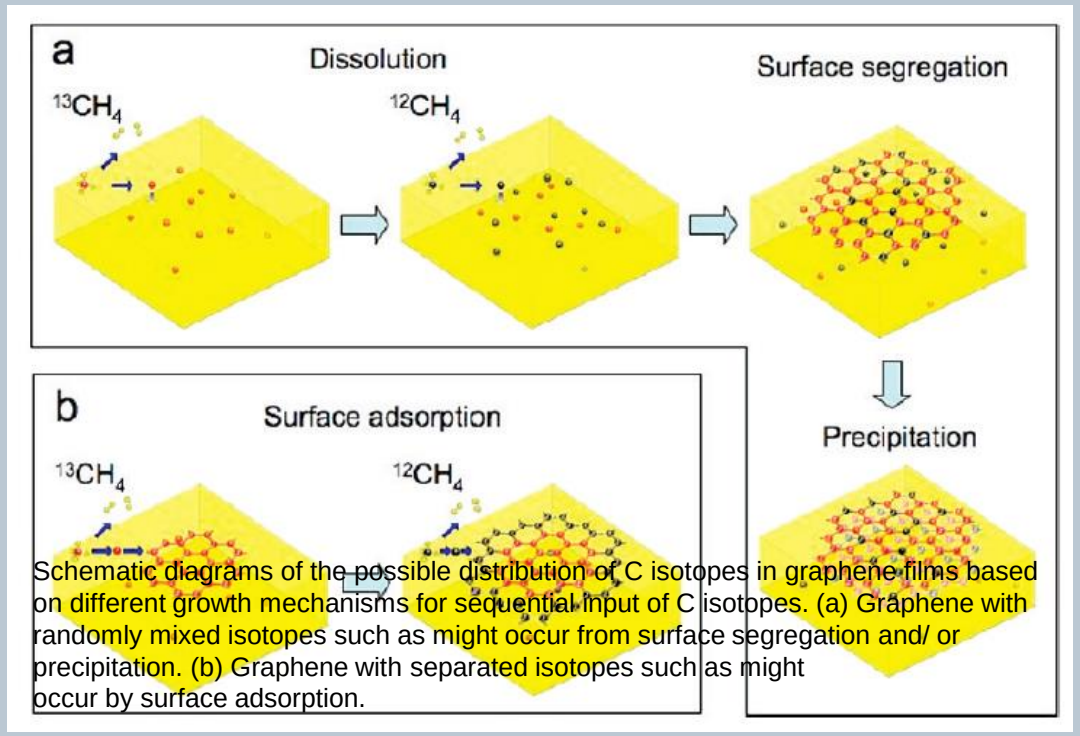

Schematic diagrams of the possible distribution of C isotopes in graphene films based on different growth mechanisms for sequential input of C isotopes. (a) Graphene with randomly mixed isotopes such as might occur from surface segregation and/ or precipitation. (b) Graphene with separated isotopes such as might occur by surface adsorption.

Evolution of Graphene Growth on Ni and Cu by Carbon Isotope Labeling Xuesong Li,† Weiwei Cai,† Luigi Colombo,*,‡ and Rodney S. Ruoff*,† *Nano Lett.,* Vol. 9, No. 12, 2009

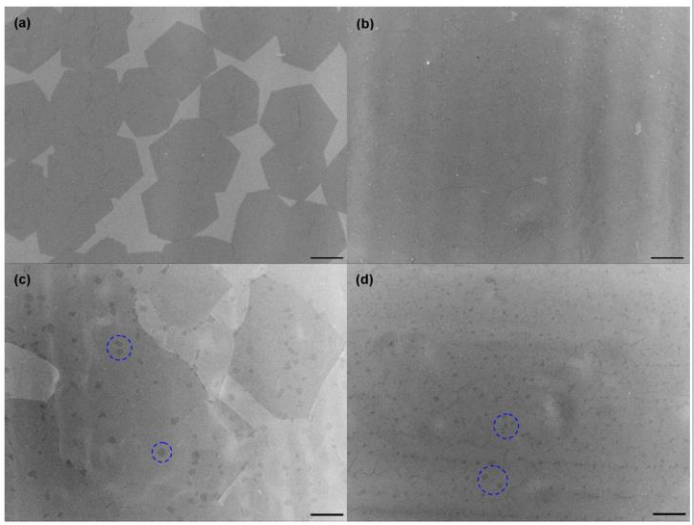

SEM images of CVD graphene on Cu. (a) 5 ppm CH4 for 60 min. (b) 10 ppm CH4 for 60 min. (c) 20 ppm CH4 for 30 min. (d) 30 ppm CH4 for 20 min. Uncovered Cu surface is brighter (images (a) and (b)). Multi-layer graphene domains are darker (some are highlighted by dashed blue circles in images (c) and (d)). The scale bars are 10 m.

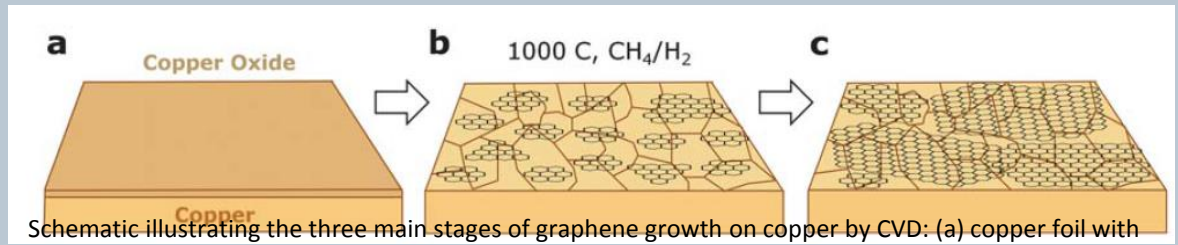

Schematic illustrating the three main stages of graphene growth on copper by CVD: (a) copper foil with native oxide; (b) the exposure of the copper foil to CH4/H2 atmosphere at 1000 C leading to the nucleation of graphene islands; (c) enlargement of the graphene flakes with different lattice orientations.

A review of chemical vapour deposition of graphene on copper† J. Mater. Chem., 2011, 21, 3324–3334 Cecilia Mattevi,*a Hokwon Kima and Manish Chhowalla

Control of thickness uniformity and grain size in graphene films for transparent conductive electrodes Wei Wu, Qingkai Yu, Peng Peng, Zhihong Liu, Jiming Bao and Shin-She

Reaction Parameters

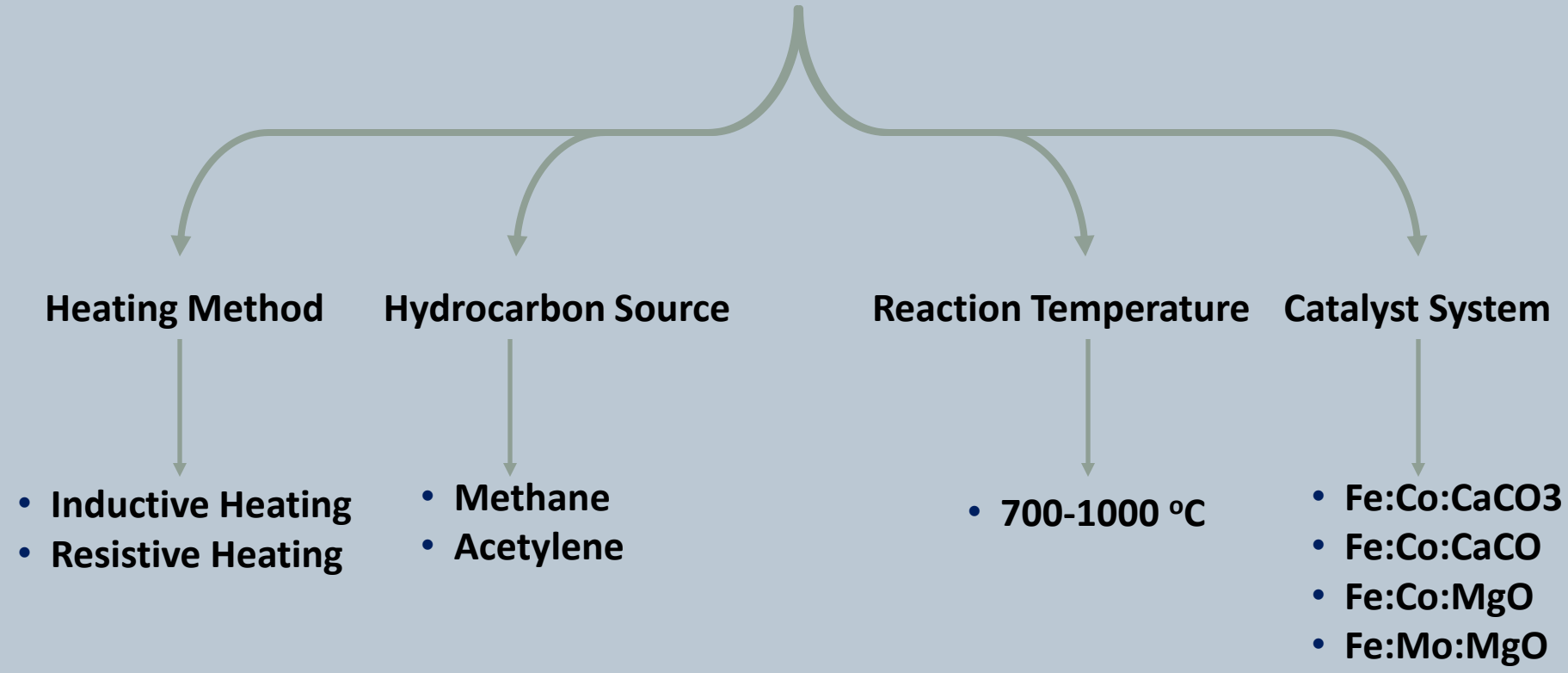

Synthesis of nanotubes with controlled properties

- Diameter distribution
- Yield
- Crystallinity
- Wall number

Catalytic Conversion of Metal Decorated Graphene into Carbon Nanotubes at Low Temperatures

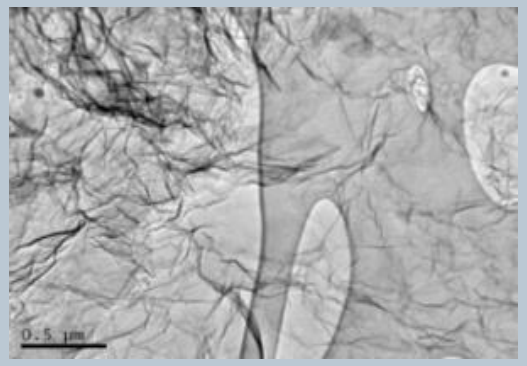

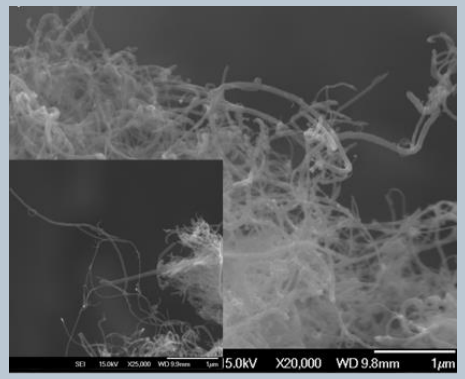

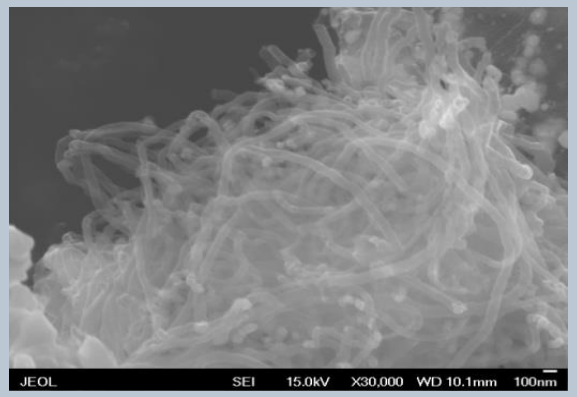

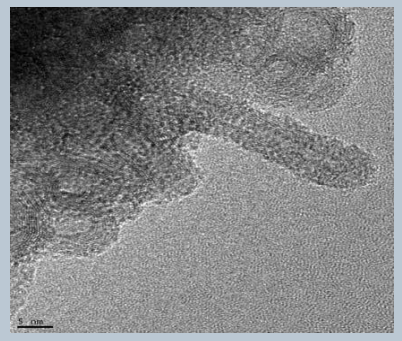

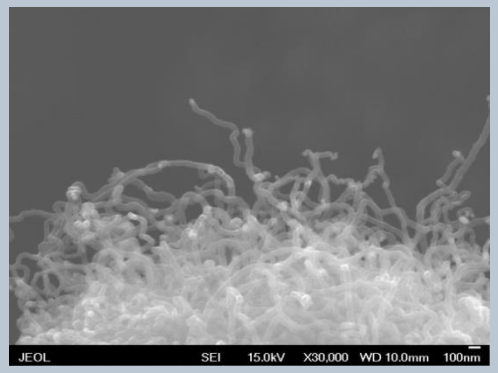

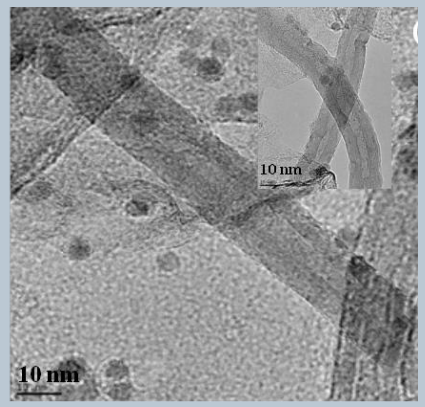

Au-decorated Graphene

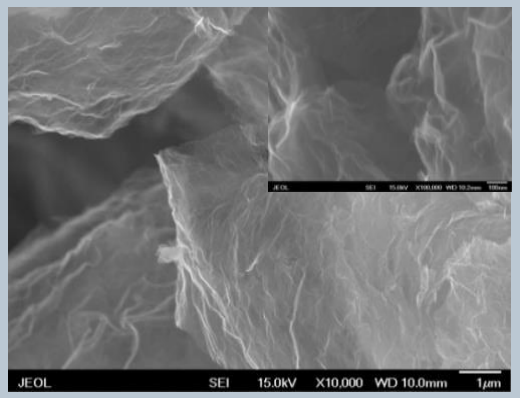

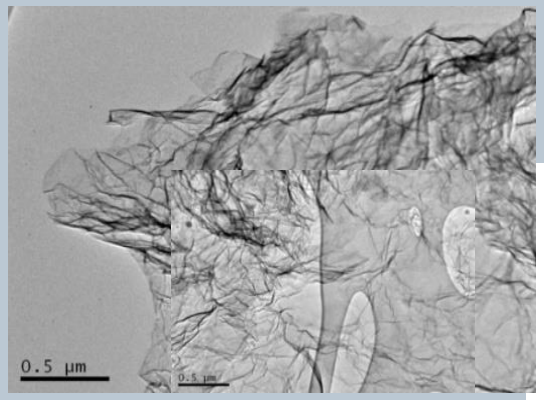

Few- layer large area commercially available graphene

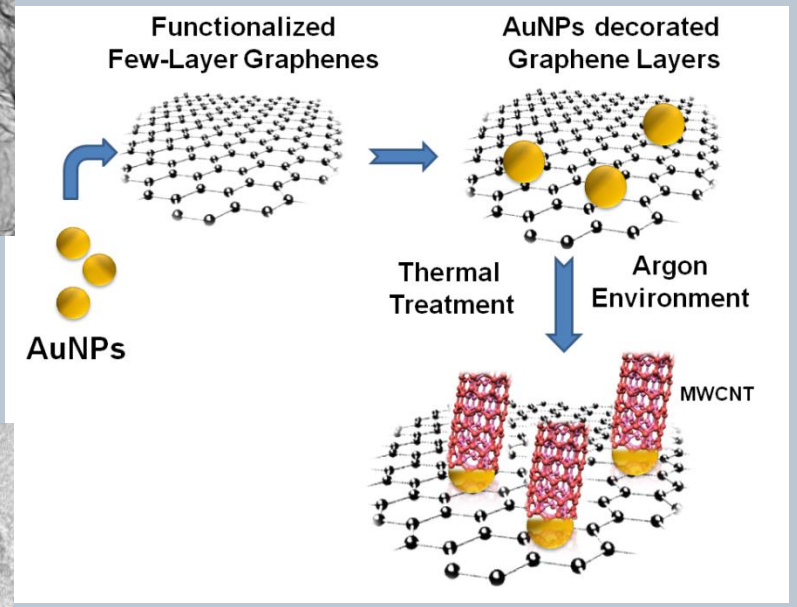

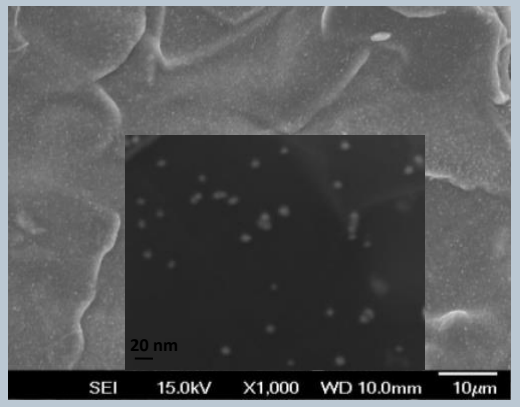

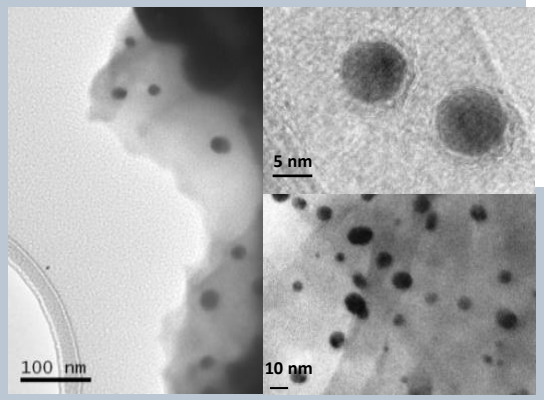

Graphene sheets decorated with Au nano-particles

E. Dervishi et al., ACS Nano, 6 (1), 501-511, 2012. Highlighted with an "In Nano" write-up in the January issue of ACS Nano entitled “Very Cool: Converting Graphene to Carbon Nanotubes at 500 °C” http://pubs.acs.org/doi/abs/10.1021/nn2050328

Synthesis with no hydrocarbon feed gas

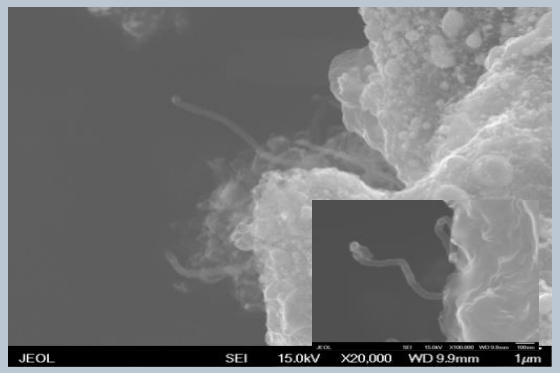

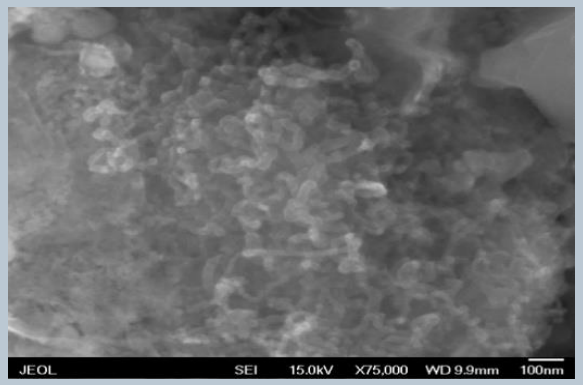

500 ˚C

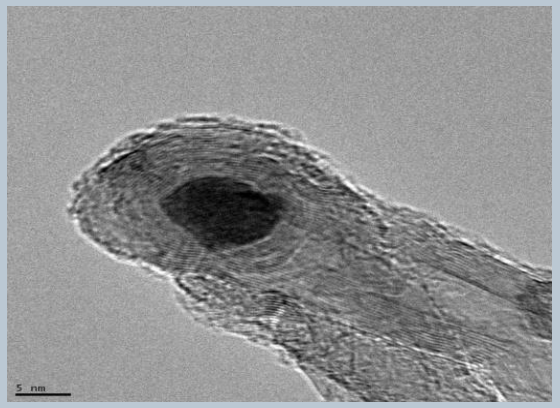

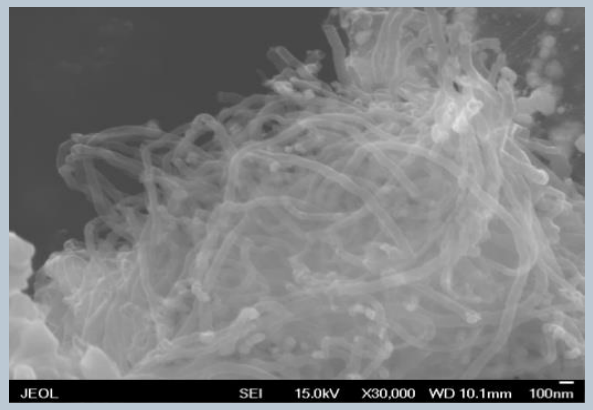

600 ˚C

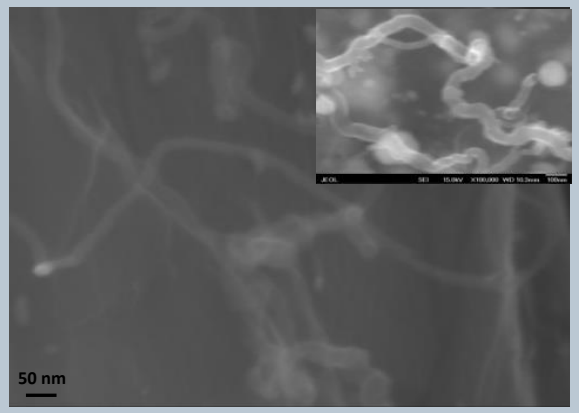

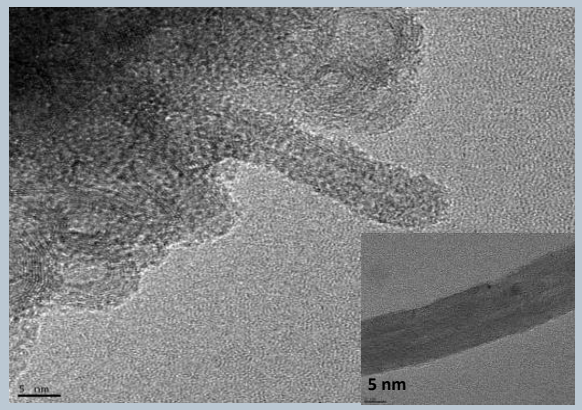

650 ˚C

Synthesis at 650 ˚C with addition of acetylene

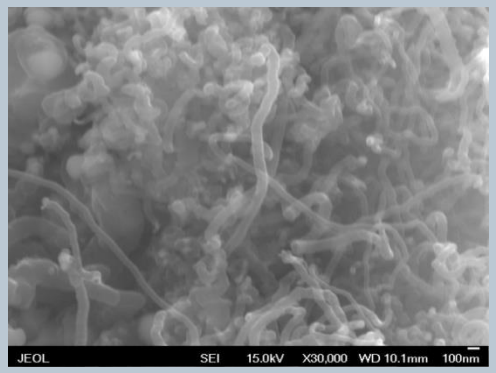

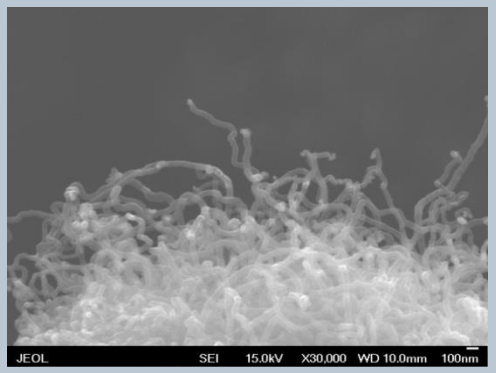

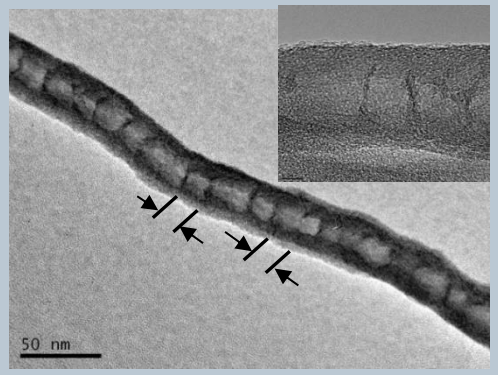

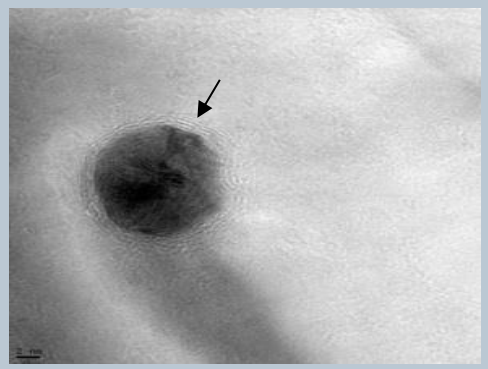

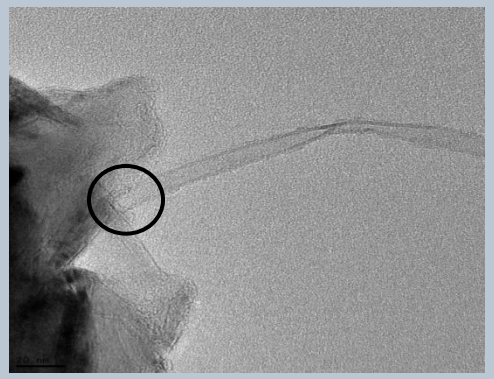

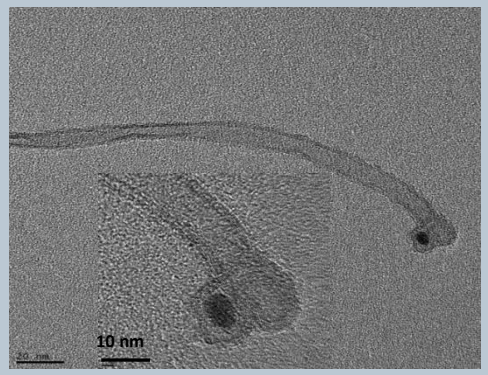

Thermo-gravimetrical analyses

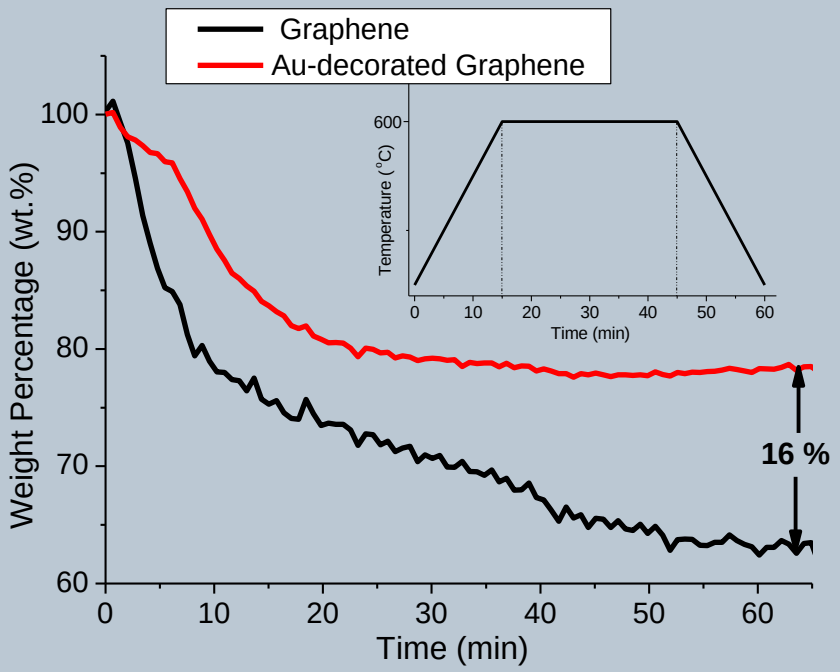

TGA curve of graphene and the decorated graphene heated to 600 ˚C under Ar, respectively. The inset presents the temperature versus time set up for every experiment in the TGA furnace.

E. Dervishi et al., ACS Nano, 6 (1), 501-511, 2012. Highlighted with an "In Nano" write-up in the January issue of ACS Nano entitled “Very Cool: Converting Graphene to Carbon Nanotubes at 500 °C” http://pubs.acs.org/doi/abs/10.1021/nn2050328

Iron oxide-graphene nano-structural system

Graphene sheets decorated with 5 nm iron oxide nano-particles

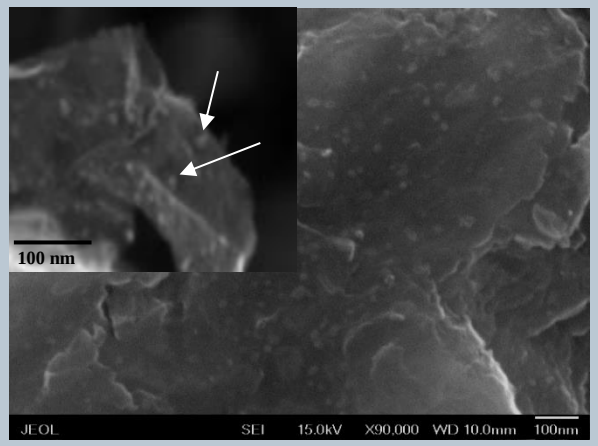

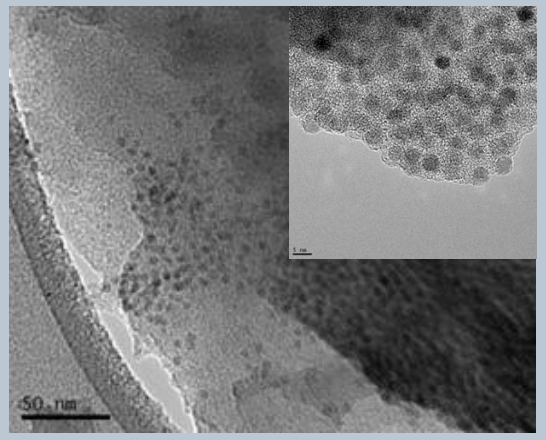

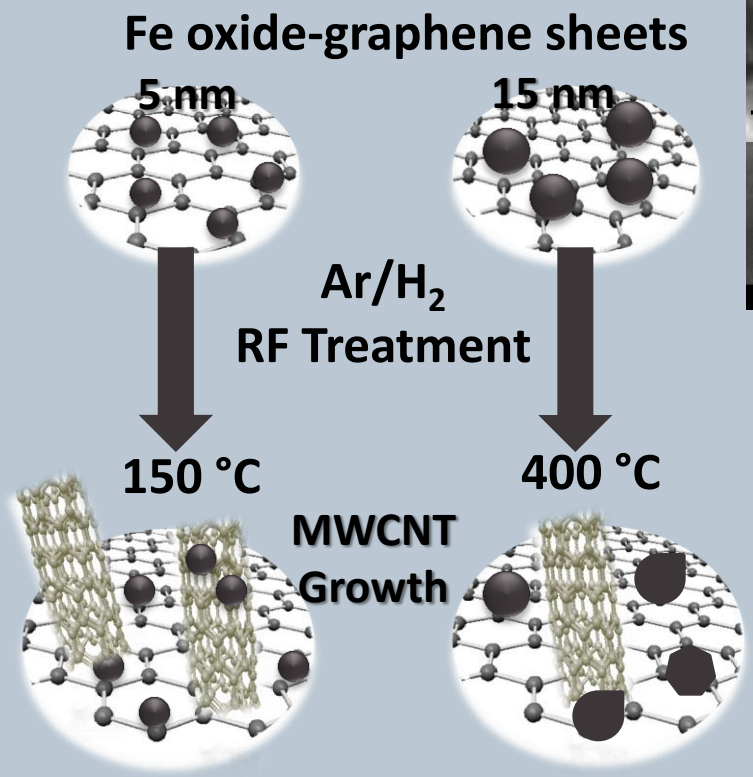

STEM image of the iron oxide nano-particles decorating the graphene structures and EDS map of Fe-K signals.

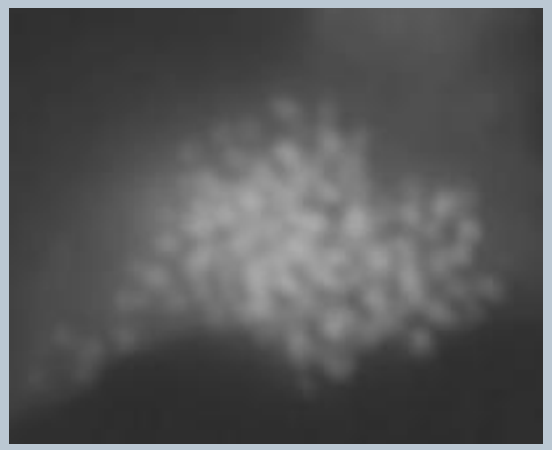

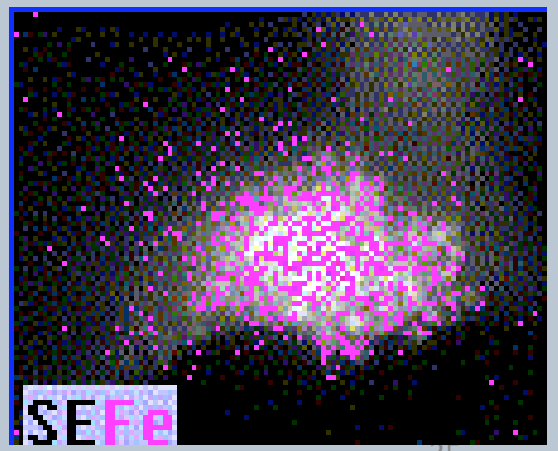

E. Dervishi at al., Journal of Catalysis, 299, 307-315, 2013.

Reaction in an Ar/H_2 environment with no hydrocarbon feed gas

External Furnace

150 ˚C

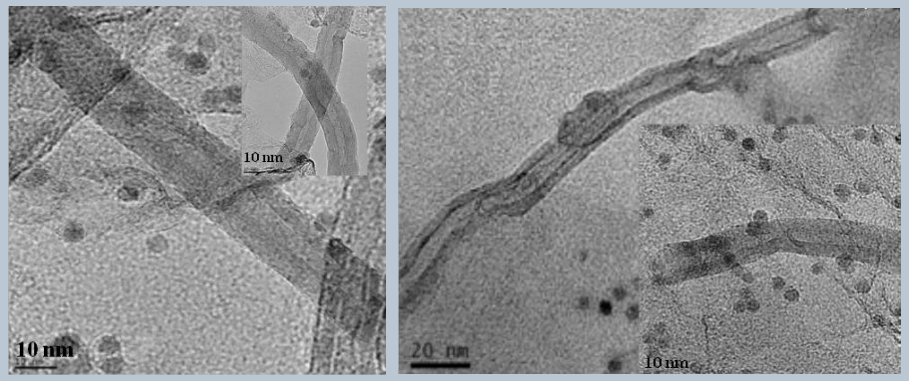

200 ˚C

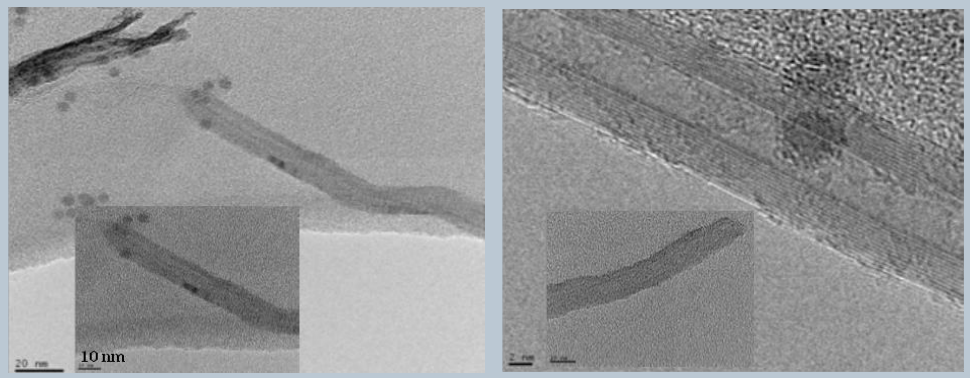

Radio Frequency

150 ˚C

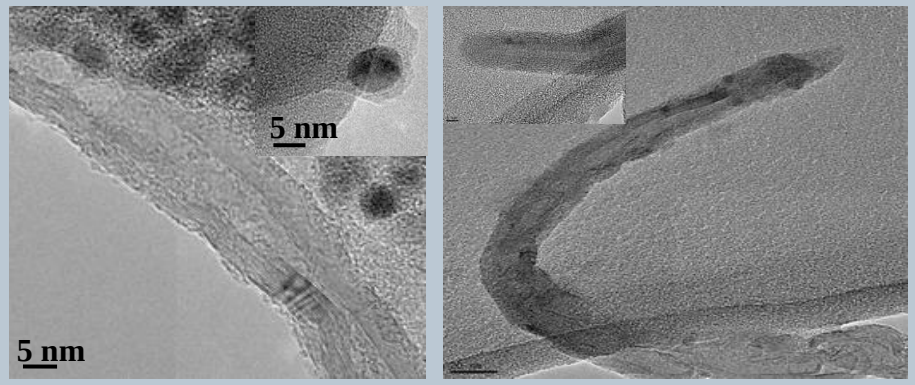

200 ˚C

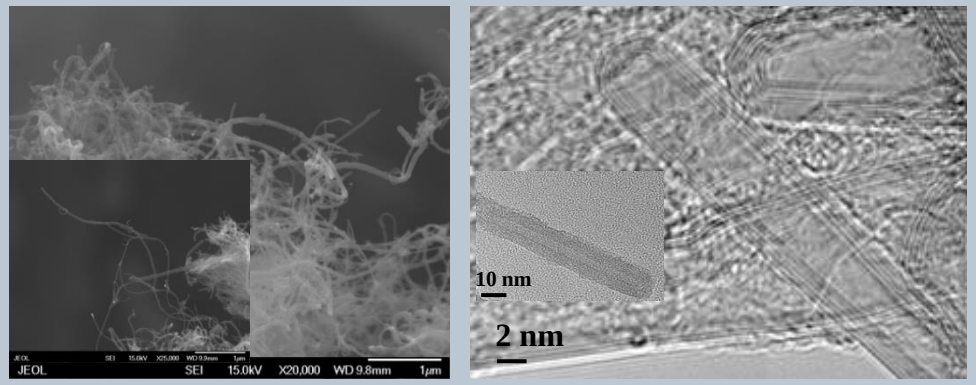

E. Dervishi at al., Journal of Catalysis, 299, 307-315, 2013.

RF treatment at 500 ˚C

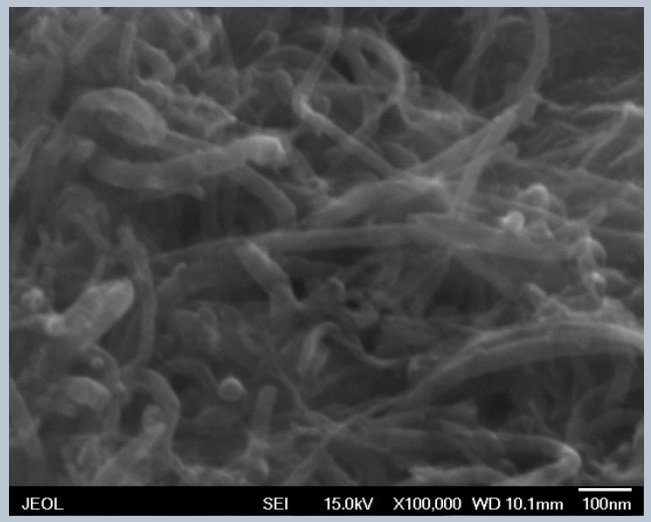

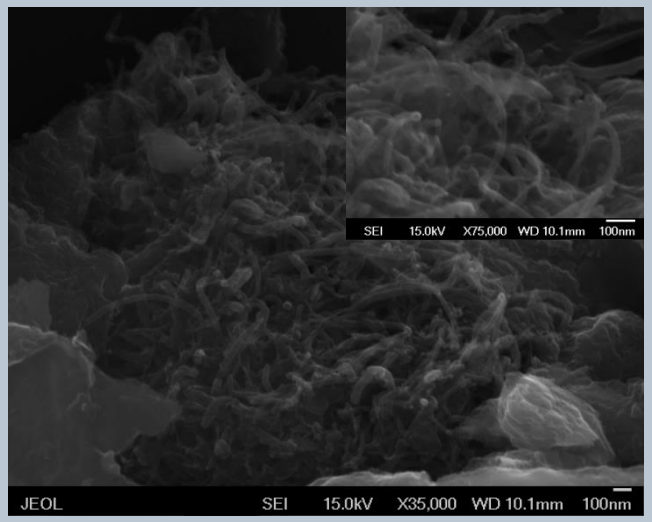

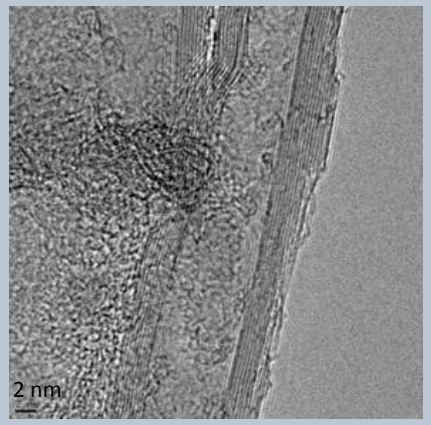

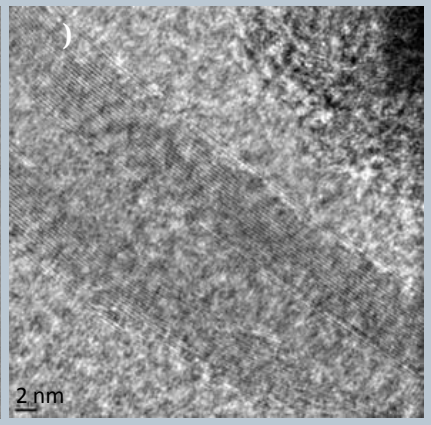

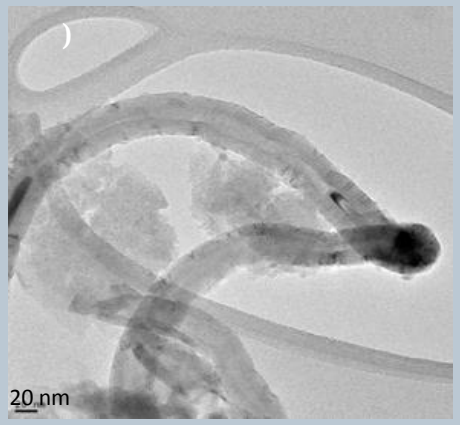

Decoration with 15 nm iron-oxide particles

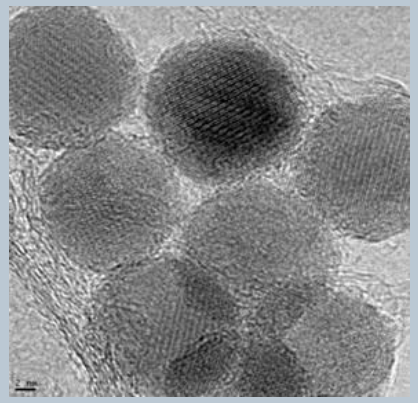

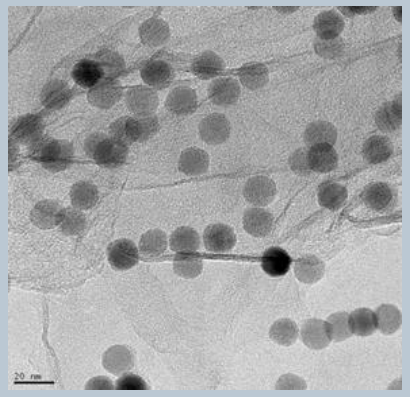

300 °C

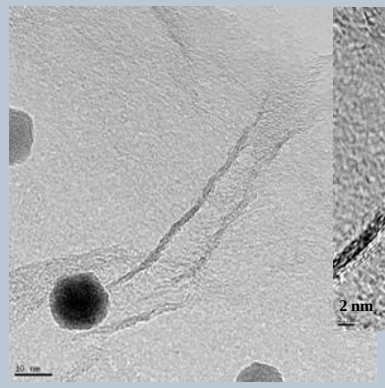

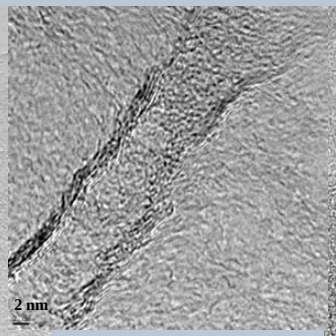

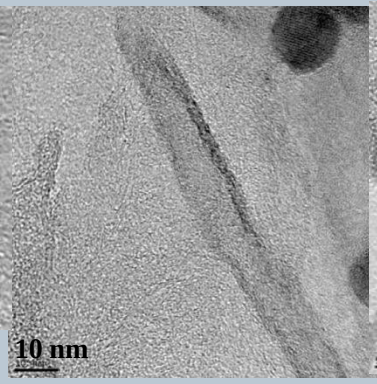

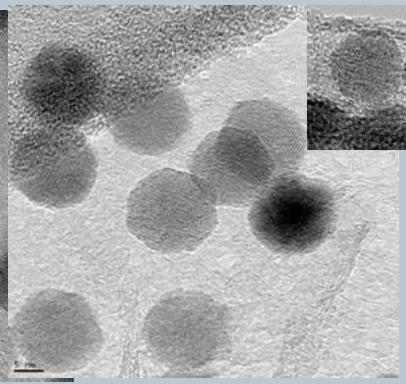

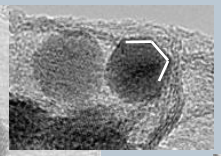

400 °C

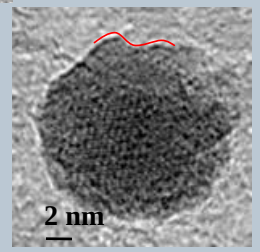

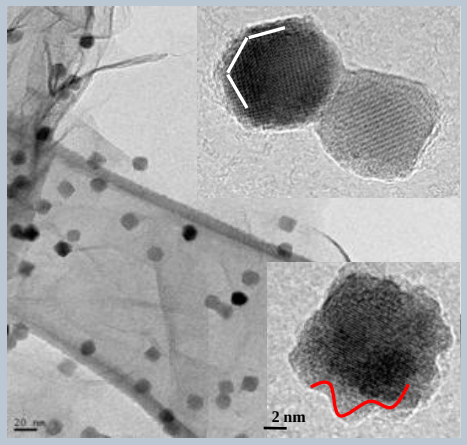

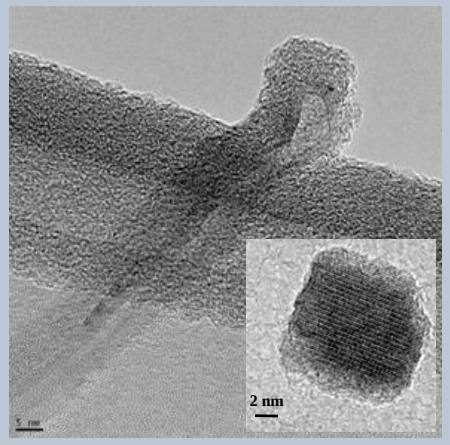

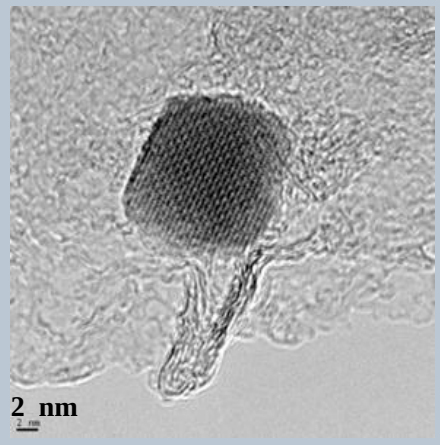

500 °C

Applications of graphene-carbon nanotube hybrids

Graphene-CNT[123] Inverter, NOR, NANAD

Graphene-CNT[245] Transistor

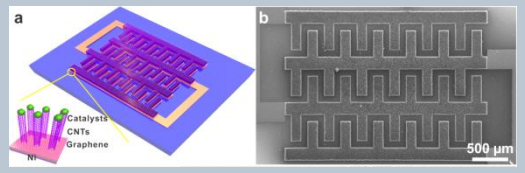

Design of microsupercapacitors and material characterizations of CNTCs. (a) Schematic of the structure of G/CNTCs-MCs. Inset: enlarged scheme of Ni-G-CNTCs pillar structure that does not show the Al2O3 atop the CNTCs;

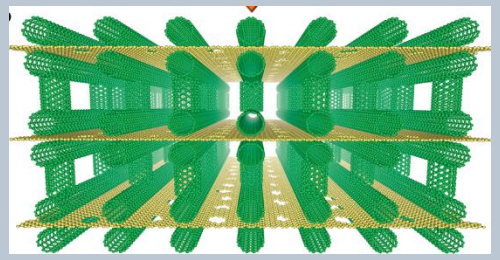

Schematic of the 3D SWCNT-bridged graphene block.

http://www.nanoconvergencejournal.com/content/pdf/s40580-014-0015-5.pdf

Duy Tho Pham,†,‡ Tae Hoon Lee,†,‡ Dinh Hoa Luong,†,‡ Fei Yao,† Arunabha Ghosh,† Viet Thong Le,†,‡ Tae Hyung Kim,† Bing Li,†,‡ Jian Chang,†,‡ and Young Hee Lee*,†,‡ACSNano VOL. 9 ’ NO. 2 ’ 2018–2027 ’ 2015

3-Dimensional Graphene Carbon Nanotube Carpet-Based Microsupercapacitors with High Electrochemical Performance

Jian Lin,†,‡ Chenguang Zhang,‡,§,⊥ Zheng Yan,§ Yu Zhu,‡,§ Zhiwei Peng,§ Robert H. Hauge,‡,§ Douglas Natelson,*,∥,# and James M. Tour* Nano Lett. 2013, 13, 72−78

Applications of carbon nanotubes and graphene

- **Bio-nano**
  - **Cytotoxicity Effects on various cell lines**
  - **Proliferation of bone cells**
  - **Cancer targeting/destruction**
  - **Gene delivery vehicles to cancerous cells**

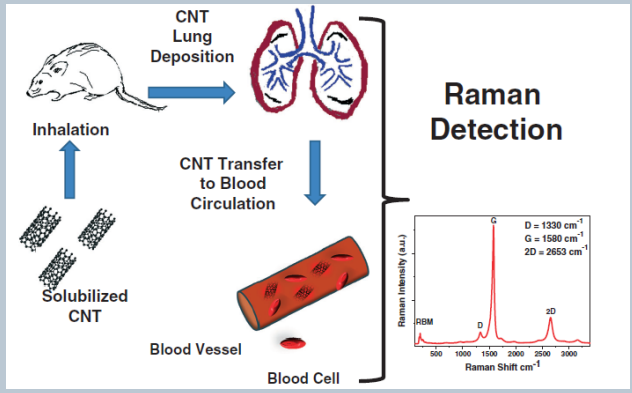

- Detection (Electrochemical Analysis of Organic Compounds)

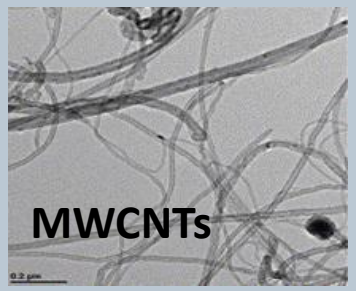

- Space explorations (Electrodynamic screens for dust mitigation of spacesuits during lunar exploration missions)
- Development of hetero-structures and polymer nano-composites
- Membranes for ion transport

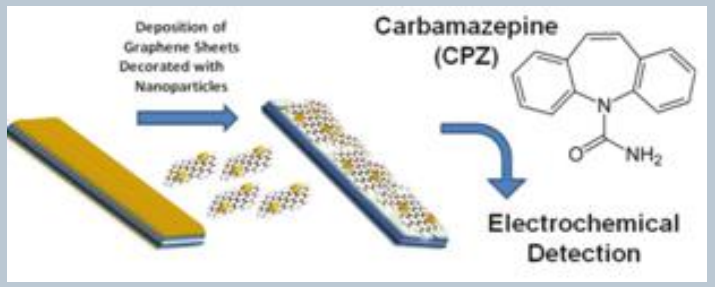

Cytotoxicity Effects of Graphene and SWCNTs in Neural Phaeochromocytoma-Derived PC12 Cells

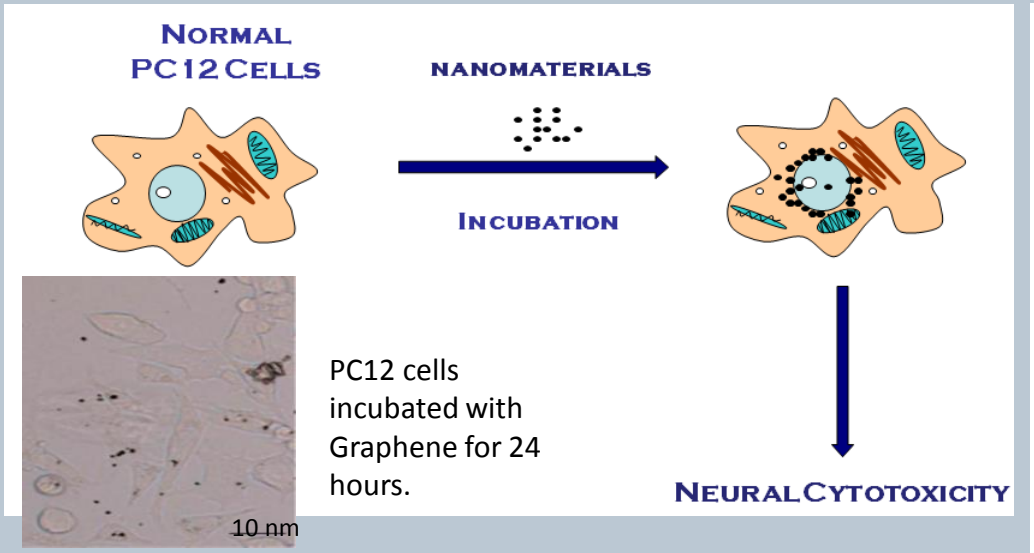

Effect of Graphene or SWCNT on mitochondrial toxicity

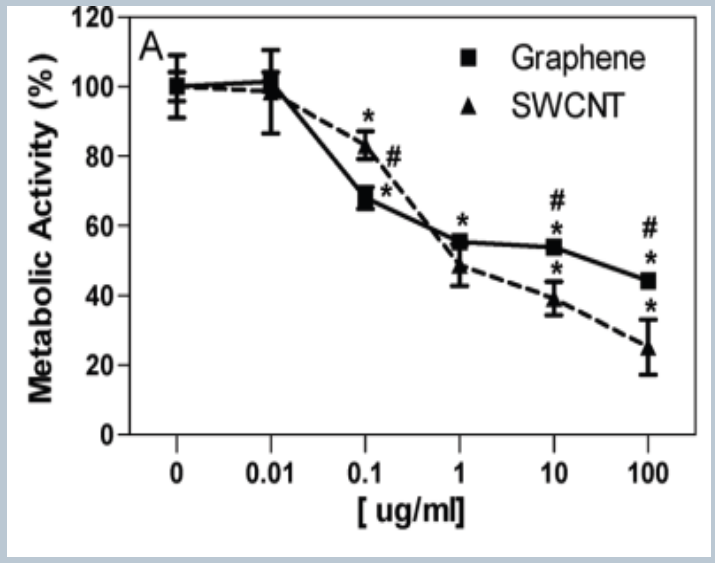

Y. Zhang et a., ACS Nano, 4 (6), 3181-3186, 2010. Article selected by Associate Editor Wolfgang Parak and Editor-in-Chief Paul Weiss and presented in the virtual Issue from ACS Nano devoted to nanotoxicology. (85 citations)

(Collaboration with scientists at NCTR/FDA)

Raman spectroscopy analysis and mapping the bio-distribution of inhaled carbon nanotubes in the lungs and blood of mice

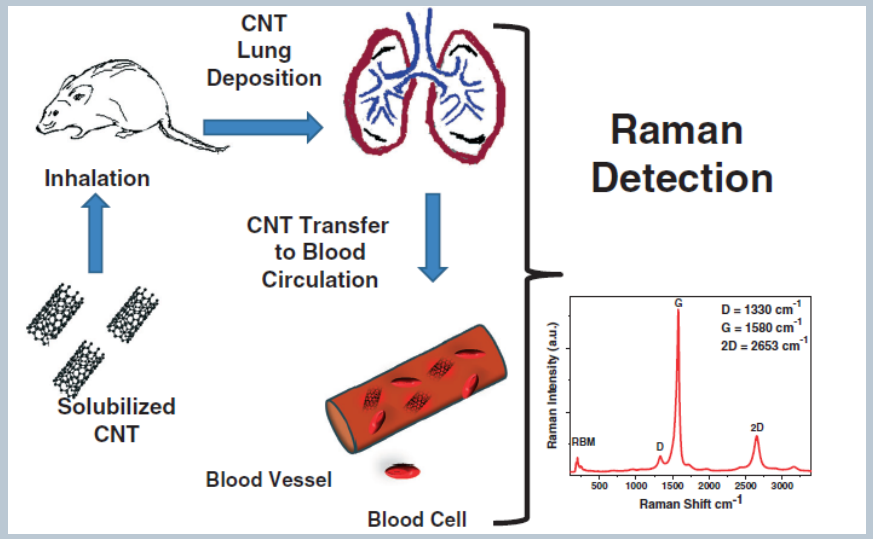

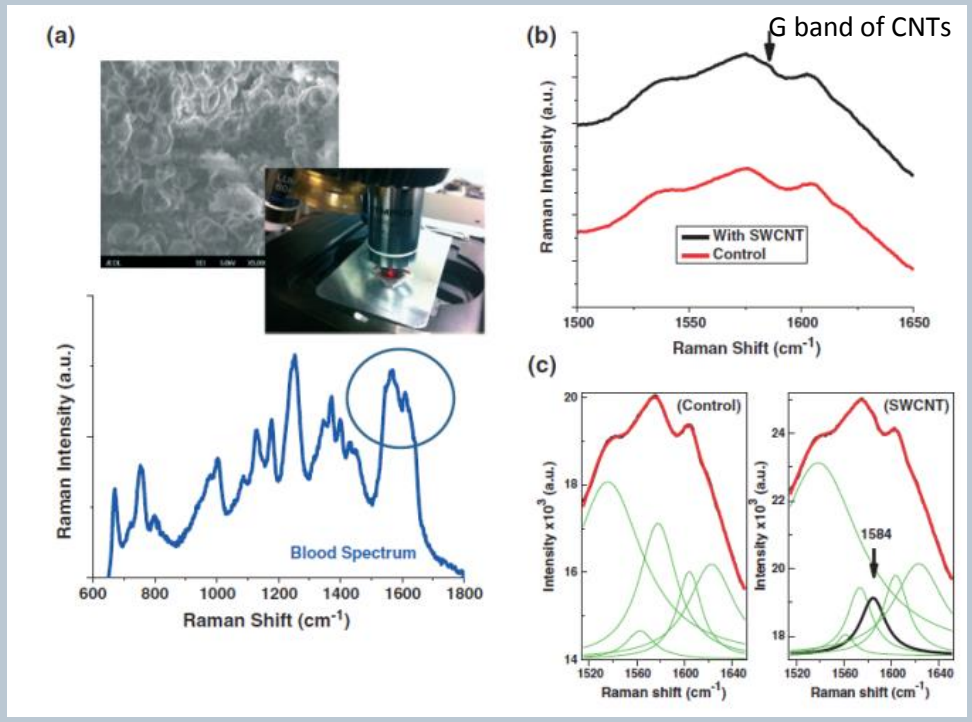

Raman analysis of the blood samples collected from the control animals that were not exposed to CNTs (A). Raman spectra of blood samples collected from animals that were not exposed to CNTs (control-red line) and animals exposed to CNTs by inhalation (black line) (B).

T. Ingle et al., Journal of Applied Toxicology, 2012, DOI: 10.1002/jat.2796.

(Collaboration with scientists at Arkansas State University)

Cancer Research

Ethylenediamine functionalized-single-walled nanotube (f-SWNT)-assisted in vitro delivery of the oncogene suppressor p53 gene to breast cancer MCF-7 cells

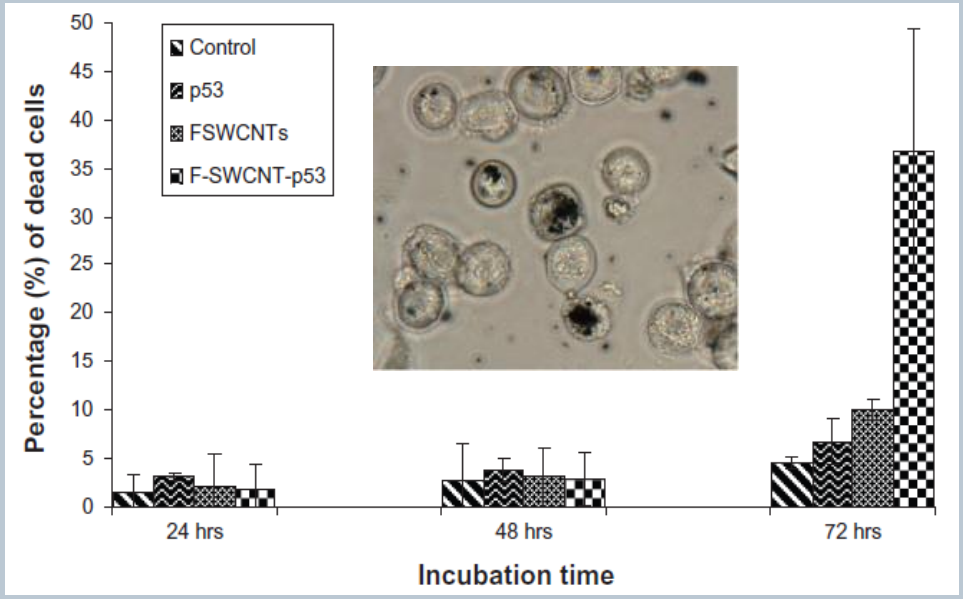

Raman Spectroscopy as a Detection and Analysis Tool for *In Vitro* Specific Targeting of Pancreatic Cancer Cells by EGF-Conjugated SWCNTs

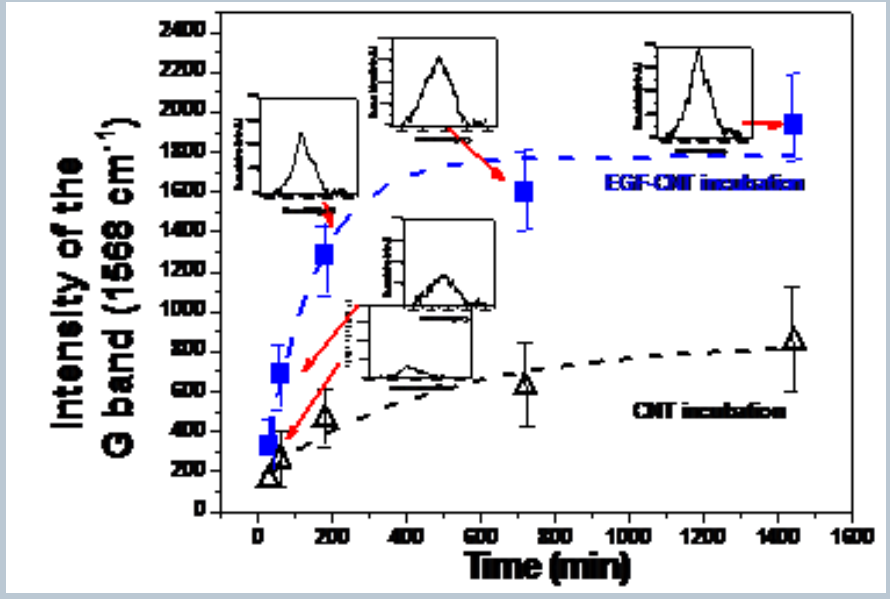

Intensity of the G band corresponding to SWCNTs (with and without EGF conjugation) measured at the surface of individual PANC-1 cells as a function of the incubation time.

A. Karmakar, et al., International Journal of Nanomedicine, 6, 1045-55, 2011.

A.Karmakar, et al., Journal of Applied Toxicology, 32 (5), 365-375, 2012.

(Collaboration with bio-nano group at UALR-CINS)

Role of the carbonaceous nanomaterials in stimulation of osteogenesis in mammalian bone cells

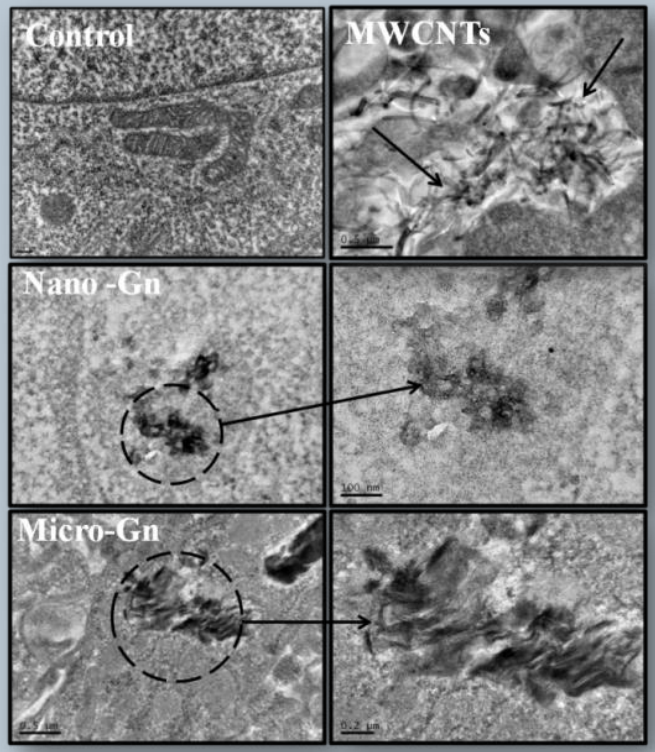

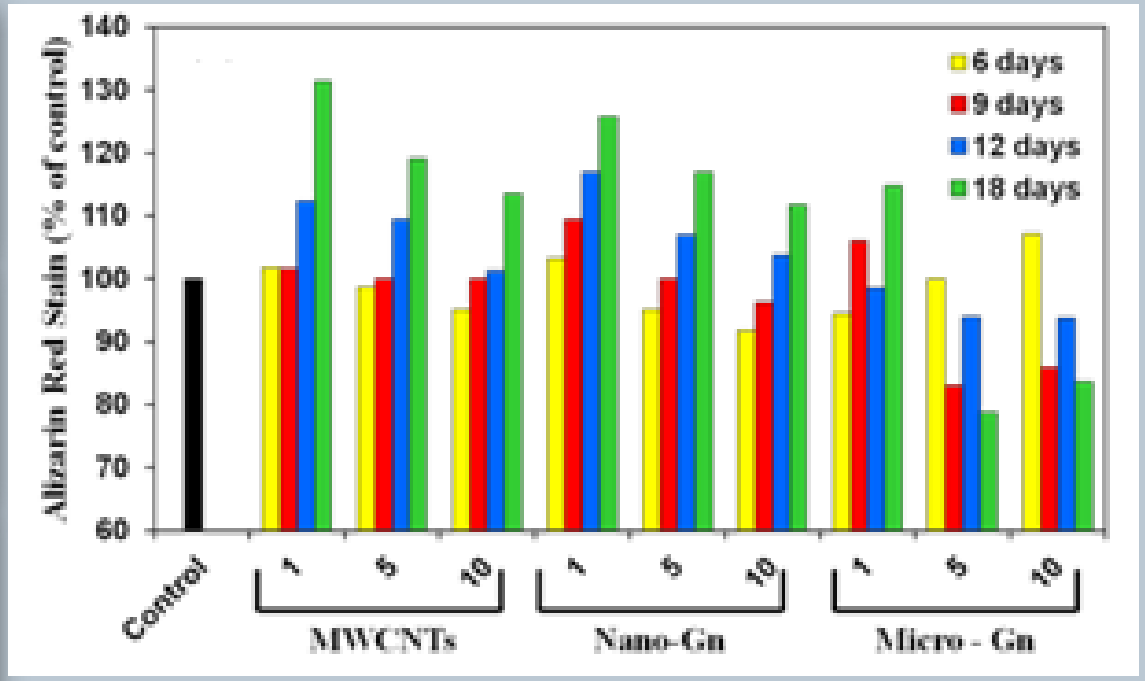

TEM images of the carbon materials within the cytoplasm of MC3T3 cells exposed to 10 µgml^{-1} of MWCNTs, nano and micro-Graphene sheets.

Alizarin Red quantification assay data in the presence of graphitic nano-materials showed that their concentration affected the level of mineralization in a time-dependent manner.

M. Mahmood et al., under review 2013.

(Collaboration with bio-nano group at UALR-CINS)

Graphene-based multiplex approach for circulating tumor cells detection in blood collaboration with Alexandru S. Biris at theUALR Center for Integrative Nanotechnology Sciences at)

Add slide for Alex work and High school kids w

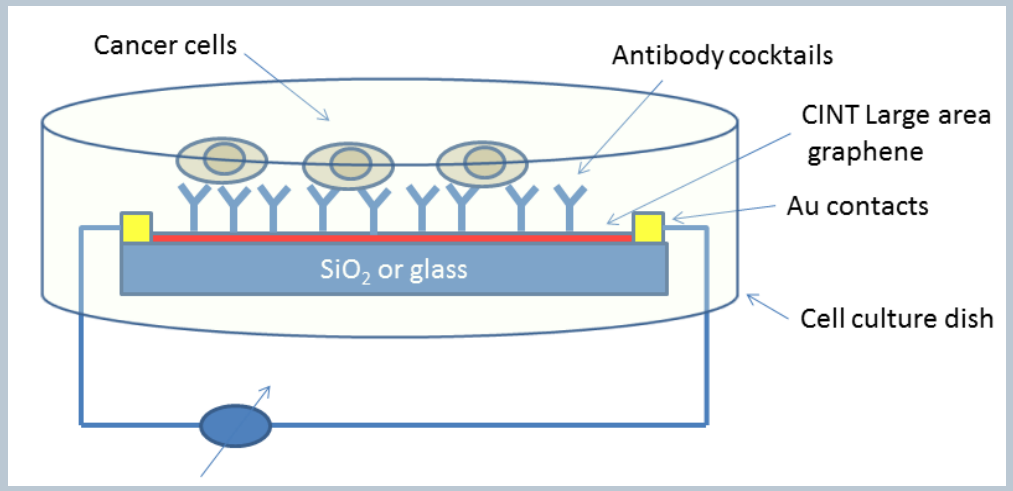

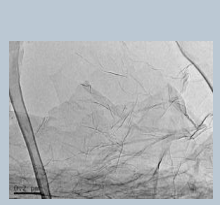

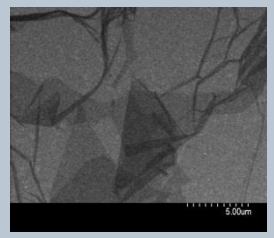

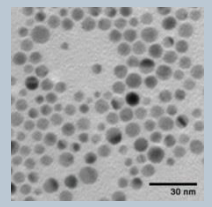

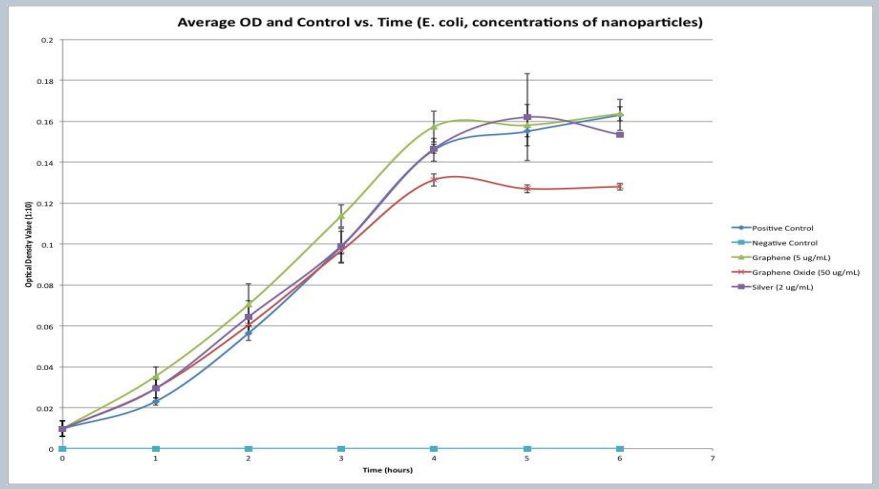

Schematic of the proposed device for circulating tumor cell detection, which integrates large-area graphene decorated with antibodies.

http://www.sigmaaldrich.com/catalog/product/aldrich/730785?lang=en&region=US

Los Alamos NATIONAL LABORATORY

U.S. DEPARTMENT OF ENERGY | Office of Science

UALR Center for Integrative Nanotechnology Sciences

Sandia National Laboratories

Applications of carbon nanotubes and graphene

- Bio-nano
  - Cytotoxicity Effects on various cell lines
  - Proliferation of bone cells
  - Cancer targeting/destruction
  - Gene delivery vehicles to cancerous cells

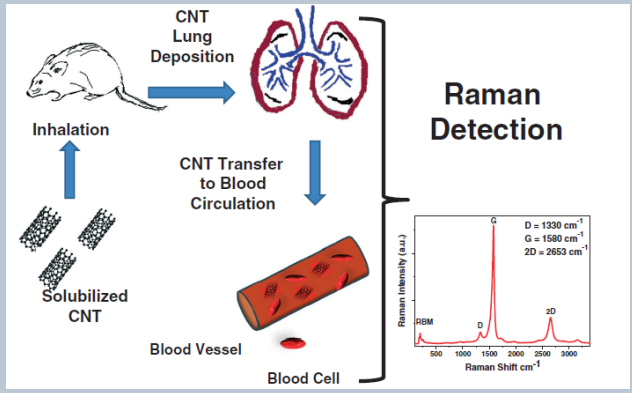

- **Detection (Electrochemical Analysis of Organic Compounds)**

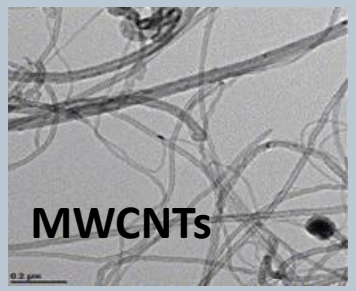

- Space explorations (Electrodynamic screens for dust mitigation of spacesuits during lunar exploration missions)
- Development of hetero-structures and polymer nano-composites
- Membranes for selective ion transport studies

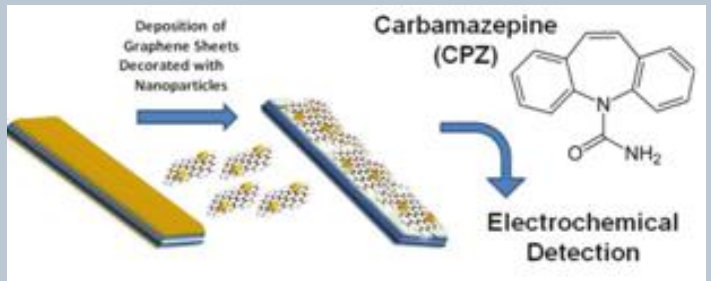

Multifunctional Graphene Sheets with Encased Nanoparticles for Detection of Organic Compounds

One-step synthesis of metal-decorated graphene sheets for electrochemical detection

Au, Ag, Au/Ag, Pt, and Pd

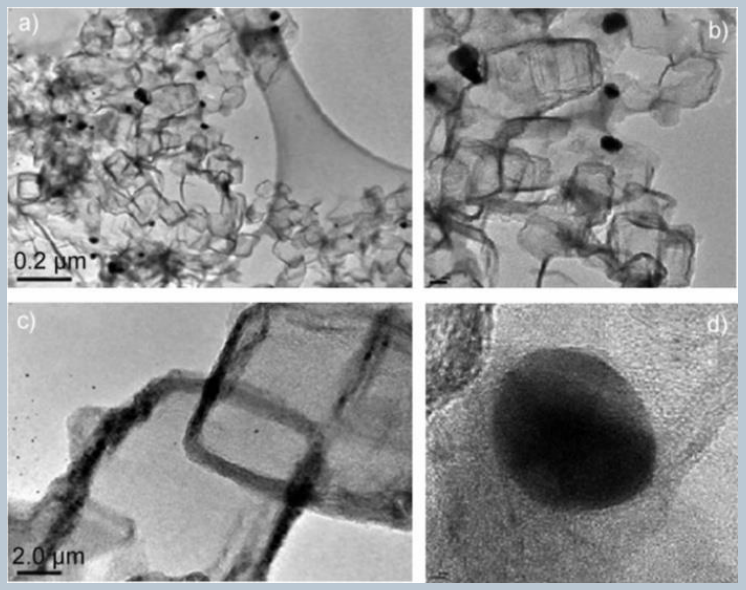

Graphene nanosheets with Au/ Ag embedded with in the graphitic layers

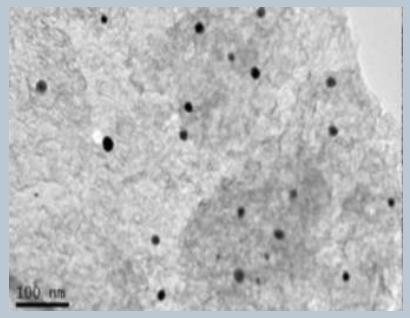

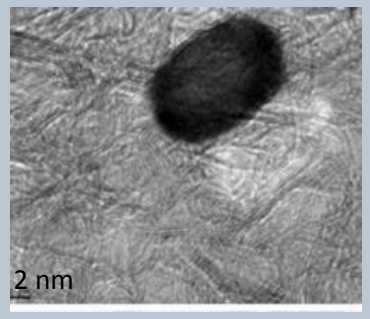

Gr-Au composites for electrochemical analysis of adenine.

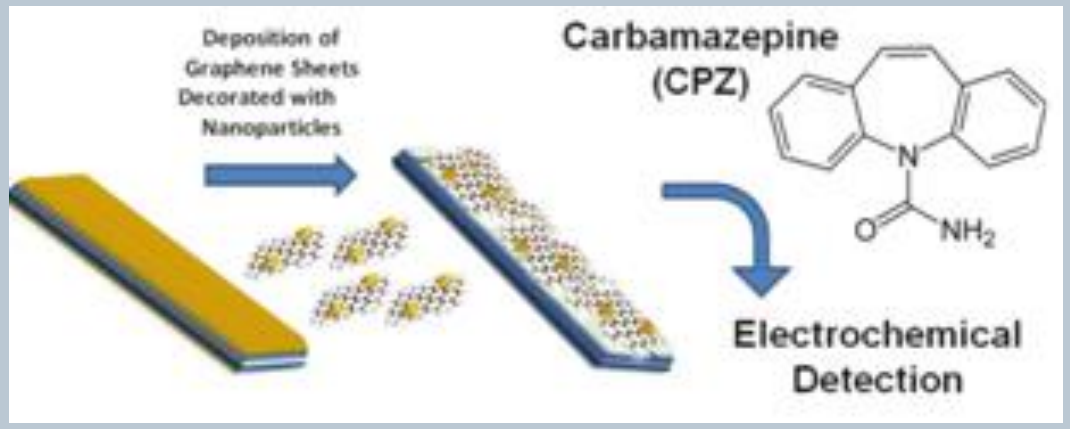

S. Pruneanu et al., International Journal of Nanomedicine, Accepted in 2013.
S. Pruneanu, et al. CHEMPHYSCHEM, 13(16), 3632-3639, 2012.
A. R. Biris et al., Carbon, 50 (6), 2252-2263, 2012.

(Collaboration with Dr. Watanabe at UALR-CINS and the scientists at the National Institute for Research and Developments of Isotopic Molecular Technologies in Romania)

Applications of carbon nanotubes and graphene

- Bio-nano
  - Cytotoxicity Effects on various cell lines
  - Proliferation of bone cells
  - Cancer targeting/destruction
  - Gene delivery vehicles to cancerous cells

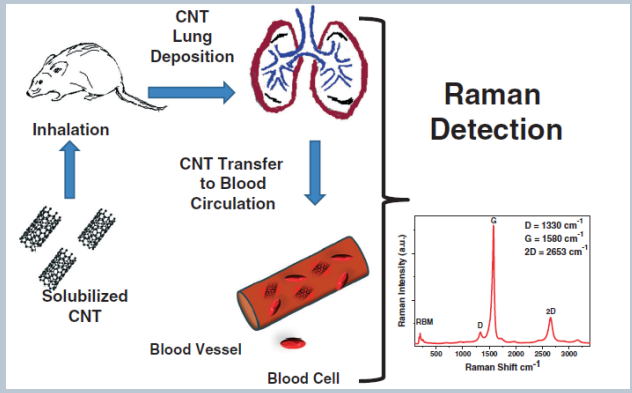

- Detection (Electrochemical Analysis of Organic Compounds)

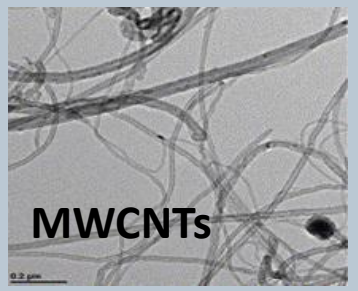

- **Space explorations (Electrodynamic screens for dust mitigation of spacesuits during lunar exploration missions)**
- Development of hetero-structures and polymer nano-composites
- Membranes for ion transport

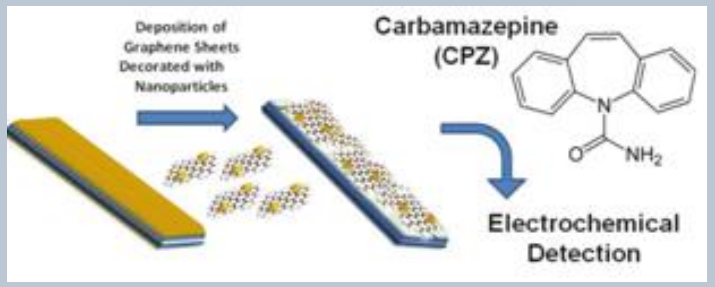

Multifunctional Coatings with Carbon Nanotubes for Electrostatic Charge Mitigation

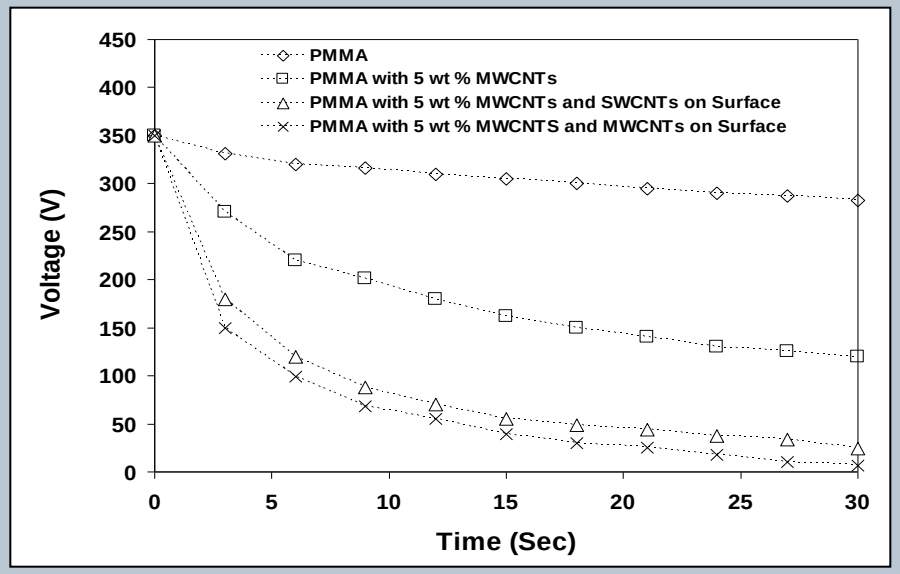

Charge decay characteristics of polymer - CNT composites

E. Dervishi et al., IEEE Transactions on Industry Applications Journal, 45 (5), 1547-1552, 2009.
S. Trigwell et al., under review 2015.

Application of conductive carbon nanotube ink electrodynamic screens for dust mitigation of spacesuits during lunar exploration missions

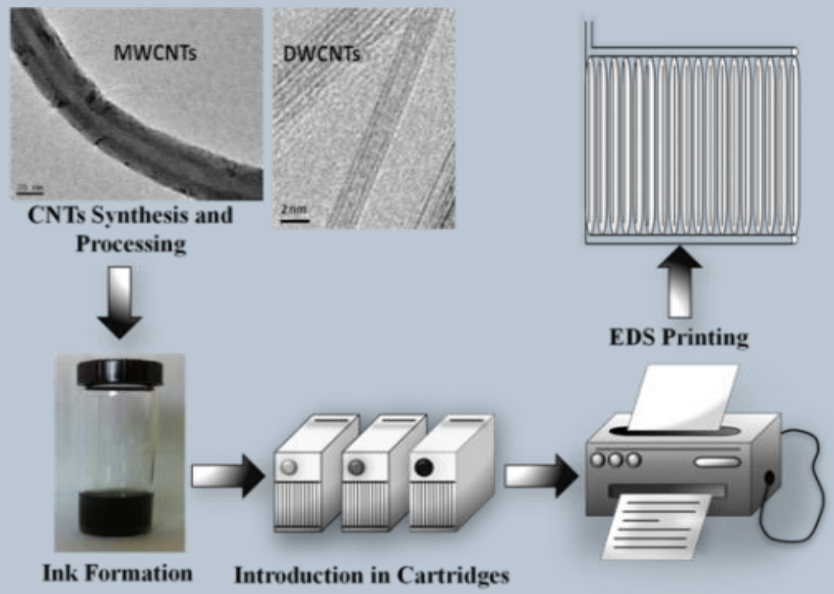

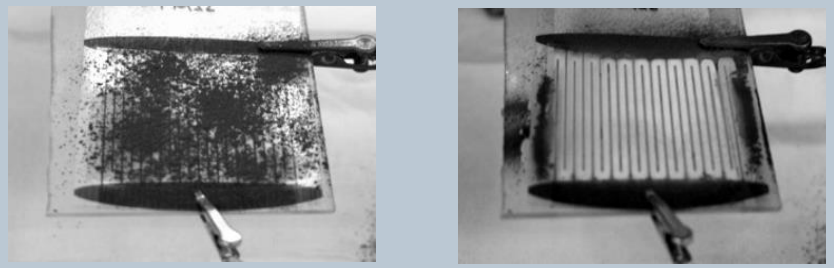

A cotton fabric shield with deposited JSC-1A lunar simulant (25-50 µm size) before and after activation with 4750 V at 10 Hz. The shield cleared in < 10 sec.

(Collaboration with Dr. Trigwell at Kennedy Space Center)

49

Applications of carbon nanotubes and graphene

- Bio-nano
  - Cytotoxicity Effects on various cell lines
  - Proliferation of bone cells
  - Cancer targeting/destruction
  - Gene delivery vehicles to cancerous cells

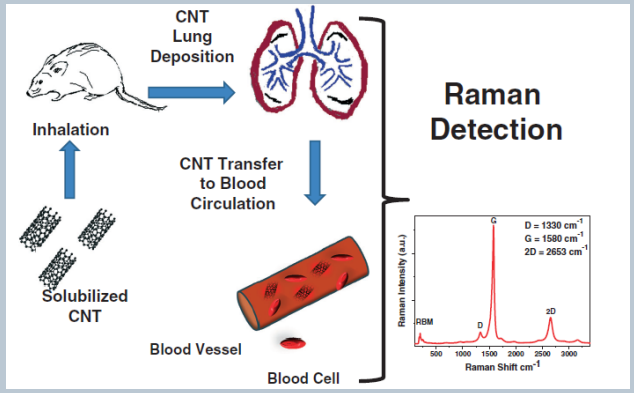

- Detection (Electrochemical Analysis of Organic Compounds)

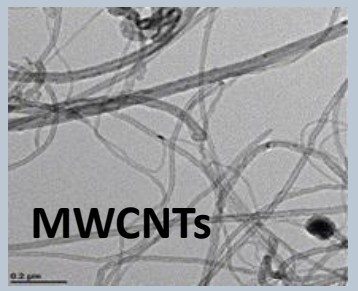

- Space explorations (Electrodynamic screens for dust mitigation of spacesuits during lunar exploration missions)
- **Development of hetero-structures and polymer nano-composites**
- Membranes for selective ion transport studies

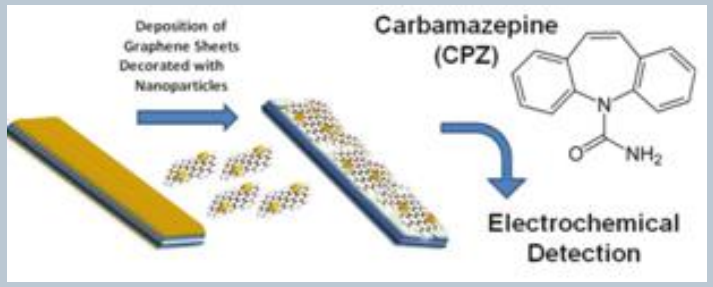

Polymer Nanocomposites

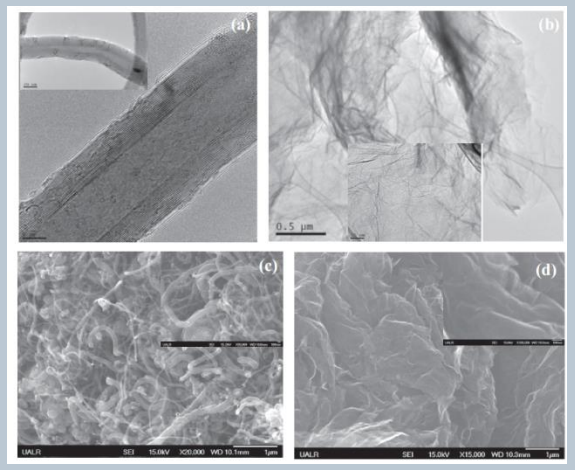

High and low magnification TEM images of the MWCNTs ((a) and inset) and few-layer graphene ((b) and inset) used in the polymer composites. SEM images of the bundled MWCNTs ((c) and inset) and graphene sheets ((d) and inset).

TEM images of the polymer nano-conposites with 1 wt.% MWCNTs ((a) and (b)), graphene ((c) and (d)), and with a MWCNT–graphene mixture ((e) and (f)).

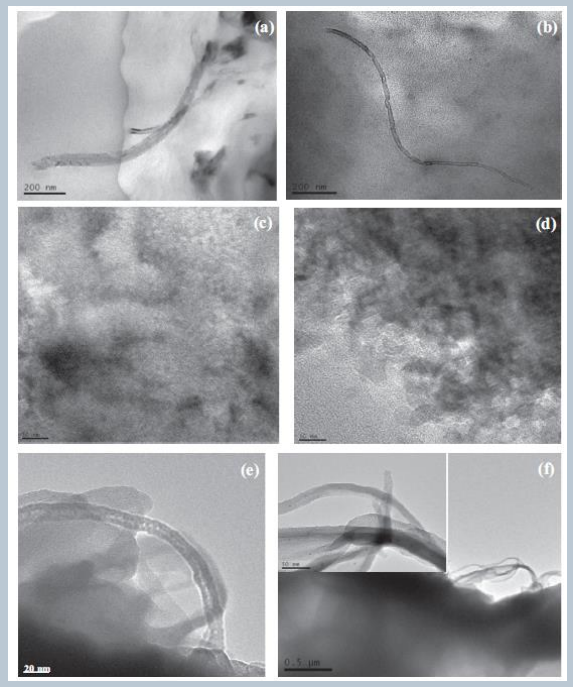

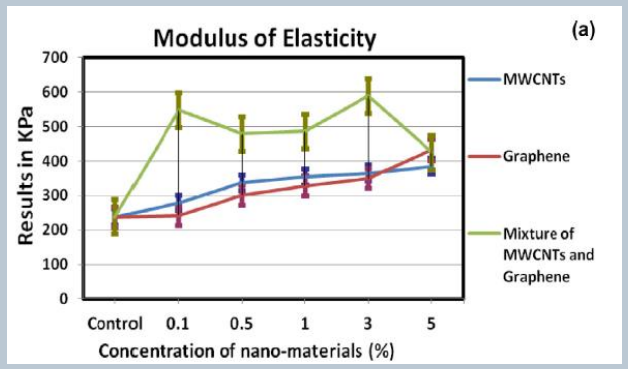

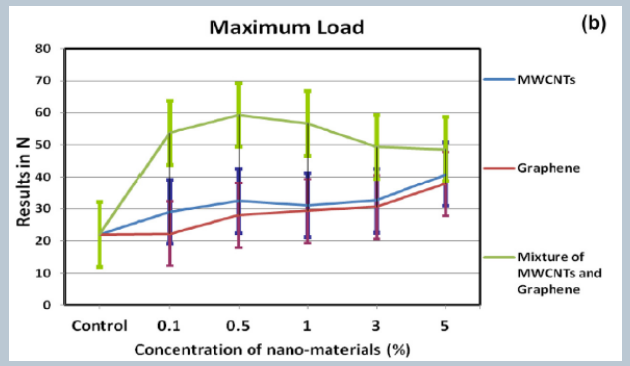

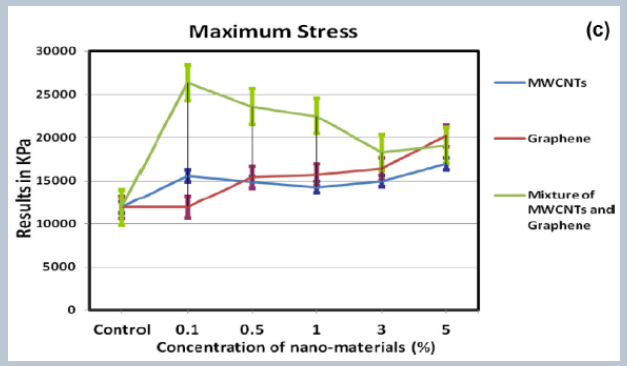

The mechanical properties of the nano-composites: moludus of elasticity (a), maximum load (b) and maximum stress (c) versus the concentration of the nanomaterials.

The effect of carbon nanotubes and graphene on the mechanical properties of multi-component polymeric composites
Enkeleda Dervishi, F. Hategekimana, L. Boyer, F. Watanabe, T. Mustafa, A. Biswas, A. R. Biris, A. S. Biris Chemical Physics Letters 590 (2013) 126–130

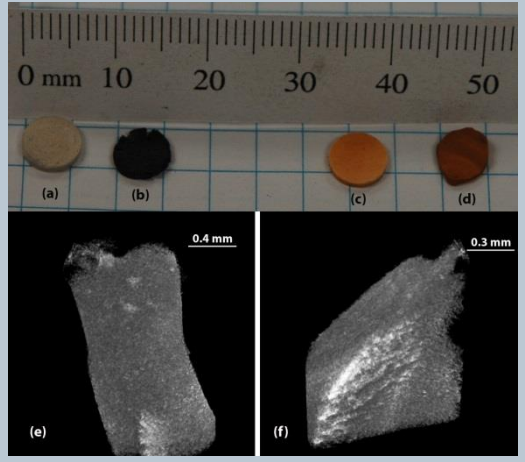

Images of Au nanofoam and pressed precursors (a) $Au(BTA)_3(NH_4)_3$, **2**; (b) nanofoam produced from (a) under 2 MPa Ar overpressure; (c) $Au(BTA)_2(NH_4)(H_2O)$, **1**; (d) Au nanofoam produced from (c) under 2 MPa Ar overpressure; (e, f) computed X-ray tomography images of a section of the Au nanofoam seen in (d).

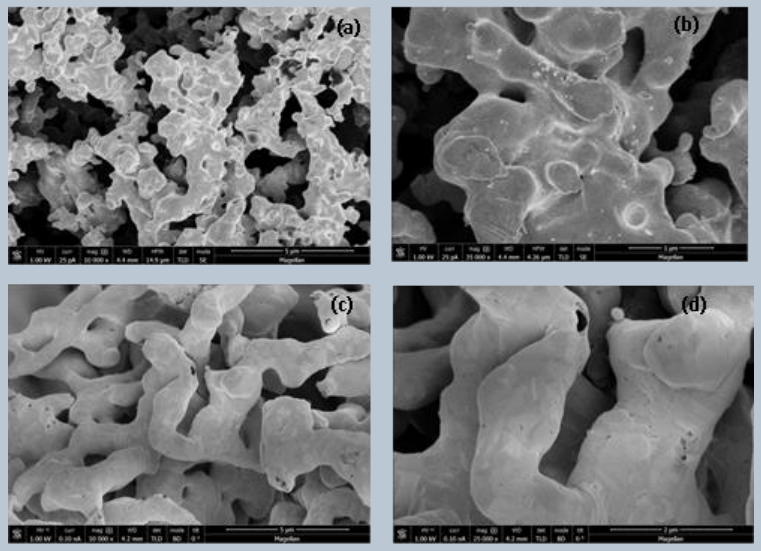

(a, b) SEM images of the as-produced nanoporous foams. (c, d) Annealed Au foams under Argon at 750 °C for 30 minutes.

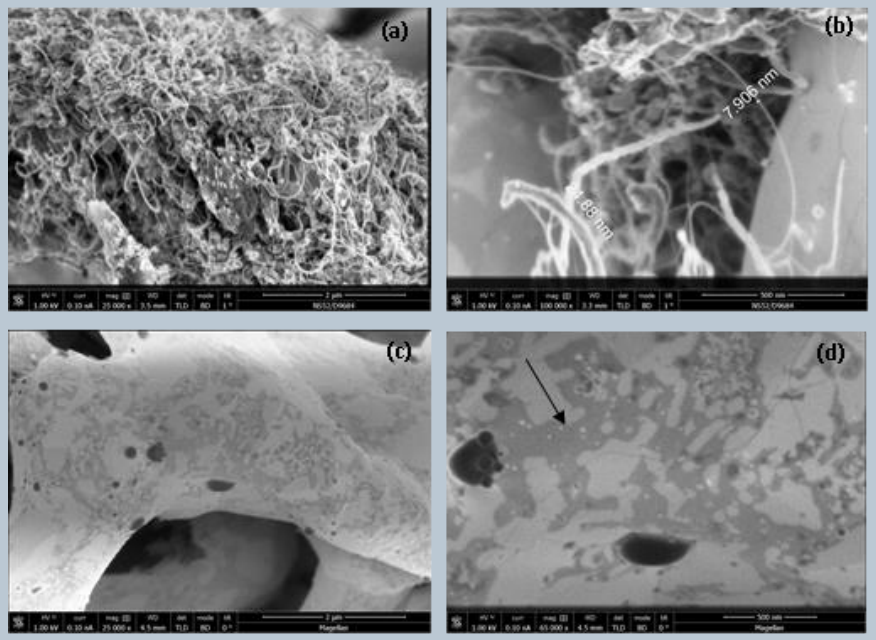

(a, b) SEM images of the nanotubes synthesized on the Au nanoporous foams using methane at 150 sccm. (c, d) Initial formation of graphitic structures (indicated by the arrow) over the Au nanofoams under methane flow of 40 sccm.

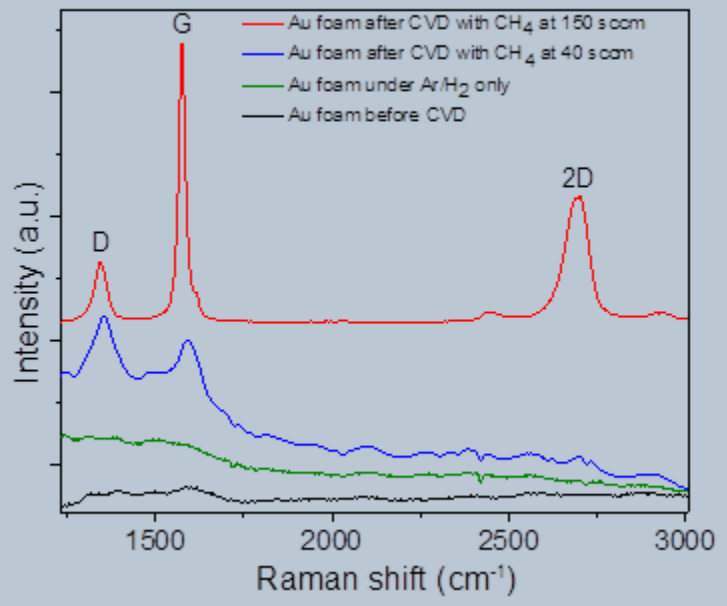

Stacked Raman spectra of the Au foams after different CVD

Probing and Engineering Lithium Ion Transport in Graphene-Nanowire Heterostructures for High-Performance Battery Anodes- Collaboration with Jinkyoung Yoo and his team

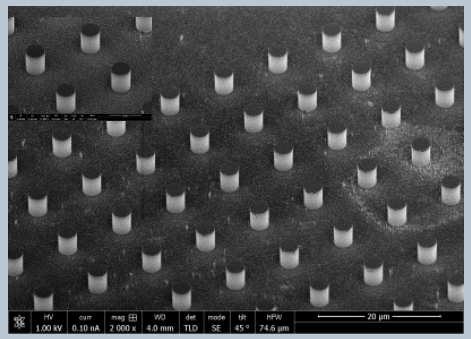

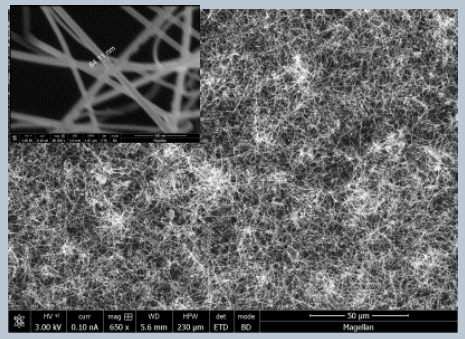

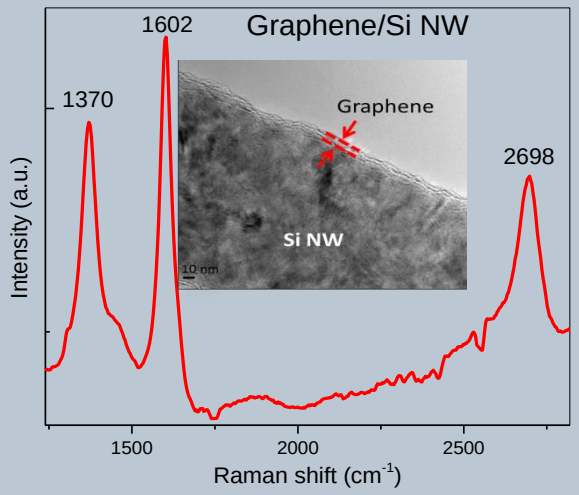

Raman spectrum of graphene/Si NW heterostructures indicating the characteristic Raman bands of graphene. Inset: High-resolution TEM image of the heterostructure.

Hybrid Graphene–Giant Nanocrystal Quantum Dot Assemblies with Highly Efficient Biexciton Emission- Collaboration with Han Htoon and Jennifer Hollingsworth

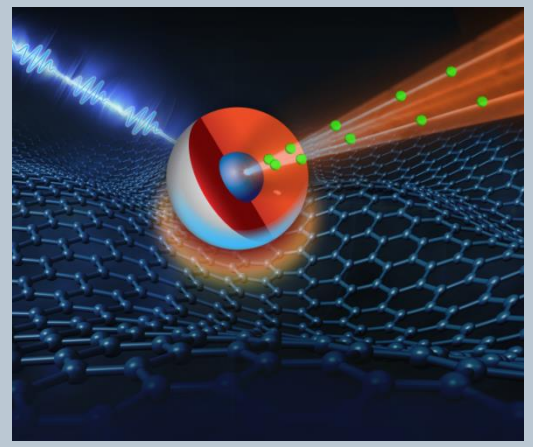

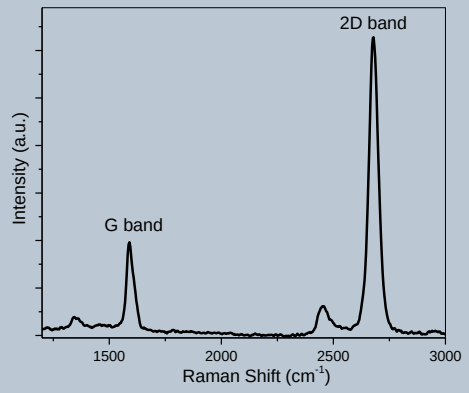

Y. Gao , O. Roslyak , E. Dervishi , N. S. Karan , S. K. Doorn , J. A. Hollingsworth , Han Htoon et. al Adv. Optical Mater. **2014**, DOI: 10.1002/adom.201400362

Applications of carbon nanotubes and graphene

- Bio-nano
  - Cytotoxicity Effects on various cell lines
  - Proliferation of bone cells
  - Cancer targeting/destruction
  - Gene delivery vehicles to cancerous cells

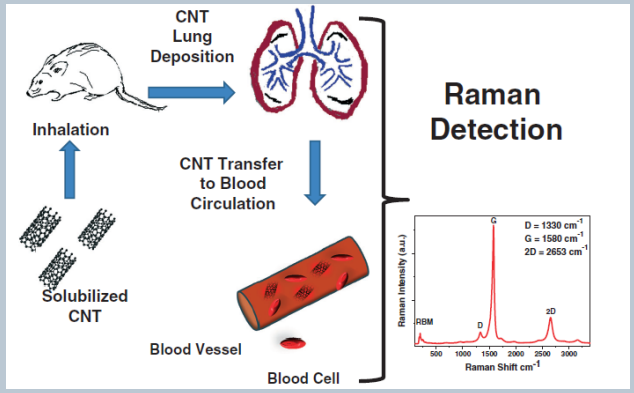

- Detection (Electrochemical Analysis of Organic Compounds)

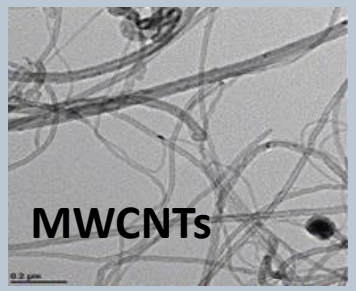

- Space explorations (Electrodynamic screens for dust mitigation of spacesuits during lunar exploration missions)
- Development of hetero-structures and polymer nano-composites
- **Membranes for selective ion transport studies**

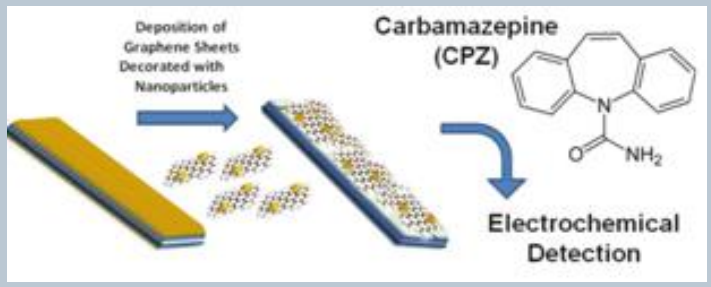

Graphene based membranes

- Large area graphene sheets were synthesized via chemical vapor deposition. Defect characterization via. Raman spectroscopy and optical microscopy
- Single layer graphene is being tested first
- Multilayer graphene may be necessary for mechanical stability and adequate pore size distribution
- Various etching agents and heating/oxidative treatments will be explored to optimize the graphene transfer process over the glass and ETFE-based substrates

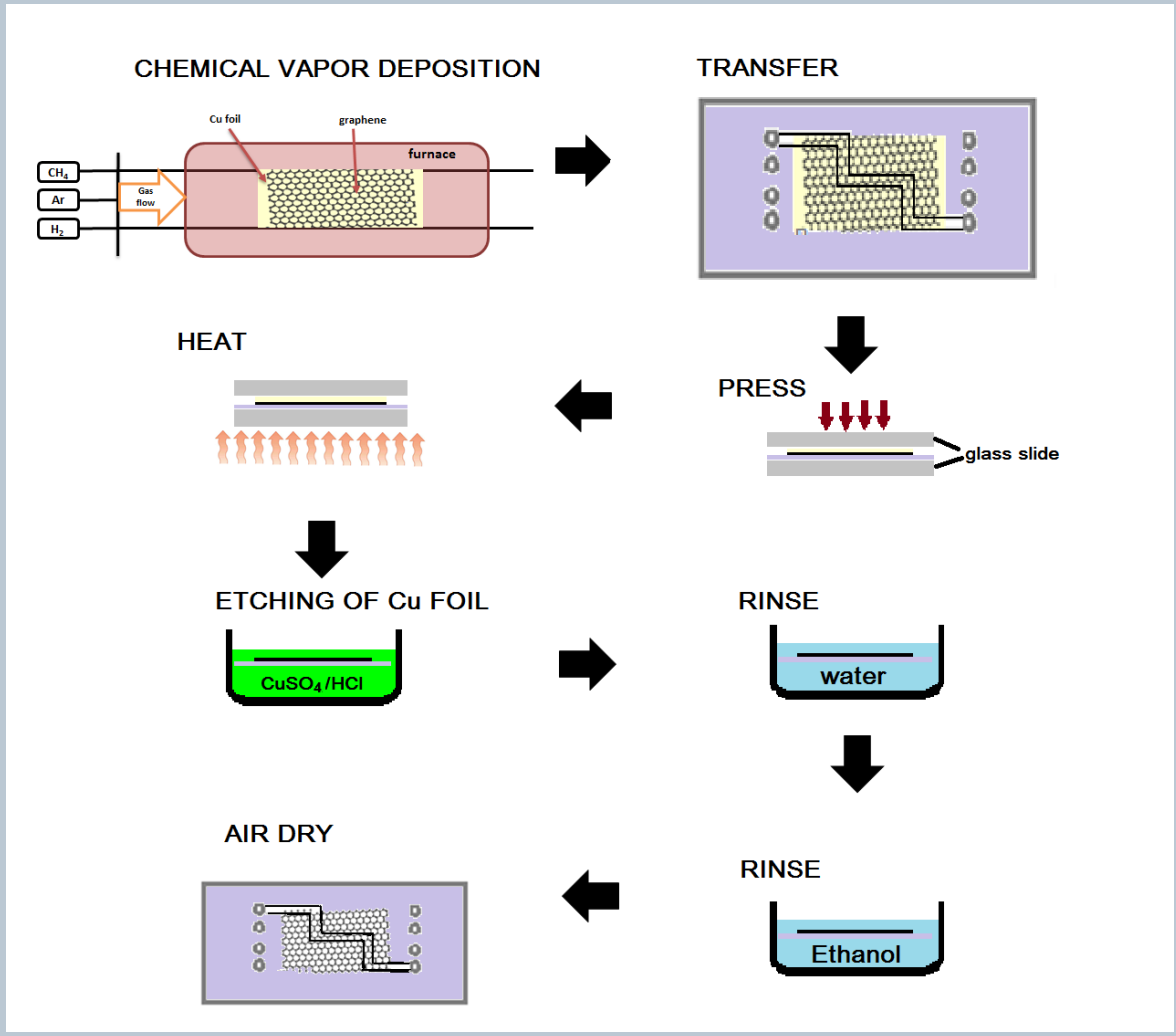

Graphene-based membranes

Large area graphene sheets were synthesized via chemical vapor deposition. The catalyst support (Cu foil) was first annealed under Ar/H_2 atmosphere at 950 °C for 1 hour. Next the furnace temperature was raised to 1005 °C and CH_4 was introduced at 15 sccm for 20 min.

Graphene was transferred on the ETFE substrates and characterized via microscopy and spectroscopy techniques. We will also develop single and few layer graphene membrane systems with tunable pores and investigate their ionic transport behavior across the channels.

The challenge will be to transfer the graphene sheets with minimal defects and completely dissolve the catalyst foil, while maintaining an intimate contact with the substrate.

Various etching agents and heating/oxidative treatments will be explored to optimize the graphene transfer process over the glass and ETFE-based substrates, which contain the ~100 µm wide channels.

Graphene is a prospective and exciting material for transparent, ultra-thin, flexible and chemically stable membrane systems with enhanced transport properties.

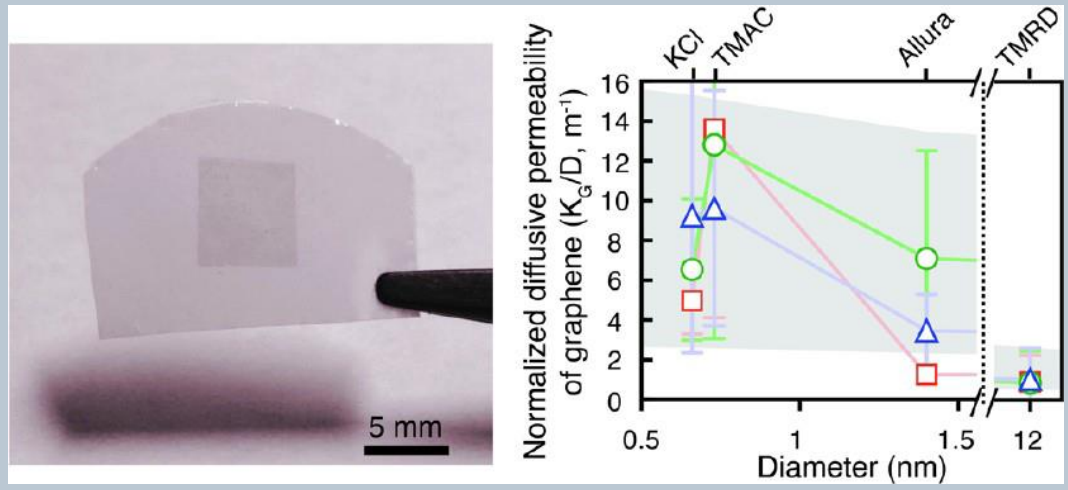

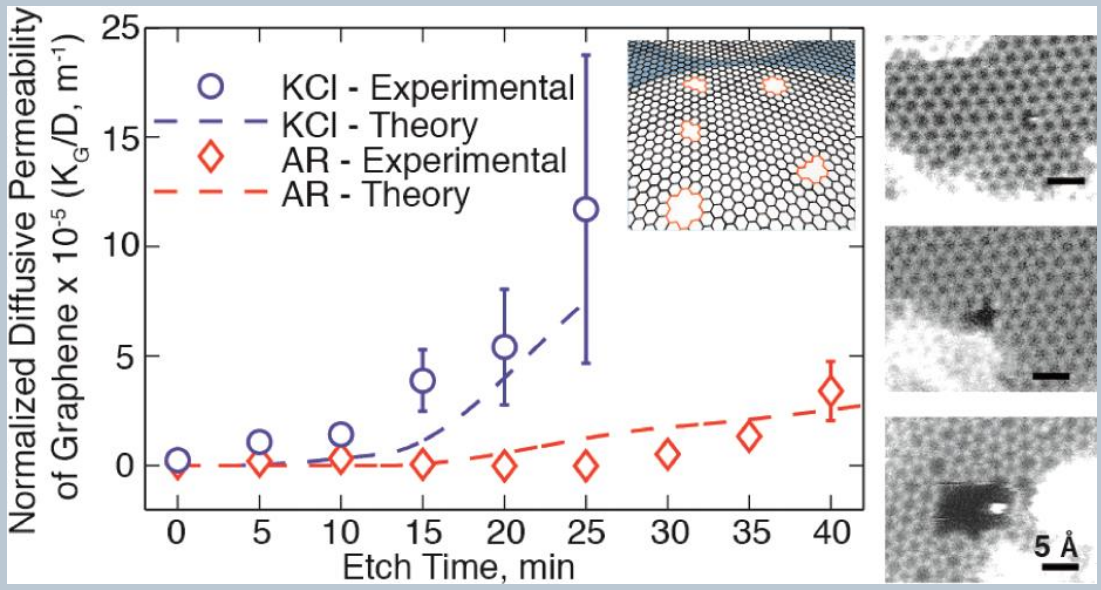

Transfer Technique

SPIN COATING

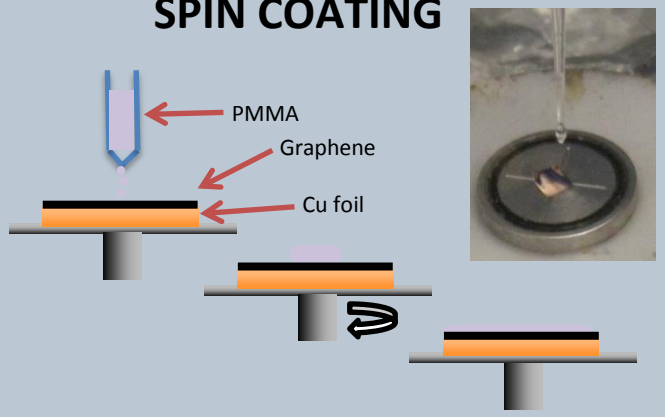

AIR PLASMA TREATMEAT

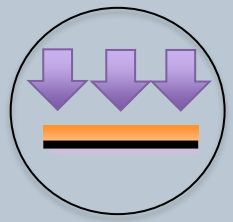

ETCHING OF Cu

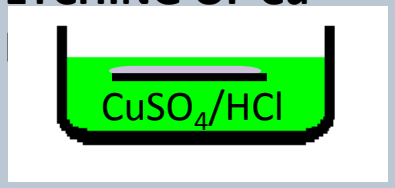

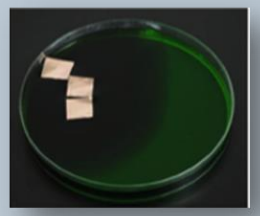

RINSE

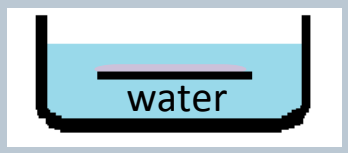

TRANSFER

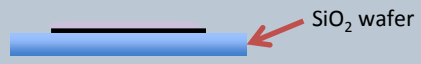

Optical images of a large area graphene sheet on Si/SiO_2 (300 nm) substrates

BAKING

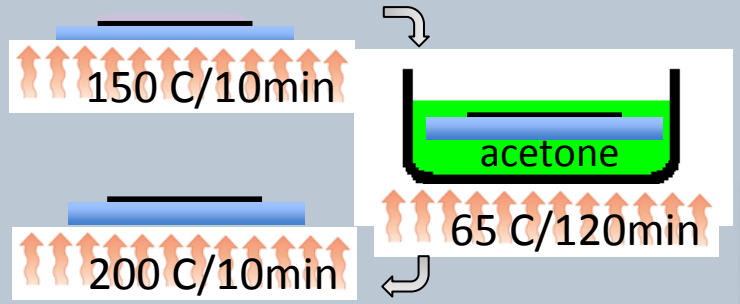

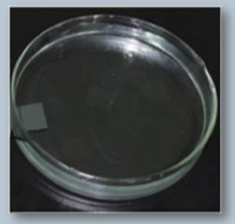

CHEMICAL VAPOR DEPOSITION

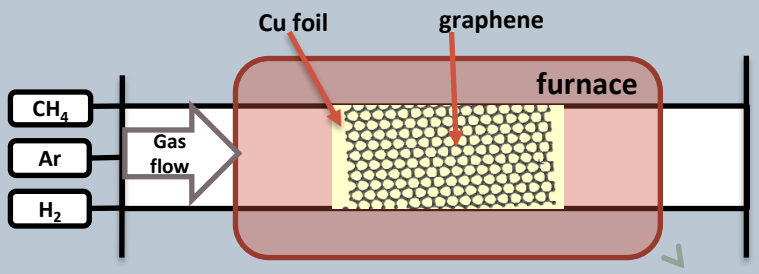

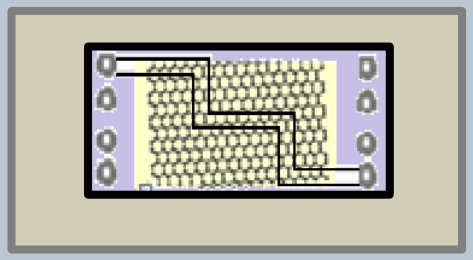

PRESS

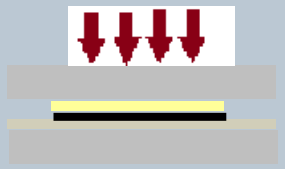

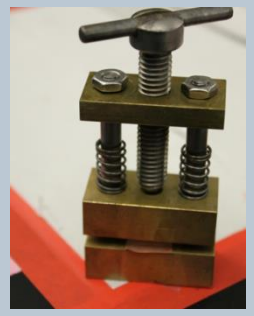

RINSE

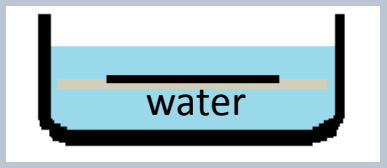

RINSE

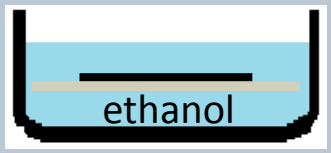

AIR DRY

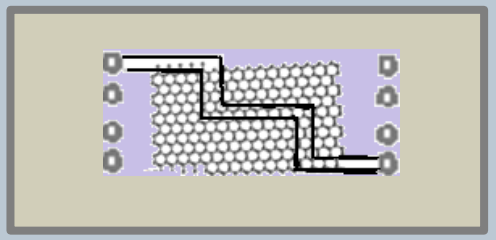

ETCHING OF Cu FOIL

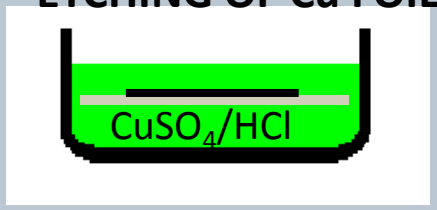

HEAT

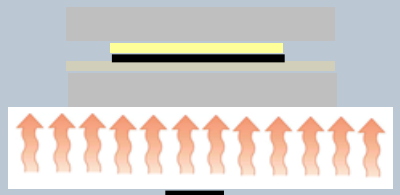

Chemical Vapor Deposition Synthesis

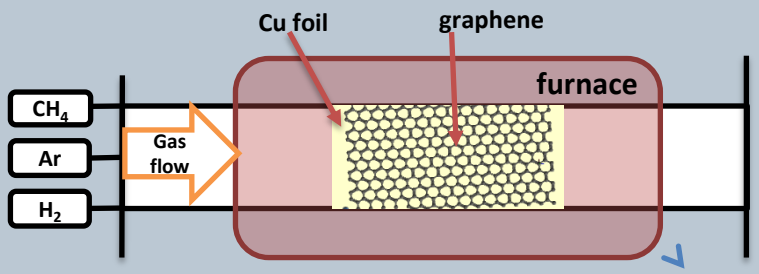

Graphene transfer using thermal release tape

Press

Etching of Cu foil

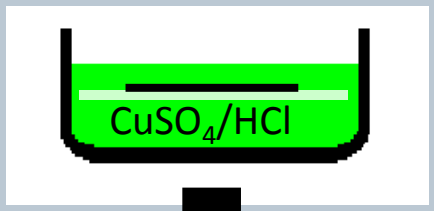

Rinse

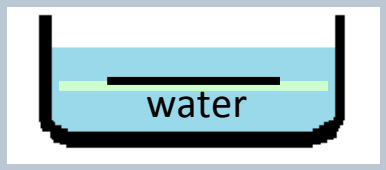

Substrate Transfer

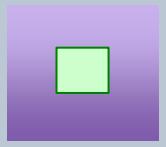

Heat/Release

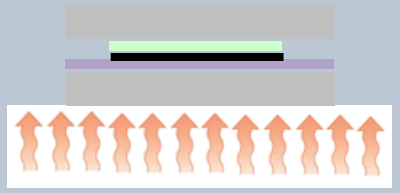

Final Product

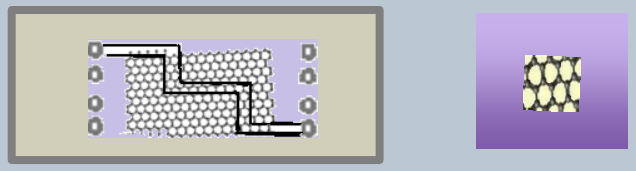

Conclusions

- The morphological properties of CNTs such as diameter distribution, yield, number of walls, and crystallinity were found to strongly depend on the catalyst composition, reaction temperature, heating method and hydrocarbon source.
- The thermal stability of $CaCO_3$ supported Fe-Co catalyst system was found to effect the diameter distribution of the MWCNTs.
- Among all the catalysts (mono or bi-metallic) the Fe-Co/MgO (2.5:2.5:95 wt.%) was found the have the highest surface area and produced SWCNTs with the highest yield and a very narrow diameter distribution.

Conclusions for Part I

- The diameter distribution of the catalyst metal nano-particles and hence the resulting nanotube diameter was controlled by varying the reaction temperature.

  E. Dervishi et al., ***Particulate Science and Technology: An International Journal, 27(3), 222 -237, 2009.***
  E. Dervishi et al., ***Journal of Materials Chemistry, 19(19), 3004-3012, 2009.***
  Identified as a 'hot article' and highlighted on the hot papers section.

- When acetylene was utilized as the hydrocarbon source, variations in temperature led to synthesis of various types of nano-structures (nanotubes or graphene) were synthesized on the same multi-functional catalyst system.

- Few-layer nano-graphene sheets were synthesized on various MgO supported catalysts. The catalyst composition, reaction temperature and type of hydrocarbon source were found to affect the morphological properties of nano-graphene.

  E. Dervishi et al., Chemistry of Materials, 21(22), 5491-5498, 2009.
  E. Dervishi et al., Chemical Communications, 27, 4061-4063, 2009.
  E. Dervishi et al., Journal of Materials Science, 47 (4), 1910-1919, 2012.

Conclusions for Part II

- The catalytic conversion of few-layer graphene into nanotubes was found to take place in the presence of metal nano-particles at the lowest temperatures reported to date (500 °C for Au and 150 °C for iron oxide).

- The synthesis temperature of nanotubes strongly depends on the nano-particle size, where smaller nano-particles yield nanotubes at lower temperatures.

- This low temperature growth technique provides a significant and promising approach for the integration of such novel nano-composites (CNT/graphene/metal) in a wide range of applications, varying from energy storage to sensing and drug delivery.

E. Dervishi et al., ACS Nano, 6 (1), 501-511, 2012. Highlighted with an "In Nano" write-up in the January issue of ACS Nano entitled "Very Cool: Converting Graphene to Carbon Nanotubes at 500 °C" http://pubs.acs.org/doi/abs/10.1021/nn2050328
E. Dervishi at al., Journal of Catalysis, 299, 307-315, 2013.

Conclusions

- Development of a versatile catalyst for an efficient growth of graphene and carbon nanotubes with controlled morphologies.
- The first to demonstrate that graphene can lower the nanotube synthesis temperature while acting as a carbon source.
- Carbon nanotubes and graphene were successfully used in a number of areas including photovoltaic devices , electrochemical detection, space exploration and bio-nano (toxicology and cancer therapy).

Y. Zhang et a., ACS Nano, 4 (6), 3181-3186, 2010. Article selected by Associate Editor Wolfgang Parak and Editor-in-Chief Paul Weiss and presented in the virtual Issue from ACS Nano devoted to nanotoxicology. (85 citations)
T. Ingle et al., Journal of Applied Toxicology, 2012, DOI: 10.1002/jat.2796.
M. Mahmood et al., under review 2013.
A. Karmakar, et al., International Journal of Nanomedicine, 6, 1045-55, 2011.
A.Karmakar, et al., Journal of Applied Toxicology, 32 (5), 365-375, 2012.
V. Saini et al., Journal of Applied Physics, 109(1), 014321, 2011. E. Dervishi et al., IEEE Transactions on Industry Applications Journal, 45 (5), 1547-1552, 2009.
V. Saini et al., The Journal of Physical Chemistry C, 113(19), 8023-8029, 2009.
S. Trigwell et al., under review 2013.
S. Pruneanu et al., International Journal of Nanomedicine, Accepted in 2013.
S. Pruneanu, et al. CHEMPHYSCHEM, 13(16), 3632-3639, 2012.
A. R. Biris et al., Carbon, 25

Acknowledgements

Mentor: Steve Doorn
Group members: Nicolai Hartmann, Erik Haroz and Navaneetha Subbaiyan

Graduate and undergraduate students: especially Rebecca Silva and Timothy O'Leary.
High-school students: Ashvini Vaidya and Esteban Abeyta

Collaborators at CINT:
Jinkyoung Yoo and Yung-Chen Lin
Han Htoon and his post-docs
Quanxi Jia and Aiping Chen
Jennifer Hollingsworth and Farah Dawood
Kristin Omberg, Quinn Mcculloch, Chris Sheehan and Darrick Williams.

Collaborators outside CINT:
Stephen Yarbro and his team (National Security Education Center)
Milan Sykora and Zhiqiang Ji (Chemistry-Division)
Zhehui Wang (P-25: Subatomic Physics)
Bryce Tappan (M-7: He Science and Technology)

Collaborators outside LANL:
Alexandru S. Biris (Center for Integrative Nanotechnology Sciences at UALR)
Vojtech Svoboda (Binergy Scientific Inc. in Atlanta, GA)

Los Alamos NATIONAL LABORATORY | U.S. DEPARTMENT OF ENERGY | Office of Science | UALR Center for Integrative Nanotechnology Sciences | Sandia National Laboratories

Thank you

Los Alamos NATIONAL LABORATORY
U.S. DEPARTMENT OF ENERGY Office of Science
UALR Center for Integrative Nanotechnology Sciences
Sandia National Laboratories

Mechanism of CNT Growth

- The longitudinal growth of the tube occurs by the continuous incorporation of small carbon clusters (C_2 dimers).
- If the nanotube has a random chirality, the adsorption of a C_2 dimer at the active dangling bond edge site will add one hexagon to the open end.
- The sequential addition of C_2 dimers will result in the continuous growth of chiral nanotubes.

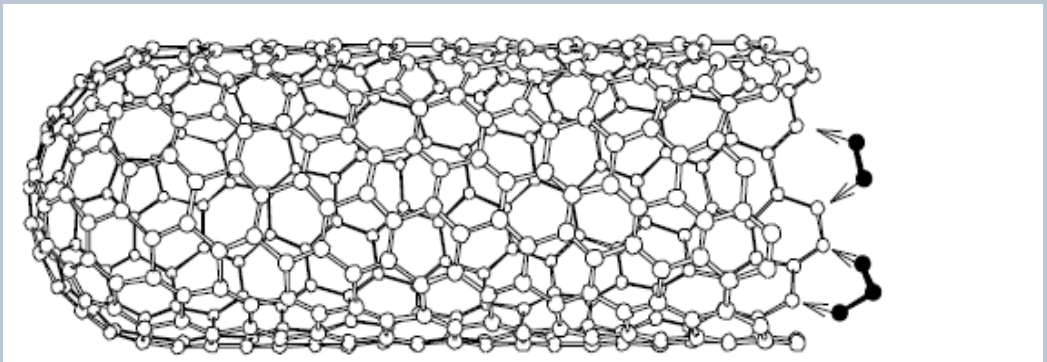

Growth mechanism of a carbon nanotube at an open end by the absorption of C_2 dimers and C_3 trimers (in black), respectively.

Charlier J. Ch. And Iijima S. "Growth Mechanism of Carbon Nanotubes", Topics Appl. Phys. 80,55-81 (2001)

Mechanism of CNT Growth cont.

- For achiral edges, C_3 trimers are sometimes required in order to continue adding hexagons, and not forming pentagons.
- The introduction of pentagons leads to positive curvature which would start a capping of the nanotube and would terminate the growth.
- Also the introduction of a heptagon-pentagon pairs leads to changes in nanotube size and orientation.

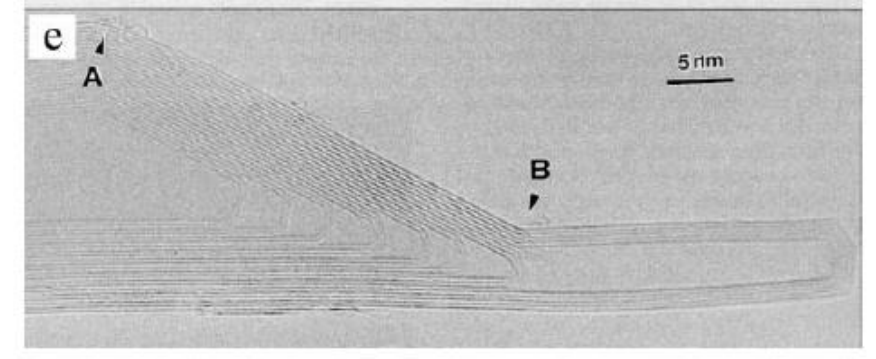

(**e**) : A positive and a negative disclamation are formed at the locations, indicated by A and B, probably due to the correlated presence of pentagons and heptagons, respectively, within the different concentric layers of the nanotube.

Charlier J. Ch. And Iijima S. "Growth Mechanism of Carbon Nanotubes", Topics Appl. Phys. 80,55-81 (2001)

Growth Models of CNTs

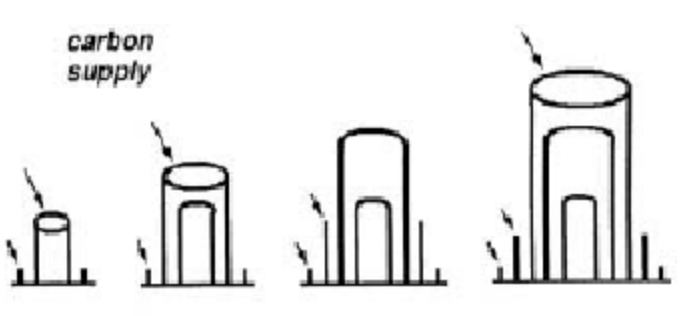

The tube ends are open while growing by accumulating carbon atoms at the tube peripheries in the carbon arc. Closure of the layer is caused by the nucleation of pentagonal rings due to local perturbations in growth conditions or due to the competition between different stable structures. Once the tube is closed, there will be no more growth on that tube but new tube shells start to grow on the side-walls.

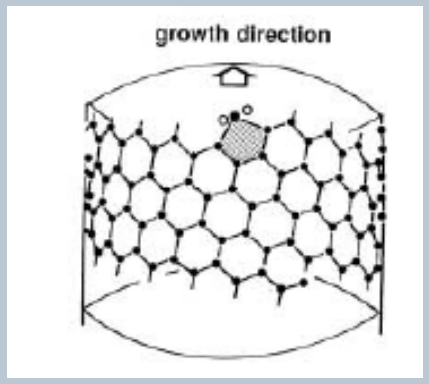

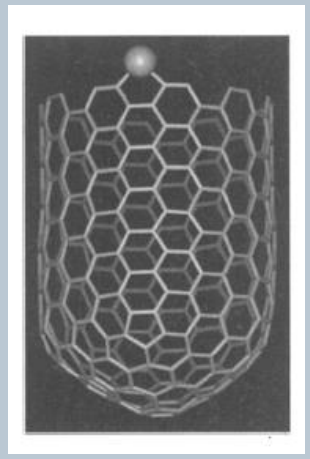

View of the critical nucleus of a (10,10) SWCNT with a Ni atom chemisorbed onto the open edge. The catalyst atom keeps the tube open by scooting around the open edge and ensuring that any pentagons or other high-energy local structures are rearranged to hexagons.

Charlier J. Ch. And Iijima S. "Growth Mechanism of Carbon Nanotubes", Topics Appl. Phys. 80,55-81 (2001)

Chemical Vapor Deposition

- It is based on the thermal decomposition of hydrocarbon (i.e., acetylene, methane) in the presence of a catalytic system (i.e., Co, Ni, Fe supported on a substrate (silica, zeolite) at elevated temperatures.

- At high temperatures, the hydrocarbon decomposes on the catalyst, whereby long nanotubes are spun from the particle.

- As the gas decomposes, carbon atoms that are produced condense on a cooler substrate that contains various catalyst systems.

Growth Process

- Based on the interaction of the catalyst with its support there are two different growth modes
- The interaction of the catalyst with the support can be characterized by its contact angle at the growth temperature, analogous to “hydrophobic” (weak interaction) and “hydrophilic” (strong interaction) surfaces.
- When there is a weak interaction between the catalyst and the support (large contact angle) tip growth mode is favored.
- When there is a strong interaction between the catalyst and the support (small contact angle) base growth mode is favored.

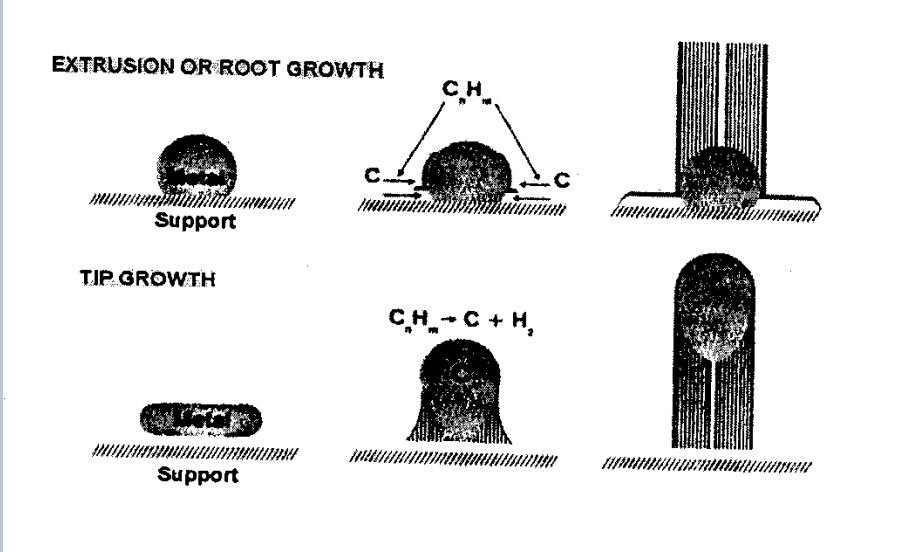

Couteau, Chemical Physical Letters, 2003;378:9-17

Raman Spectroscopy

What is the Raman Effect?

Light Scattering: A laser photon bounces off a molecule and loses a small amount of energy equal to the vibrational energy of the molecule.

Based on Inelastic or Raman Scattering (Exchange of Energy)

Raman Spectrum Provides a "Fingerprint" for Identification

- **Molecular Species**
- **Chemical Composition**
- **Crystalline Phase**

Raman for Carbon Nanotubes

Vibrational Modes

- Radial Breathing Mode (RBM) Single-Wall CNTs, 100-400 cm^{-1}
- D-band

  Disorder induced band, 1330-1360 cm^{-1}
- G-band

  Tangential band, 1550-1605 cm^{-1}
- G’-band

  Second order harmonic of the D band,2700 cm^{-1}

Photovoltaics

Photovoltaic devices based on high density boron-doped single-walled carbon nanotube/n-Si heterojunctions

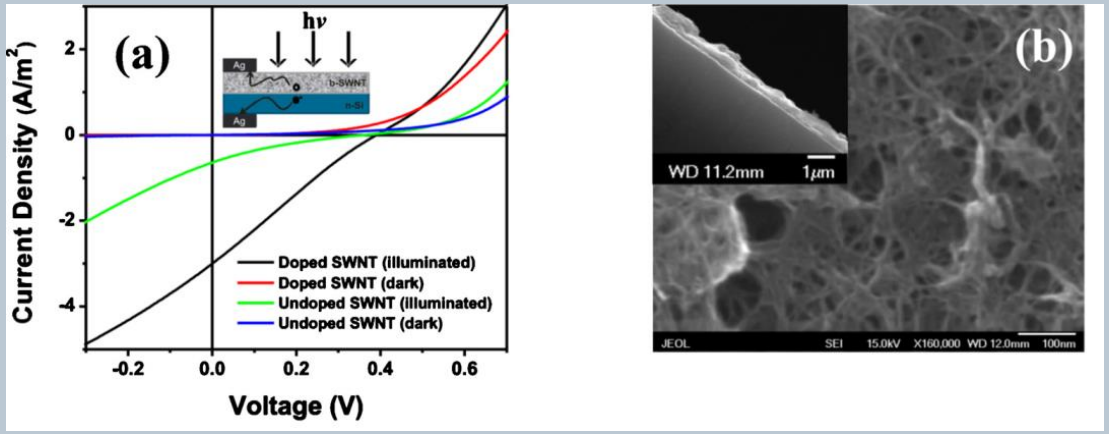

(a) Current-voltage characteristics of a typical pristine-SWNT/n-Si and B-SWNT/n-Si heterojunction photovoltaic device, with the device schematic and electrical connections. (b) Top view and inset image side view of B-SWNT film deposited over n-Si substrate.

Morphological Properties of P3HT-MWNT Nanocomposites prepared by in Situ Polymerization

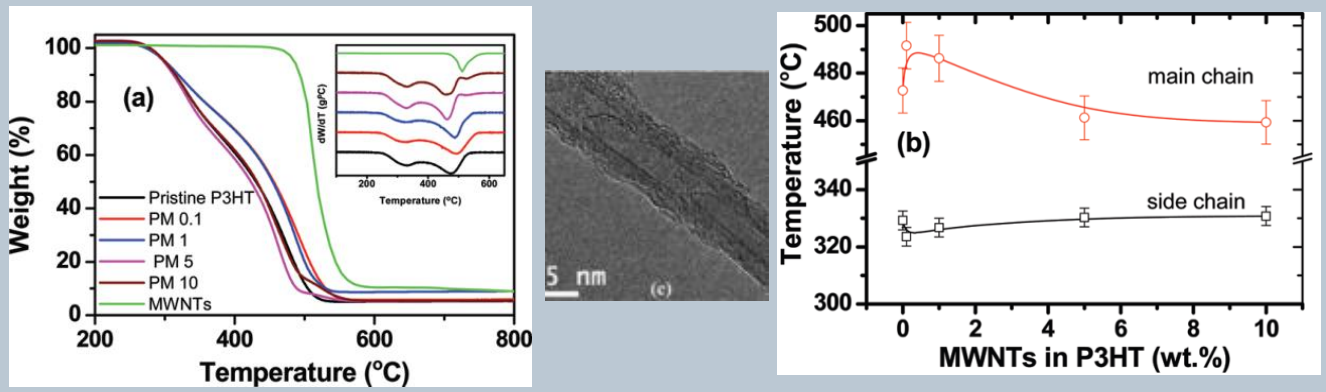

a) TGA and DTA (inset) of pristine P3HT, P3HT-MWNT nano-composites, and purified MWNTs. (b) Decomposition temperatures (*Td) of P3HT side chain (squares) and main chain (circles) in P3HTMWNT* composites.

V. Saini et al., Journal of Applied Physics, 109(1), 014321, 2011.
V. Saini et al., The Journal of Physical Chemistry C, 113(19), 8023-8029, 2009.

(Collaboration with Dr. Saini and the photovoltaic group at UALR-CINS)